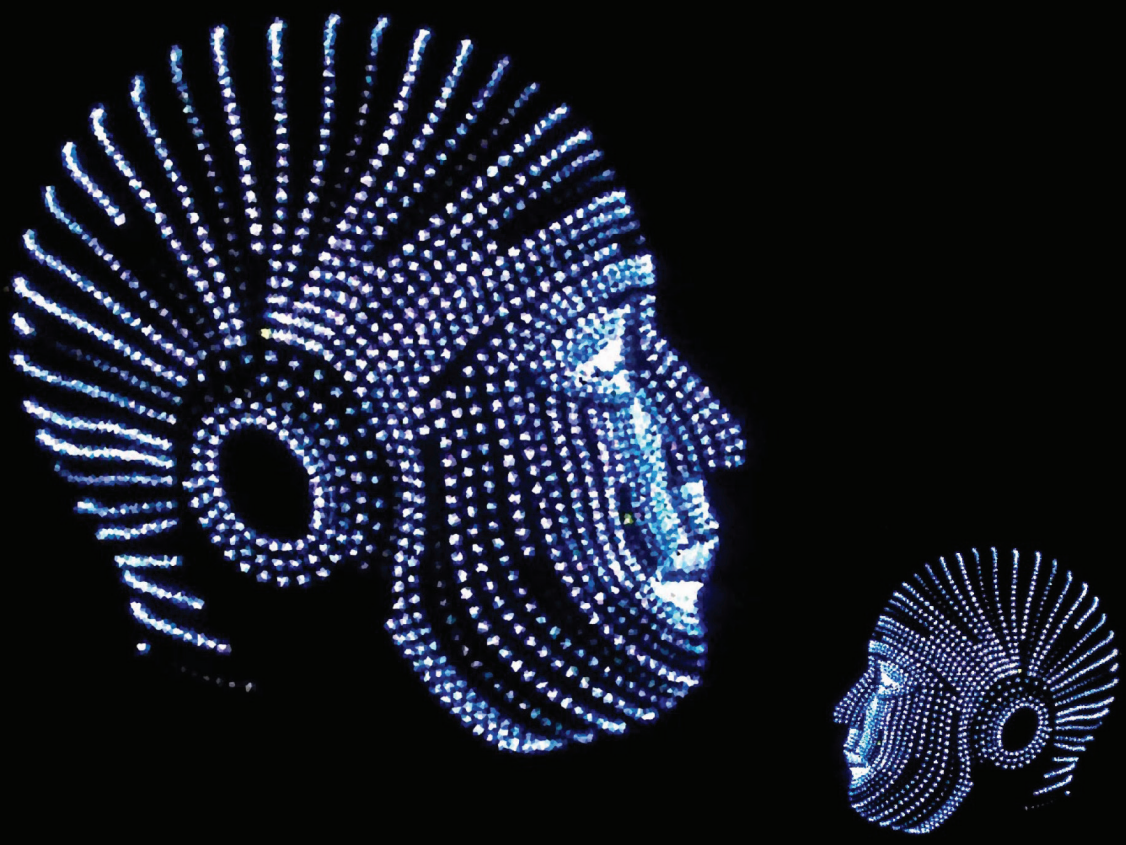
EXPRESSION AND ROLE OF TISSUE TRANSGLUTAMINASE IN LEUKOCYTES IN MULTIPLE SCLEROSIS AND EXPERIMENTAL AUTOIMMUNE ENCEPHALOMYELITIS



Navina L Chrobok

EXPRESSION AND ROLE OF TISSUE TRANSGLUTAMINASE IN LEUKOCYTES IN MULTIPLE SCLEROSIS AND EXPERIMENTAL AUTOIMMUNE ENCEPHALOMYELITIS

Navina L Chrobok

The research described in this thesis was conducted at the department of Anatomy and Neurosciences, Neuroscience Campus, VU University Medical Center, Amsterdam, The Netherlands.

The project was financially supported by the European Union Framework Program 7 Marie Curie TRANSPATH ITN (grant number 289964). Printing of this thesis was kindly supported by Stichting MS Research.

All publications in this thesis were reproduced with the permission of the respective publisher. See http://creativecommons.org/licenses/by/4.0 for additional information regarding chapters 1 and 4 (published in Amino Acids). Changes were applied for this thesis.

© Navina Laura Chrobok, 2020

ISBN 978-94-6380-755-5

Cover design:	Navina Chrobok
Layout:	Navina Chrobok / ProefschriftMaken.nl
Printing:	ProefschriftMaken.nl

VRIJE UNIVERSITEIT

EXPRESSION AND ROLE OF TISSUE TRANSGLUTAMINASE IN LEUKOCYTES IN MULTIPLE SCLEROSIS AND EXPERIMENTAL AUTOIMMUNE ENCEPHALOMYELITIS

ACADEMISCH PROEFSCHRIFT

ter verkrijging van de graad Doctor of Philosophy aan
de Vrije Universiteit Amsterdam,
op gezag van de rector magnificus
prof.dr. V. Subramaniam,
in het openbaar te verdedigen
ten overstaan van de promotiecommissie
van de Faculteit der Geneeskunde
op donderdag 14 mei 2020 om 15.45 uur
in de aula van de universiteit,
De Boelelaan 1105
door

Navina Laura Chrobok

geboren te Hannover, Duitsland

promotor:	dr. B. Drukarch
copromotoren:	dr. A.M.W. van Dam dr. M.M.M. Wilhelmus

Πάντες ἄνθρωποι τοῦ εἰδέναι ὀρέγονται φύσει.
Aristotle, *Metaphysics I 21, 980a*

CONTENTS

CHAPTER 1	General introduction and outline of the thesis	9
CHAPTER 2	Tissue Transglutaminase contributes to experimental multiple sclerosis pathogenesis and clinical outcome by promoting macrophage migration	27
CHAPTER 3	Tissue Transglutaminase appears in monocytes and macrophages but not in lymphocytes in white matter multiple sclerosis lesions	55
CHAPTER 4	Monocyte behavior and tissue Transglutaminase expression during experimental autoimmune encephalomyelitis in transgenic CX3CR1$^{gfp/gfp}$ mice	71
CHAPTER 5	Characterization of Transglutaminase 2 activity inhibitors in monocytes *in vitro* and their effect in a mouse model for multiple sclerosis	93
CHAPTER 6	Summarizing discussion	115
APPENDICES		129
	References	131
	Summary	155
	Acknowledgements	159
	Curriculum Vitae	161
	List of publications	163



Chapter 1

GENERAL INTRODUCTION AND OUTLINE OF THE THESIS

Partially based on:
Chrobok NL, Sestito C, Wilhelmus MM, Drukarch B, van Dam AM (2017):
Is monocyte- and macrophage-derived tissue transglutaminase involved in inflammatory processes?
Amino Acids. 2017 Mar;49(3):441-452.

1. MULTIPLE SCLEROSIS

Multiple Sclerosis (MS) is an inflammatory disease of the central nervous system (CNS). It was first described in detail in 1868 by Jean-Martin Charcot as scar tissue in the CNS [1]. More precisely, MS is characterized by an autoimmune attack to components of the myelin sheath guarding the integrity of neurons and axons. Infiltrating cells from the bloodstream, together with local cells of the CNS, damage this insulating myelin sheath. This results in demyelination, axonal damage and inhibited saltatory nerve conduction leading to a plethora of symptoms in MS patients. MS onset occurs mostly in young adults between 20 and 40 years of age and is up to thrice as frequent in women than men [2]. The prevalence of MS varies highly and is highest in western countries where it affects about 100-200 patients per 100.000 inhabitants (North America, Europe). Consequently, MS is one of the most common neurological disorders. Physical disabilities together with cognitive problems and the early onset of MS can have a high impact on the quality of life and life expectancy (reduction of 5-10 years). The disease can lead to the inability to work, a permanent requirement of daily help and/ or wheelchair dependency as well as social isolation due to fatigue and incapacity to maintain active social relationships. Each of these factors, as well as a combination of them, affects the personal life of the patient and their immediate surroundings by reducing the patient's quality of life. Furthermore, the inability to work as well as extended and expensive health care treatment also affects the economy [3, 4]. Therefore, further investigation in the causes, as well as treatment of MS, is highly desired to reduce its impact on patients and society.

1.1 Etiology and demographics

The precise etiology of MS remains largely elusive, despite tremendous research efforts. Nowadays it is commonly accepted that MS arises from a combination of environmental factors on the background of genetic predisposition. The observed geographical distribution of MS is possibly caused by the distribution of genetic factors in different populations. Depending on the racial background, some populations exhibit a high prevalence, such as Caucasians from Scandinavia and Scotland. In contrast, Mongolians, Japanese, Chinese, and American Indians show a low disease susceptibility [5]. Furthermore, studies with affected parents [6], twins [7], adoptees and half-siblings [6] support the notion of MS as a partially hereditary disease.

In addition to the genetic background, a plethora of environmental factors have been studied in association with MS. A correlation of MS susceptibility was found with low exposure to sunlight/UV radiation [8]. This might directly be related to Vitamin D, as sunlight exposure is the major factor for Vitamin D production and nutritional supplementation with the vitamin reduced relapses in MS patients [8]. Furthermore, MS is associated with viral infections such as the Epstein Barr virus and other viruses [9, 10]. However, the underlying mechanisms linking viral infections and the onset of MS remain unclear.

1.2 Clinical features and diagnosis

Clinical features of MS are manifold and divided into motor deficits and cognitive symptoms, which are further described below, and attributed to the disturbances in the stimulus transmission of axons by demyelination. Depending on the disease course, symptoms either manifest as sudden attacks or show a steady progression. On this basis, four distinct forms of MS are described. Approximately 80 % of the patients initially show a disease course known as a relapsing-remitting disease (RRMS). This form is characterized by disease symptoms adjourned by their (complete) absence. The frequency between symptomatic attacks and the absence of symptoms can be several weeks, but also years without any clinical signs of disease are described. About 10-15 % of patients present the primary progressive type, which is characterized by slow but continuous worsening of symptoms. The rarest initial disease form, progressive relapsing MS, shows continuous worsening disease that is broken up by occasional relapses. The fourth and last type of MS describes a common secondary disease phase. Most of the RRMS patients enter, after a certain disease duration, a disease state that is characterized by continuous disease progression. They are therefore described as having entered the secondary progressive disease phase, which occurs in approximately 90 % of RRMS patients after a disease duration of more than 25 years.

The most common presenting symptoms of MS are muscular spasms and weakness, sensory and visual disturbances and neuropsychological symptoms including cognitive impairment. Optic neuritis is also often seen and leads to an impaired vision of the patient. The occurrence of symptoms largely depends on the site of MS lesions in the brain, which is distinct in each patient. For example, cognitive impairment is caused by cerebellar lesions, whereas spinal cord lesions cause muscle weakness and spasms [4].
Due to the variety of clinical symptoms, MS diagnosis often depends on the experience of the neurologist. Nevertheless, there are specific criteria determined for the diagnosis of the disease. MS diagnosis is mostly based on clinical symptoms, which are described in the Poser criteria [11]. Criteria for the clinical presentation of the disease include at least two clinical attacks and/or lesions as well as dissemination in time [12]. In most cases, this is supported by magnetic resonance imaging (MRI) as described in the McDonalds criteria [13]. Although more than 96 % of patients show white matter abnormalities in MRI, their occurrence needs to be backed up by clinical diagnoses, since the MRI criteria are not intended to distinguish MS from other neurologic conditions [14]. Another confirmation of MS disease can be gained by the analysis of oligoclonal bands of autoantibodies in the cerebrospinal fluid of the MS patients, that indicate neuroinflammation [15].

1.3 Pathology

The pathological hallmarks of MS are demyelinated focal lesions in the white matter central nervous tissue (CNS) of the brain and spinal cord. These MS plaques are characterized by a focal accumulation of inflammatory cells, axonal damage, neurodegeneration, and glial scar formation. Recent research revealed that MS lesions might also be observed in the grey matter brain tissue. In contrast to white matter lesions,

their demyelination is associated with a lower level of inflammation caused by activated local astrocytes and microglia in the absence of immune cell infiltration [16-19].

The inflammatory plaques in the white matter consist mainly of cells infiltrated from the blood such as leukocytes, i.e. lymphocytes and monocytes, as well as activated local cells such as microglia and oligodendrocytes [20]. The inflammatory cells are found in and around areas of demyelination and can be visualized with MRI for the diagnosis of MS. They are also important in the neuro-pathological diagnosis of the disease. Immunohistochemical analysis on biopsies or post-mortem tissue shows that MS lesions display different characteristics depending on their activation status. The distinction in pre-active lesions, active lesions, chronic active lesions, and inactive lesions is based on the presence of HLA-DR positive cells, i.e. lymphocytes and macrophages, and the level of demyelination. Pre-active lesions are characterized by intact myelin sheets with clusters of HLA-DR positive cells. Active lesions show a hyper-cellular demyelinated area with an evenly distributed massive HLA-DR positive cell infiltration, whereas chronic active lesions have a hypo-cellular demyelinated core as the HLA-DR positive cells recede to form a rim around the demyelinated area. Inactive plaques are mostly devoid of macrophages but demyelinated. As a lesion develops from a chronic active towards an inactive state, progressing astrocytic fibrillary gliosis results in a glial scar that fills the demyelinated area. Also, remyelination is observed in MS, especially in the earlier disease phases [21]. However, the myelin quality and amount does not reach the natural state from before MS onset and remains a weak spot for further inflammatory attacks [22].

1.3.1 Cellular CNS infiltration

The blood-brain barrier (BBB) is a physical barrier that specifically protects the CNS from toxic substances, pathogens and immune cells from the bloodstream, that might cause swelling and therefore cause damage to the brain and spinal cord. In healthy individuals, the BBB highly limits the infiltration of immune cells from the blood into the CNS. In MS patients however, this barrier is dysfunctional and allows cells to migrate into the CNS where they exert damage leading to MS symptoms [23]. This process of cellular infiltration is highly regulated and involves many factors such as chemokines and adhesion molecules (Figure 1). Inflammation leads to the expression of chemoattractants (chemokines) which are secreted on the surface of endothelial cells [24]. This attracts leukocytes from the bloodstream and results in simultaneous upregulation of adhesion molecules on the attracted leukocytes and also on the endothelial cells of the blood vessel lumen. The initial capturing and rolling of leukocytes is mediated by selectins and their counter receptors on the endothelial cells [24]. This is followed by leukocyte activation via chemokine signaling pathways including the Rho family of GTPases and activation of surface adhesion molecules [25]. The next step is subsequent adhesion strengthening via binding of integrins, which initiates a firm arrest [26]. Now cells start to crawl along the blood vessel lumen, a process that is integrin-mediated and helps the cells to find suitable extravasation sites. Once a suitable site is encountered, the cells migrate through the endothelial cell layer into the perivascular space, either by paracellular or transcellular route, promoted by luminal chemokines. Continuing on their path, the cells progress via

the BBB specific glia limitans into the brain parenchyma, a process whose details are not fully understood yet, despite the availability of *in vitro* BBB models.

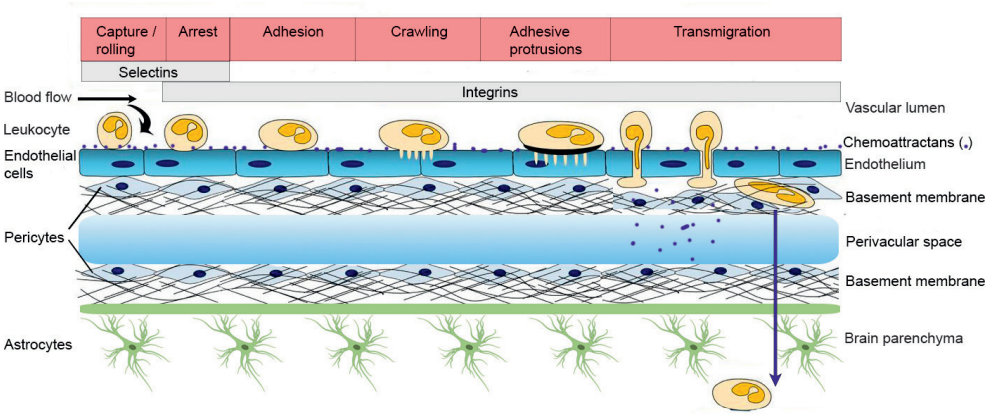


Figure 1: Multistep cascade of leukocytes recruited into the CNS. The extravasation process of leukocytes from the blood into the CNS is a multistep process. Capture/rolling: selectins on the leukocytes and endothelial surface initiate capture and subsequent rolling in the direction of the blood flow. Chemokines on the lumen initiate this capture/rolling and initiate integrin upregulation and a firm binding is established that leads to the arrest and adhesion of the leukocytes. Then the search for suitable extravasation sites starts by crawling of the cells along the endothelial lumen. Transmigration into the perivascular space can either be paracellular or transcellular and is promoted by luminal chemokines. The chemokines also are crucial for further extravasation of the cells across the glia limitans into the brain parenchyma. Adapted from Schaefer and Hordijk, Cell-stiffness-induced mechanosignaling - a key driver of leukocyte transendothelial migration. J Cell Sci, 2015. 128(13): p. 2221-30.

1.3.2 Cell types in inflammatory MS lesions

The immune cells present in inflammatory MS lesions are depicted in Figure 2 and described in more detail in this paragraph. Despite the multitude of cells present in MS lesions, the currently accepted hypothesis is that activation of auto-reactive T cells that infiltrate the CNS and induce or facilitate a chronic inflammatory response, is the main mediator of MS development [4, 27]. It is believed that defects in immune tolerance (central and peripheral) permit the existence of self-reactive T cells that are responsible for MS induction.

The other lymphocyte type, B cells, plays a pathogenic role in MS development via antibody production in the CNS and is therefore likewise addressed in MS therapies. In healthy patients, B cells do not cross the BBB, while in MS patients leukocytes are found in the CNS. MS patients show increased levels of antibodies in the cerebrospinal fluid, which indicates local antibody production by B cells. This local antibody production is a prerequisite for the analysis of oligoclonal bands of autoantibodies in the cerebrospinal fluid of MS patients, one of the biomarkers used for MS diagnosis [15]. Furthermore, autoantibodies specific for proteins of the myelin sheath are indicators of demyelination [28]. Additional to antibody production, B cells can also produce and secrete cytokines which may aid or dampen the inflammatory processes via the stimulation of T cells [29-31].

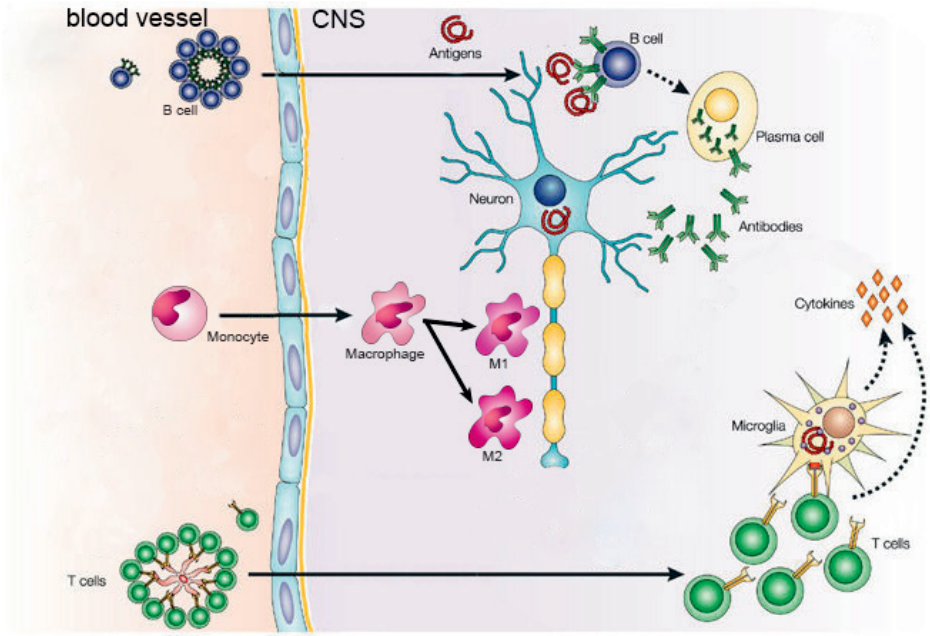


Figure 2: Cells involved in the pathology of MS. Leukocytes from the bloodstream infiltrate the CNS in MS patients. The most prominent inflammatory cell types present in MS lesions are B cells, T cells, macrophages and the local microglia of the CNS. The cells are attracted by a multitude of factors including cytokines produced by microglia and T cells that lead to further recruitment of immune cells. After extravasation, B cells develop into plasma cells and secrete antibodies into the CNS. Monocytes differentiate into macrophages upon entering the CNS and further differentiate into macrophage phenotypes (M1, M2). T cells develop into different subsets and secrete, together with stimulated microglia, cytokines. Adapted from Hemmer, et al., New concepts in the immunopathogenesis of multiple sclerosis. Nat Rev Neurosci, 2002. 3(4): p. 291-301.

Despite the importance of lymphocytes ins MS pathology, one of the biggest cell populations found in MS lesions are macrophages. They can be either CNS residential microglia or macrophages differentiated from monocytes that had extravasated from the bloodstream. Macrophages can play opposing roles in MS: On the one side, they contribute to lesion formation, inflammation and axonal damage, on the other side, they induce repair mechanisms via secretion of neurotrophic factors, clean up (myelin-)debris and produce anti-inflammatory factors [32]. The infiltration of monocytes in the CNS is specific for neuroinflammation, but even under healthy conditions, a limited number of monocytes enter the CNS and exert a surveillance function [33]. Once in the CNS tissue, monocytes differentiate depending on the encountered stimuli in different phenotypes. These can be either classically activated macrophages (M1) or alternatively activated macrophages (M2) [34]. Generally, M1 macrophages are considered pro-inflammatory while M2 macrophages are anti-inflammatory [35]. Unfortunately, the distinction in macrophage subsets is based on *in vitro* studies and *in vivo* the division is less pronounced [36]. Nevertheless, in an MS animal model, M1 macrophages were shown to increase disease severity whereas cells of the M2 type improved the disease [37]. In MS patients,

however, the difference between the two macrophage subtypes is less clear and most cells co-express M1 and M2 markers, indicating an intermediate phenotype [38].

1.4 Treatment

No treatment is currently known to prevent or cure MS. The current therapeutic strategy for MS focuses on dampening the symptoms, postponing and reducing the number of relapses and preventing permanent disability acquired through disease progression. This is achieved by long-term treatment with immune-modulatory agents that suppresses the inflammatory response to reduce lesion formation and consequently disease progression and are called disease-modifying treatments (DMTs) [39]. To dampen the symptoms and duration of relapses, the most commonly used treatment is immunosuppression with oral or intravenous administration of corticosteroids. They inhibit the production of pro-inflammatory cytokines and are mostly applied in the form of methylprednisolone [14, 40]. Systemic corticosteroids are the most established and validated first-line treatment options to reduce the duration of acute MS relapses. In addition, β-interferons have been proven very potent in that regard [41]. Amongst other effects, they lead to downregulation of inflammatory cytokines and decreased T cell interaction with the BBB [42]. Observed side effects for these immunosuppressing treatments are flu-like symptoms injection-site reactions and potentially liver damage caused by elevation of liver transaminases and therefore require very close monitoring. Overall, immunosuppression increases the risk for common infections and is, therefore, to be handled with care and specific precaution.

In contrast to general immunosuppression, a more specific approach in MS treatment is to counteract the number of leukocytes or specific subsets that infiltrate the CNS and thereby limit inflammation and subsequent demyelination and axonal damage. Although these new(er) therapies often have several modes of actions, they can roughly be divided into two main groups according to their mechanism: a) specific immunosuppression and b) inhibition of cellular adhesion and CNS infiltration of leukocytes. The specific reduction of leukocyte recruitment into the CNS dampens the inflammation at the site of interest without the drawbacks of general immunosuppression. The whole leukocyte population can be targeted in such a way or, more specific, only cell subsets that might infiltrate the CNS. However, also targeted therapies that focus on more specific cell subsets, for example only lymphocytes or T cells or B cells have been approved. The modes of actions of these therapies result in specific immunosuppression including the depletion of cells (e.g. alemtuzumab) [43, 44], inhibition of cell proliferation (e.g. mitoxantrone and leflunomide) [45-48] and cell activation (i.e. daclizumab) [49, 50], tethering of lymphocytes in the lymph node (e.g. FTY720 and fingolimod) [51-53], and the inhibition of pro-inflammatory signaling (i.e. BG-12) [48]. These therapies, including dimethyl fumarate and natalizumab, inhibit the cell-cell interaction, migration on the BBB and/ or diapedesis across the endothelium [54-58].

This short summary of possible therapeutic strategies for MS indicates that DMTs have quite diverse modes of actions with a common denominator in reducing inflammation and cellular migration into the CNS. Unfortunately, some of these agents

show serious adverse effects such as concomitant infections and progressive multifocal leukoencephalopathy [59]. Consequently, the search for better MS treatments is still ongoing and aims at developing specific, safe and effective therapies with minimal side effects. Targeting immune cell inflammation and specific molecules involved in the interaction of cells and the BBB might be the direction of choice to prevent the destruction of myelin without the adverse side effects of general immunosuppression.

2. ANIMAL MODELS FOR MS

MS is a human disease with no naturally occurring equivalent in other species. To overcome this drawback for research, numerous artificially induced animal models in rodents and non-human primates have been developed over the last century. Despite being highly valuable in evaluating therapy options for MS, one nevertheless needs to point out that none of these models completely resembles all features of MS. Each model resembles specific aspects of the disease such as the inflammatory component or de-/remyelination but no model reflects the complexity of MS and its diverse disease manifestations. Therefore an *in vivo* model for MS research has to be chosen carefully, depending on the focus of interest [60].

The available MS animal models can be divided into two groups: a) Induced neuroinflammation in the experimental autoimmune encephalomyelitis models and b) demyelination induced by toxins or viruses in absence of inflammation. Wide knowledge regarding basic mechanisms of de-/remyelination, neuroinflammation, and their pathomechanisms are derived from these models and many available MS therapies evolved, at least partly from *in vivo* research.

2.1 Neuroinflammation in experimental autoimmune encephalomyelitis (EAE)

EAE is the most commonly used animal model for inflammation of the CNS and resembles the histopathology of MS. Most frequently, rats and mice [61, 62] are used in these experiments but EAE models for other rodents and non-human primates have been developed similarly [63-65]. The EAE model is a good model to study immune-related pathological processes as well as treatment effects [66].

To induce EAE, CNS-derived antigenic components [myelin basic protein, myelin proteolipid protein, myelin oligodendrocyte protein (MOG) or spinal cord lysates] are injected with or without an immune reaction booster, i.e. an adjuvant. The immune response induced by the CNS-antigens results in an autoimmune response against the myelin sheath in the CNS resulting in BBB loosening, leukocyte infiltration, and demyelination. The occurring symptoms are gradual paralysis by neurological deficits paired with weight loss. The choice of antigen, adjuvants, application process and possibly other essential substances are dependent on the species, the strain and the desired aspects of MS to be mimicked. Animals induced with EAE show a gradual incline in motor-symptoms that are caused by inflammatory infiltrates of the CNS and especially the spinal cord, concomitant with demyelination. In addition to the immunization and active

immune response approach, a passive model is available: Transfer of myelin autoreactive T cells either from an EAE immunized animal or *in vitro* differentiation/stimulation induces EAE in experimental animals. This so-called passive EAE allows to specifically study the role of T lymphocytes during EAE.

The two active EAE animal models used in this thesis are the chronic-relapsing EAE model in dark agouti rats and the monophasic acute EAE model in mice of the C57BL/6 strain.

2.1.1 Chronic relapsing EAE in dark agouti rats

Chronic relapsing EAE (cr-EAE) in rats of the dark agouti strain resembles RRMS, which is the most common form of initial MS diagnosed patients. Mostly, the rats are injected with MOG in combination with Freund's adjuvants [67] and exhibit a disease that starts with worsening of symptoms followed by a (complete) remission. This phase is then followed by a relapse and therefore mimics the relapsing remitting-course of MS. On a cellular level, cr-EAE is mainly mediated by monocytes/macrophages making this model predestined for research regarding these cell types [67].

2.1.2 Monophasic acute EAE in C57BL/6 mice

The most widely used EAE mouse model is in animals of the C57BL/6 strain. The peptide MOG_{35-55} (representing amino acids 35-55 of the MOG protein) is injected in complete Freund's adjuvants complemented with Mycobacterium tuberculosis. Besides, the animals receive pertussis toxin to finish disease induction. This immunization scheme results in a monophasic disease that is mainly mediated by a predominant T cell component, supported by monocytes/macrophages [68]. The main advantage of this experimental model is the genetic manipulation of this mouse strain which is relatively easy to achieve and therefore the majority of commercially available transgenic and mutant animals are either derived from C57BL/6 mice or are back-crossed to this particular mouse strain. Unfortunately, no relapses or clinical progression can be studied in this monophasic disease model. Thus, it is mainly used to study immune cell infiltration and neuroinflammation and potential treatments affecting these.

2.2 Demyelination in the absence of inflammation

The second type of MS animal models is not focused on inflammation but purely on demyelination and the underlying pathological processes and can be induced either by toxins or viruses.

2.2.1 The cuprizone model: toxin-induced demyelination

Feeding mice with chow supplemented with the copper-chelator cuprizone (bis-cyclohexanone-oxalyldihydrazone) for several weeks results in CNS demyelination [69, 70]. Within 4-6 weeks, complete demyelination is reached and after ablation of a cuprizone-

supplemented diet, successive remyelination occurs. After prolonged exposure to cuprizone (>12 weeks) chronic demyelination without signs of remyelination is achieved. The detailed mechanism of cuprizone-induced demyelination is not completely understood but it seems that cuprizone leads to oxidative stress and selective toxicity for oligodendrocytes [71]. Oligodendrocytes undergo subsequent apoptosis which explains a lack in (re-)myelination. Neither a breakdown of the BBB, leukocyte infiltration nor primary immune-modulated effects are observed in this model. This model is used for detailed studies regarding oligodendrocyte death and simultaneous de- and remyelination, as seen in MS patients, can be studied in parallel.

2.2.2 Theiler's murine encephalomyelitis virus: virus-induced demyelination

Virus-induced demyelination is observed in the Theiler's murine encephalomyelitis virus (TMEV) model in which mice are subjected to picornavirus. This model allows insight into progressive neurological disability, resembling the progressive forms of MS, and the origin of some behavioral signs in line with demyelination of the murine CNS [72, 73].

3. TISSUE TRANSGLUTAMINASE

3.1. Tissue Transglutaminase and the Transglutaminase family

Tissue Transglutaminase (tTG, TG2) is a multifunctional enzyme that was first described in the late 1950s [74, 75]. Upon discovery in guinea pig liver, it was demonstrated to be able to catalyze protein-protein cross-linking. Later on, TG2 turned out to be a multifactorial enzyme associated with important functions in both physiological and pathological conditions. It is part of the family of transglutaminases (TGs), which consists of nine structurally and functionally related enzymes in mammals [76]. The members of the TG protein family (expect Band 4.2) are best known for their enzymatic cross-linking activity but highly differ in their expression patterns. Keratinocyte TG (TG1), epidermal TG (TG3) and TG5 are mostly found in keratinocytes and the skin where they are involved in epidermal terminal differentiation [77, 78]. Prostate TG (TG4) is involved in semen coagulation [76], whereas relatively little is known about TG6 and TG7 [79, 80]. The outsider of the family, Band 4.2, lacks the typical enzymatic cross-linking activity and is present in red blood cells and regulates cytoskeleton integrity [81, 82]. The blood-derived Factor XIIIa is a soluble zymogen involved in blood coagulation and wound closure as well as gene expression in alternatively activated macrophages [83, 84]. The family member that has been most studied is TG2, which is ubiquitously expressed in many cell types under physiological conditions [85]. Both neuroinflammation and degeneration facilitated by dysregulated expression and activity of TG2 have been implicated in many neurodegenerative diseases such as Alzheimer's [86], Parkinson's [87] and Huntington's disease [88, 89] and therefore make it a promising target for neuroinflammatory and neurodegenerative research.

3.2 TG2: Structure, function, and regulation

Human TG2 is a 78 kDa protein and consists of 686 amino acids. The molecular structure of TG2 consists of four domains, which are involved in distinct functions: the N terminal β-sandwich (binds fibronectin and integrins), the catalytic core (transamidation activity) and two C terminal β-barrels of which the latter includes a phospholipase C binding sequence [85]. The transamidation function gave TG2 and its family the name and catalyzes cross-linking of glutamine to lysine residues within or between proteins, resulting in a stable isopeptide bond [76]. This means that cross-linked substrates are not only more protease-resistant, but they also result in altered biological functioning, metabolism and/or immunogenicity of the substrates [76]. Moreover, amine incorporation into substrates and deamidation are catalyzed by the same enzymatic domain [76, 90].

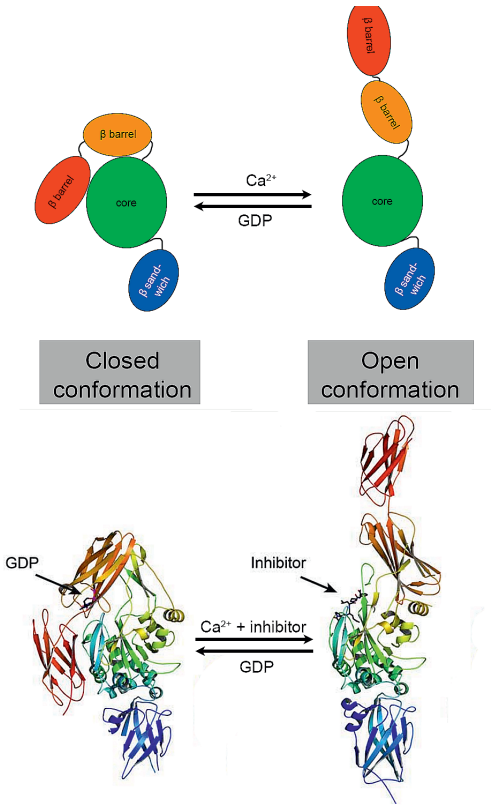


Figure 3: TG2's open and closed conformation. Inactive TG2 is present in a GDP bound closed conformation, in which the two β barrels bend around the core and shield the catalytic triad. Calcium-binding induces a large conformational change of the two β-barrels towards an elongated open conformation that is catalytically active. Adding an inhibitory compound, TG2 is kept in the open state but is catalytically inactive. The open and closed conformations are reversible. Adapted from Pinkas et al., Transglutaminase 2 undergoes a large conformational change upon activation. PLoS Biol, 2007. Dec;5(12):e327.

The transamidation activity of TG2 is regulated in the catalytic domain with the catalytic triad consisting of cysteine 277, histidine 335 and aspartic acid 358. The transamidation activity is regulated by guanosine diphosphate/triphosphate (GDP/GTP) and calcium-binding (Figure 3) [91]. Calcium-binding of TG2 induces a conformational change towards an open, elongated and therefore active conformation that makes the catalytic core

accessible (Figure 3) [92]. The calcium concentration needed for transamidation activity lays in the supraphysiological range, indicating that TG2 is mostly inactive intracellularly and probably requires disturbed calcium homeostasis for activation [93]. Besides, extracellular TG2 is inactive due to the redox state of the transamidating site or binding to extracellular matrix (ECM) proteins and can be transiently activated upon mechanical injury, oxidation or inflammatory stimuli [94-96]. This open active conformation of TG2 can also be targeted by chemical TG2 activity inhibitors which lock the enzyme in an open but inactive conformation.

Alike some other members of the family, TG2 has various additional enzymatic functions, i.e. disulfide isomerase function [97], G protein (GTPase) function during which TG2 is better known as Ghα [98, 99] and protein kinase activity [100]. However, these functions are not the focus of this thesis since their participation in the processes and functions studied in it is mostly unknown.

As various as TG2's functions are the reported subcellular locations. Although predominantly present in the cytoplasm, TG2 has also been found in the nucleus, mitochondria, endoplasmic reticulum and on the cell surface [101-105]. Furthermore, TG2 can be secreted from the cell into the ECM [76, 106, 107]. TG2 is constitutively expressed in endothelial and smooth muscle cells, but many tissues and cell-types show up-regulated expression in a cell type-dependent manner by several physiological and pathological stimuli including astrocytes, fibroblasts, lymphocytes, and monocytes/ macrophages. Increased TG2 expression and transamidation activity are often observed under inflammatory conditions in which cytokines, retinoids and growth factors, released by injured or activated cells, regulate TG2 expression and activity and this function [108]. Due to the manifold functions that TG2 can exert, its expression needs to be tightly regulated. The regulation occurs mainly at the transcriptional level and is mediated by the presence of several transcription factor-binding sites located in the promoter-region of the TGM2 gene, including NFκB [109, 110] and TGF-β responsive elements [111]. Although some evidence exists that anti-inflammatory mediators can induce TG2 expression, the majority of TG2 stimulation in various cell types during inflammation is caused by pro-inflammatory mediators [112-117]. However, the exact mechanisms behind TG2 regulation as well as the role of TG2 in the different cell types are still not fully understood. Furthermore, the discrepancy of some published results as well as contradicting results in different cell types indicate that the regulation and function of TG2 expression are cell type and time point dependent and therefore general conclusions remain unclear.

3.3 TG2 function in cellular adhesion and migration

TG2 participates in cell adhesion and extravasation, processes crucial for inflammatory cells to reach sites of inflammation [118-120]. In MS, these cellular processes provide specific and valuable targets for new treatment options to fight the disease and therefore make TG2 an interesting study object in this context. TG2 on the cell surface is complexed with integrins, i.e. β1/β3/β5-integrins and bridges the intracellular cytoskeleton with fibronectin in the ECM and thus facilitates adhesion of cells [119, 121, 122]. Reduction of TG2 expression by TG2 knock-down or inhibition of TG2-fibronectin-binding by function-

blocking antibodies strongly reduced the cellular adhesion and migration capacities of macrophages [119]. Additionally, cell surface TG2-integrin complexed in specialized adhesive structures on macrophages, so-called podosomes, point towards a strong link between TG2-integrin complexes and adhesion and extravasation of cells [123, 124]. Interestingly, the interaction between TG2 and β-integrins does not require transamidation activity to increase adhesion, spreading and cell motility [76, 122, 125-128]. In addition to its involvement in direct adhesion of cells, TG2 is also involved in assembly, re-modeling, and stabilization of the ECM via crosslinking of several ECM substrates [80, 106]. ECM stabilization by TG2-mediated transamidation increases the rigidity of the ECM, potentially resulting in increased cell adhesion to the ECM [129, 130].

The above described contribution of TG2 to adhesion and migration is mediated by cell surface and/or extracellular TG2 [131]. However, also intracellular TG2 might have an effect by stabilizing and/or reorganizing the actin cytoskeleton [132-135]. Migration and especially diapedesis of cells through the blood vessel endothelium require high motility of the actin cytoskeleton to change the shape of the cell in an efficient and fast manner. This reorganization of the cytoskeletal structure and re-arrangement is mediated by focal adhesion kinase and Rho-associated protein kinase [134, 136]. Both of these are stimulated by TG2 induced clustering of cell surface integrins, which leads to higher initiation of cell adhesion and cytoskeletal flexibility [135]. Furthermore, TG2 can induce expression and activation of matrix metalloproteinases (MMPs) that are involved in adhesion and migration processes [127, 137-139]. Although this has not been shown yet in monocytes or macrophages, increased stimulation of MMPs might further promote their cellular migration and especially facilitate diapedesis by loosening up tissue structures [137, 139].

3.4 TG2 inhibition

Although TG2 is involved in a variety of cell functions and is observed in many cellular locations, the enzyme is generally catalytically silent under physiological conditions. Under pathological conditions, however, TG2 activity has been associated with a wide range of conditions including inflammatory [140], autoimmune [141] and neurodegenerative [142, 143] diseases and certain types of cancer [144, 145]. In some of these pathologies, TG2 transamidation activity has been proposed and studied as a possible druggable target to counteract the pathological events. As described above, the cross-linking activity is highly regulated under physiologic conditions and TG2 remains predominantly in its inactive conformation. Yet, under pathological conditions not only the expression is increased but also TG2 adapts the active open state conformation. This suggests that targeting TG2 activity will not interfere with its various functions in physiology. Indeed, the complete absence of TG2 in TG2-knockout mice first did not result in a specific phenotype, although later studies revealed reduced apoptosis and signs of autoimmunity due to insufficient efferocytosis with increasing age [146]. The fact that in healthy mice the absence of TG2 results in no apparent changes suggests that dysregulated TG2 in disease provides an interesting druggable target with limited effects on physiology.

TG2 inhibitors can be divided into several classes according to their structure and/or inhibitory mechanism. The earliest investigated inhibitors are reversible inhibitors that are often alternative substrates such as primary amines [147]. They compete with the natural enzyme substrates and therefore reduce the enzymatic activity for natural substrates. However, they completely lack specificity. The second group of reversible inhibitors is specifically designed to inhibit the binding of native substrates to the enzyme while not being substrates of TG2, and thus do not participate in the enzymatic reaction. Although in some cases reversible inhibition might be desired, the bigger potential is believed to lay in irreversible inhibition. The design of this class of inhibitors has led to compounds with a higher selectivity for the TG2 enzyme over other transglutaminases, higher potency and permanent inhibition with long-term effects. These inhibitors are usually either peptide-based or small molecules.

Although tremendous efforts have been made to develop and study the described TG2 inhibitors, the majority of our knowledge on these inhibitors is based on cell-free assays with limited data from *in vitro* assays. Unfortunately, *in vivo* data is even more scarce and mostly only available for the 'older' and less specific (i.e. interaction with other transglutaminases) TG2 inhibitors.

So far, beneficial effects of *in vivo* pharmacological inhibition of TG2's transamidating activity with cysteamine have been observed in experimental models for neurodegenerative diseases and fibrosis. The competitive reversible TG2 inhibitor cysteamine and its oxidized form cystamine are effective in inhibiting TG2 activity *in vivo*. Cyst(e)amine was reported to be effective in murine models of Parkinson's and Huntington's disease where it extended survival and improved neuropathological symptoms through reduced neuronal loss [148-150]. However, the pleiotropic effects on all transglutaminases and possible additional off-target effects make it difficult to narrow down the source of its beneficial outcome. Conversely, further evidence indicated that some of the observed effects of TG2 inhibition by cyst(e)amine cannot be confirmed in TG2 knockout mice and might be independent of TG2 activity inhibition [151].

Apart from reversible TG2 inhibitors, irreversible TG2 inhibitors have also been tested *in vivo*. One category of these are dihydroisoxasole derivatives like KCC and ERW1041E. They effectively reduced the size of implanted glioblastoma, extended survival in a glioblastoma mouse model and were also effective in celiac disease (reduce intestinal TG2 activity) and a pulmonary hypertension model (reduced hypertrophy of the heart) [152-154]. Problematic is the low potency and cross-reactivity with other transglutaminases that these inhibitors show (TG1, TG3, FXIII)[152]. Another group of irreversible TG2 inhibitors has successfully been applied in (renal) fibrosis animal models where they reduced transglutaminase activity, ECM crosslinking and scarring [155, 156]. Recently, the new irreversible inhibitor ZED1227 was the first irreversible TG2 inhibitor to enter clinical trials (press release, 2018, www.Zedira.com). It proved to have sufficient safety and tolerability to be further investigated in a phase 2a clinical trial as a treatment of celiac disease.

All the above-mentioned compounds target TG2 transamidating activity. Another approach is to target the interaction of TG2 with its specific substrates. One example of such an approach is the small TG53 molecule which disrupts the binding of TG2 to

fibronectin and inhibits cell adhesion to fibronectin *in vitro* [157]. Despite the lack of *in vivo* availability of such data, this is an interesting start to develop TG2 inhibitors that specifically block the interaction of TG2 with one of its binding partners. In addition to peptidergic and small molecule inhibitors, another relatively new approach is the use of inhibitory antibodies either to inhibit enzymatic activity or interaction with other TG2 binding partners. Successfully applied *in vitro*, they still need to demonstrate their effectivity *in vivo* [158].

Although there are many publications on the use of TG2 inhibitors in cell-free and cell/tissue-based assays, there is a gap in our knowledge on their kinetic properties and selectivity *in vivo*. This lack of knowledge hampers the transition of the compounds into animal models of different diseases, and thus proof of concept that these TG2 inhibitors are feasible therapeutic agents remains to be demonstrated.

4. AIMS AND OUTLINE OF THE THESIS

MS is pathologically characterized by inflammation, demyelination and axonal damage within the CNS. Functional disturbances of the blood-brain barrier facilitate an influx of leukocytes from the bloodstream into the CNS. These cells, together with local glial cells, cause inflammation and the typical demyelinating MS lesions that are responsible for serious disabling symptoms in MS patients. As one of the most common neuroinflammatory disorders that affect mainly young adults, specific and tailored pharmacological treatments for MS are highly sought after. MS therapy traditionally includes general anti-inflammatory treatment to dampen the inflammatory response. Recently, more dedicated treatments for MS have been developed, many of them focusing on the inhibition of adhesion and migration of leukocytes, e.g. T cells and thereby preventing their infiltration into the CNS

As described in detail in this introductory chapter, TG2 is a well-studied enzyme that is ubiquitously expressed and involved in many disease pathologies. Inflammatory mediators are known to increase TG2 expression and its enzymatic transamidation activity. The increased presence and activity of TG2 during inflammation *in vivo* can contribute to many fundamental processes, including cell adhesion and migration, ECM deposition, cytoskeletal rearrangement, cell differentiation, apoptosis and phagocytic processes such as efferocytosis. The potential involvement of TG2 in at least some of these processes makes it an interesting protein to study in the context of MS pathology. Also, TG2 may be considered a novel pharmacological target to counteract inflammatory processes contributing to MS.

Therefore, the aims of the studies described in this thesis were to

1) identify the presence of TG2 and the cell types expressing
it in post-mortem material of MS patients and of relevant MS animal models, i.e. experimental autoimmune encephalomyelitis (EAE) in rats and mice.

2) determine the contribution of TG2 to EAE symptoms and pathology and its potential as a druggable target.

The first aim is addressed in chapters 2, 3 and 4. At first, we studied whether TG2 was present in post-mortem brain tissue from MS patients in a pattern distinct from that of healthy control subjects (chapter 2). As MHC-II positive cells showed TG2 expression in white matter MS lesions, we followed this up with a more extensive characterization of TG2 expressing cells present in inflammatory active white matter MS lesions (chapter 3). In addition, the presence of TG2 in infiltrating leukocytes (i.e. monocytes), was identified in the MS models chronic-relapsing EAE in dark agouti rats (chapter 2) and monophasic EAE in C57BL/6 mice (chapter 4). Furthermore, in chapter 4, the behavior of crawling monocytes and their interaction with the spinal cord endothelium was studied *in vivo* in EAE mice. To this end, we visualized fluorescent monocytes in transgenic CX3CR1$^{gfp/gfp}$ mice with 2-photon microscopy at various time-points during EAE disease and analyzed their behavior and movement patterns.

The second aim of this thesis, the contribution of TG2 to EAE symptoms and pathology and its potential as a druggable target, is the focus of chapters 2 and 5. The functional role of TG2 in rat chronic-relapsing EAE and mouse monophasic EAE was investigated using a pharmacological approach with a TG2 activity inhibitor known as KCC009 and TG2 knock-out animals, respectively. The consequences of these interventions on motor symptoms and spinal cord pathology was assessed. Furthermore, using an *in vitro* blood-brain-barrier model, the role of TG2 in adhesion onto and migration of rat monocytes over endothelial cells was elucidated further (chapter 2). Also, novel TG2 inhibitors that have recently entered the research field were the subject of research in chapter 5. Two small molecule TG2 activity inhibitors, BJJF078 and ERW1041E, were first characterized *in vitro* on their selectivity and potency. Subsequently, their effect on the clinical and pathological outcomes of the monophasic EAE model in C57BL/6 mice was evaluated.

Finally, in chapter 6, the results described in the other chapters of this thesis are summarized and discussed in a broader perspective and suggestions for further research are provided



Chapter 2

TISSUE TRANSGLUTAMINASE CONTRIBUTES TO EXPERIMENTAL MULTIPLE SCLEROSIS PATHOGENESIS AND CLINICAL OUTCOME BY PROMOTING MACROPHAGE MIGRATION

Brain Behav Immun. 2015 Nov;50:141-154

ABSTRACT

Multiple sclerosis is a serious neurological disorder, resulting in e.g., sensory, motor and cognitive deficits. A critical pathological aspect of multiple sclerosis (MS) is the influx of immunomodulatory cells into the central nervous system (CNS). Identification of key players that regulate cellular trafficking into the CNS may lead to the development of more selective treatment to halt this process. The multifunctional enzyme tissue Transglutaminase (TG2) can participate in various inflammation-related processes and is known to be expressed in the CNS. In the present study, we question whether TG2 activity contributes to the pathogenesis of experimental MS, and could be a novel therapeutic target.

In human post-mortem material, we showed the appearance of TG2 immunoreactivity in leukocytes in MS lesions and particular in macrophages in rat chronic-relapsing experimental autoimmune encephalomyelitis (cr-EAE), an experimental MS model. Clinical deficits as observed in mouse EAE were reduced in TG2 knock-out mice compared to littermate wild-type mice, supporting the role of TG2 in EAE pathogenesis. To establish if the enzyme TG2 represents an attractive therapeutic target, cr-EAE rats were treated with TG2 activity inhibitors during ongoing disease. Reduction of TG2 activity in cr-EAE animals dramatically attenuated clinical deficits and demyelination. The mechanism underlying these beneficial effects pointed toward a reduction in macrophage migration into the CNS due to attenuated cytoskeletal flexibility and RhoA GTPase activity. Moreover, iNOS and TNFα levels were selectively reduced in the CNS of cr-EAE rats treated with a TG2 activity inhibitor, whereas other relevant inflammatory mediators were not affected in CNS or spleen by reducing TG2 activity. We conclude that modulating TG2 activity opens new avenues for therapeutic intervention in MS which does not affect peripheral levels of inflammatory mediators.

Miriam E. van Strien[a], Navina L. Chrobok[a2], Helga E. de Vries[a2], John G.J.M. Bol[a], John J.P. Breve[a], Susanne M.P. van der Pol[b], Gijs Kooij[b], Jaap D. van Buul[c], Marcela Karpuj[d], Lawrence Steinman[e], Micha M. Wilhelmus[a], Claudia Sestito[a], Benjamin Drukarch[a] and Anne-Marie Van Dam[a]

[2]authors contributed equally to the study

VU University Medical Center, Neuroscience Campus Amsterdam, [a]Dept. Anatomy & Neurosciences, [b]Dept. Molecular Cell Biology and Immunology, Amsterdam; [c]Dept. Molecular Cell Biology, Sanquin Research and Landsteiner Laboratory, Academic Medical Center, University of Amsterdam, Amsterdam, The Netherlands, [d]BioA2z. Inc, San Francisco, CA, USA; [e]Beckman Center for Molecular Medicine, Stanford University, Stanford, USA

INTRODUCTION

Multiple sclerosis (MS) is a chronic neuro-inflammatory and neurodegenerative disease, affecting mostly young adults in the prime of their lives. Clinically, MS is characterized by major motor and sensory deficits, and in addition, patients develop cognitive dysfunction, e.g., memory impairment, which has a dramatic impact on their quality of life [159]. With regard to the pathogenesis of MS, the influx of leukocytes into the central nervous system (CNS) has been focused upon as a main driver of the disease, resulting in inflammation, demyelination and axonal damage [160, 161]. During MS, the entry of leukocytes into the CNS across the blood-brain barrier is stimulated by chemokines interacting with their corresponding receptors [162] and by leukocyte integrins (e.g., α4β1) binding to endothelial adhesion molecules (e.g., VCAM-I and ICAM-I) [163] resulting in firm adhesion of immunomodulatory cells onto the vascular endothelium [164]. Following endothelial transmigration, cells traverse the endothelial basement membrane and glia limitans and migrate into the brain parenchyma, a process that is facilitated by local tissue destruction via activation of MMPs [165]. Infiltrated, activated leukocytes are a key source of inflammatory mediators that stimulate myelin phagocytosis resulting in subsequent demyelination [166, 167]. Current therapies for MS are predominantly immunosuppressive or immunomodulatory but may lead to severe side effects and can disturb the immune balance [168-170], emphasizing the need for alternative targets to treat MS.

Tissue Transglutaminase or Transglutaminase type 2 (TG2, EC:2.3.2.13) is a 78-kD multifunctional enzyme belonging to a multigene family of protein cross-linking enzymes [76], is localized in the cytoplasm, on the cell surface and in the extracellular matrix (ECM), where it can act in a Ca2+-dependent or Ca2+-independent way [76, 85, 105]. Of the Transglutaminase family, TG1, TG2, and TG3 are expressed in the healthy human CNS [171], of which TG2 is almost ubiquitously present. TG2 plays a role in the pathogenesis of various neurodegenerative disorders (reviewed in [172]). More recently, it has been shown that TG2 activity is enhanced during inflammation [113, 173, 174]. In addition, TG2 acts as a co-receptor for β1- and β3-integrin subunits thereby contributing to cell adhesion [122], TG2 regulates MMP2 and MMP9 activity [138] and is involved in cytoskeletal remodeling [175] pointing to a role in cell migration. Since TG2 is known to be expressed in the CNS and can have effects on immune cells, we question whether TG2 activity contributes to the pathogenesis of experimental MS, and could be an interesting novel therapeutic target.

MATERIALS AND METHODS

Human brain material

Cortical brain tissue from 5 patients with clinically diagnosed and neuropathologically confirmed MS was obtained at autopsy and immediately frozen in liquid nitrogen. Five subjects without neurological disease acted as control subjects. White matter MS tissue

samples containing lesions were selected using postmortem magnetic resonance imaging as published [176, 177]. Additional relevant information was retrieved from the medical records and summarized in Table 1. All patients and control subjects had given informed consent for autopsy and use of their brain tissue for research purposes.

Table 1: Summary of MS patient details

Age	Gender	Type of MS lesion	Disease duration (years)	PMD (hours)	Cause of death
78	female	Control	NR	6:30	decompensatio cordis
82	male	Control	NR	12:00	heart failure
81	male	Control	NR	6:40	Euthanasia
52	female	Control	NR	6:00	Leiomyosarcoma
88	female	Control	NR	6:15	Aging
52	female	Active	13	8:25	respiratory insufficiency/pneumonia
53	female	Active	27	8:30	Euthanasia
70	male	Active	Unknown	6:25	Unknown
69	female	Active	26	13:20	viral infection
76	female	Active	53	14:15	respiratory insufficiency/pneumonia

MS, multiple sclerosis; NR, not relevant; PMD, post-mortem delay

Lesion classification

Classification of white matter lesions was based on standard histopathological stainings for myelin-specific proteolipid protein (PLP) and inflammatory cells (LN3: anti-major histocompatibility complex class II) as described before [178-180]. Active lesions were characterized by abundant phagocytic, perivascular and parenchymal macrophage infiltration throughout the lesion area.

Immunohistochemistry on human material

Cryosections (6 µm) were air-dried and fixed in 4% paraformaldehyde in 0.1 M phosphate buffer (pH 7.6) for 10 min (min) (TG2). Subsequently, sections were preincubated for 15 min with 2% normal donkey serum in Tris-buffered saline (TBS) containing 0.5% Triton-X100. Thereafter, sections were incubated for 60 min at room temperature (RT) with goat anti TG1 (Santa Cruz Biotechnology Inc., Santa Cruz, CA USA, 1:100), goat anti TG2 (Upstate, Charlottesville, USA; 1:3000) or mouse anti TG3 (Santa Cruz Biotechnology Inc., 1:200). After washes in TBS, the sections were incubated for 2 h (h) at RT with biotinylated donkey anti goat IgG or biotinylated donkey anti mouse IgG (Jackson ImmunoResearch, Suffolk, UK; 1:400). Following washes in TBS, the sections were incubated for 60 min at RT with ABC-HRP complex (Vectastain; Vector Laboratories, Burlingame, USA; 1:400).

Peroxidase activity was visualized by 3,3-diaminobenzidine (DAB, Sigma–Aldrich, St. Louis, USA). Finally, the sections were counterstained with hematoxylin. All antibodies were diluted in TBS containing 0.5% Triton-X100 and 2% normal donkey serum. Omittance of the primary antibodies served as a negative control.

The specificity of the anti TG2 antibody was determined by pre-adsorption of the anti TG2 antibody derived from Upstate with at least 100-fold (w/w) excess of guinea pig TG2 (Sigma–Aldrich). After 6 h of pre-adsorption, adjacent tissue sections were incubated with the pre-adsorbed or non-adsorbed antibodies and further treated as regular immunohistochemical staining.

Quantification of the number of TG2 positive infiltrating cells in active MS lesions was performed manually by unbiased counting of TG2 positive cells localized in the perivascular space or the parenchyma localized within 2 mm of a blood vessel. Seventeen lesion areas from five MS patients were included. Blood vessel wall and luminal staining were excluded from the examined area. In control subjects, no TG2 positive infiltrating cells were observed.

Immunofluorescent double labeling on human MS material

Co-localization of TG2 with MHC class-II positive cells was determined by co-incubation of 4% paraformaldehyde-fixed cryosections with a monoclonal antibody to HLA-DR (LN3, Labvision Fremont, CA, USA, 1:100) and with goat anti TG2 (Upstate, 1:4000). Subsequently, sections were co-incubated with Alexa Fluor (AF) 488 labeled donkey anti mouse IgG's and AF594 labeled donkey anti goat IgG's (Invitrogen, Carlsbad, USA; 1:400). In addition, co-localization of TG2 with T cells was performed on acetone-fixed cryosections by incubation with goat anti TG2 (1:1000) and rabbit anti CD3 (DAKO, Glostrup Denmark; 1:200). Subsequently, sections were co-incubated with biotinylated donkey anti-goat IgG's and AF488 labeled donkey anti rabbit IgGs. Finally, the sections were incubated with streptavidin-labeled AF594 (Molecular Probes; 1:400). Incubation procedures were performed as described above, and sections were mounted with an anti-fading medium containing DABCO (Fluka). The presence of fluorescent double immunolabeling was identified by confocal laser scanning microscopy (Leica TCS-SP2-AOBS; Leica Microsystems, Wetzlar, Germany).

***In vivo* experiments**

Chronic-relapsing experimental autoimmune encephalomyelitis (cr-EAE)

Adult male dark agouti rats (Harlan, Horst, The Netherlands) weighing 240–290 g, were anesthetized with isoflurane and immunized intradermally in the dorsal tail with 75 µg of the N-terminal sequence of recombinant rat myelin oligodendrocyte glycoprotein (rrMOG$_{1–125}$) emulsified in incomplete Freund's adjuvant (IFA; Difco, Detroit, MI, USA) with 0.01 M NaAc (pH 3.0). Control rats received IFA + NaAc only. Rats were weighed and examined daily for neurological symptoms that were scored on the following scale: 0, no symptoms; 0.5, partial loss of tail tone; 1, complete tail atony; 2, paresis, partial hind limb

paralysis; 3, complete paralysis of the hind limbs and/or lower part of the body; 4, moribund or dead.

TG2 expression during the course of rat cr-EAE

cr-EAE rats (n = 10/group) were sacrificed at different phases of disease, i.e., during the first phase of neurological symptoms (day 12–13 post immunization (p.i.)), remission (∼day 15 p.i.) and relapse (∼day 22 p.i.) to study TG2 expression at the mRNA and protein level.

KCC009 treatment in cr-EAE rats

Thus far, a little number of small peptidergic, irreversible inhibitors of TG2 activity have been used in an *in vivo* setting. Of these, KCC009 [181], has been shown to be effective *in vivo* when given intraperitoneally to mice to suppress TG2 activity. KCC009 significantly suppressed TG2 activity within 15 min, whereas enzyme activity fully recovers after 24 h [182]. The characteristics and positive *in vivo* effects of the compound determined our choice for KCC009 to perform our therapeutic experiments. To ensure the continuous reduction of TG2 activity, cr-EAE animals were injected i.p. once daily with KCC009 (40 mg/kg, kind gift from Alvine Pharmaceuticals, San Carlos, USA) in PBS/DMSO (1:1) (n = 8/group). The animals were treated from initial clinical signs (day 11), from the abundant presence of clinical signs during the first phase of disease (day 13) or the remission (day 17) of cr-EAE onwards. Control animals were injected i.p. daily with vehicle (PBS/DMSO 1:1) from initial clinical symptoms (day 11) onwards (n = 8). Animals were sacrificed by decapitation under isoflurane anesthesia when vehicle-treated cr-EAE rats reached peak clinical symptoms during the relapse (day 28).

Cystamine treatment in cr-EAE rats

For comparison with KCC009, we used cystamine, a traditionally used TG activity inhibitor, in the same rat experimental MS model. In addition to inhibiting TG activity, cystamine has been described to act as an antioxidant and to inhibit caspase-3 [183, 184]. Cr-EAE rats were injected i.p. daily with 75 mg/kg cystamine (Sigma–Aldrich), a competitive substrate for TG activity, in PBS (n = 12) or with PBS only (n = 12, vehicle) starting from initial clinical symptoms (day 9) onwards. Animals were sacrificed when vehicle-treated cr-EAE animals reached the remission phase (day 16).

EAE in TG2 knock-out mice

To determine, as proof of principle, whether TG2 is of importance for the development of EAE, we performed an experiment in TG2−/− and wildtype mice. To this end, 8–10 week old C57Bl/6 female $TG2^{-/-}$ (n = 10) [185] that were backcrossed for at least 12 generations, and littermate female $TG2^{+/+}$ genotype control (n = 14) mice were kept in individually ventilated cages with food and water accessible ad libitum. All mice were immunized

subcutaneously with 100 µg recombinant myelin oligodendrocyte glycoprotein peptide 35–55 ($MOG_{35–55}$; Cambridge Research Biochemicals, Billingham, UK) in an emulsion mixed (volume ratio 1:1) with Complete Freund's Adjuvant (CFA; Difco Laboratories) to which 600 µg of heat-killed Mycobacterium tuberculosis H37Ra (MBT; Difco) was added. All animals were additionally injected i.p. with 200 ng pertussis toxin (PTX) derived from *Bordetella pertussis* (Sigma, Zwijndrecht, The Netherlands) in 200 µl saline at the time of, and 48 h after immunization [186]. On day 15, all mice were sacrificed by decapitation under isoflurane anesthesia.

Monodansylcadaverine treatment in EAE mice

In addition to the rat cr-EAE model, we performed an experiment in a mouse model using a therapeutic approach to inhibit TG activity. To this end, 6–8 weeks old female PLSJL/J mice (Jackson labs, Bar Harbor, USA, n = 16) were anesthetized with isoflurane and immunized subcutaneously in the hind legs and tail with 200 µg of recombinant proteolipid protein peptide 139–151 (PLP139–151), emulsified in complete Freund's adjuvant (CFA; Difco Laboratories, Detroit, MI, USA). PTX (Sigma–Aldrich, 0.2 µg/animal) was injected i.p. on days 0 and 3 after immunization. Monodansylcadaverine (MDC, Sigma–Aldrich, 17 mg/animal), a competitive substrate for TG activity, in PBS (n = 8) or PBS only (n = 8, vehicle) was injected i.p. on day 10 when initial clinical symptoms were present. All animals were sacrificed on day 15 when vehicle-treated EAE mice reached maximal clinical score. Additionally to inhibiting TG activity, MDC has been described to affect other enzymes, e.g., phosphatidylcholine synthetase, 17-ketosteroid reductase or calmodulin activation of cyclic nucleotide phosphodiesterase [187]. Animal experiments as described above were approved by the local animal ethical committees.

Immunohistochemistry on rat material

Fresh frozen rat spinal cord sections were fixed for 10 min with acetone, washed in TBS, blocked in 5% milk in TBS with 0.5% Triton X-100 (TBS-T) and 0.03% H_2O_2 and incubated with the first antibody overnight at 4 °C. To detect TG2, a mouse monoclonal antibody raised against guinea pig TG2 was used (Ab2, Labvision, 1:1000). Mouse monoclonal antibodies raised against MHC-II (OX6, Serotec Ltd., 1:1000) or to CD68 (ED1, Serotec Ltd., 1:500) was used to detect macrophage-like cells. To detect T cells, a mouse-anti CD3 antibody (kind gift from Dept. Molecular Cell Biology, VU University Medical Center, Amsterdam, 1:100) was used. For myelin staining, a rat-anti-myelin basic protein (MBP) antibody was used (Chemicon, 1:250).

Subsequently, sections were washed in TBS and incubated for 2 h at RT with appropriate secondary biotinylated IgGs (Jackson ImmunoResearch, 1:400), followed by washes in TBS and incubation for 1 h at RT with HRP-coupled ABC complex (Vector Laboratories, 1:400). After washes in TBS and Tris–HCl, immunoreactivity was visualized using 0.5 mg/ml of DAB (Sigma–Aldrich) in Tris–HCl. Demyelination in the rat spinal cord was assessed using Luxol Fast Blue (LFB) staining. Sections were stained in LFB at 56 °C for 16 h and counterstained with cresyl violet solution for 30–40 s. All sections were

examined microscopically (Vanox-T, Olympus). The white matter area size containing MHC class II (activated particularly infiltrated monocytes) or CD-3 (T cells) positive cells was quantified using a grid in which the positive area was manually counted and related to the total white matter area of the spinal cord examined (AnalySIS software; Olympus). Blood vessel wall and luminal staining were also manually determined using the grid and excluded from the examined area. Per treatment group, 4 areas in the cervical and thoracic part of the spinal cord per section, 2 sections per animal in 4 representative rats per group were examined.

Immunofluorescent double labeling on rat cr-EAE material

For immunofluorescent double stainings, fresh frozen rat spinal cord and spleen sections were fixed with acetone (OX6 or CD3 and laminin) or 4% paraformaldehyde (Iba1 and TG2) for 20 min, washed in TBS, blocked in 5% milk in TBS with 0.5% Triton X-100 (TBS-T) and 0.03% H_2O_2 and incubated with the first antibodies overnight at 4 °C. Rabbit polyclonal anti laminin (Cappel, MP Biomedicals, Illkirch, France, 1:250) and mouse monoclonal OX6 (Serotec Ltd., 1:1,000) or mouse monoclonal CD3, a pan-marker for T cells (gift from Dept. Molecular Cell Biology and Immunology, VU Medical Center, Amsterdam, The Netherlands 1:100) or mouse monoclonal anti TG2 (Ab2, Labvision, 1:1000) and a goat antibody to Iba1 (Abcam Inc., Cambridge, MA, USA, 1:1000), a specific marker for microglia/monocytes [188], were used followed by appropriate fluorescent secondary antibodies to detect laminin or Iba-1 (Alexa fluor-488, Invitrogen, 1:400) and OX6, CD3 or TG2 (Alexa fluor-594, Invitrogen, 1:400) immunoreactivity. Sections were embedded in Vectashield mounting medium (Vector Laboratories) and examined on a Leica confocal laser scanning microscope (Leica).

Semi-quantitative RT-PCR

To determine the mRNA transcript levels in cr-EAE animals, spinal cord and spleen tissues were homogenized in Trizol reagent (Invitrogen, Carlsbad, CA, USA). Total RNA was isolated and of 1 µg cDNA was synthesized using the Reverse Transcription System (Promega, Madison, WI, USA) with oligo-dT primers and AMV enzyme according to the manufacturer's instructions. For semi-quantitative RT-PCR, the SYBR Green PCR Core reagents kit (Applied Biosystems, Foster City, CA, USA) was used. Amplification of cDNA was performed in MicroAmp Optical 96-well Reaction Plates (Applied Biosystems) on an ABI PRISM 7700 Sequence Detection System (Applied Biosystems). The reaction mixture (20 µl) was composed of 1× SYBR Green buffer, 3 mM $MgCl_2$, 875 µM dNTP mix with dUTP, 0.3 U AmpliTaq gold, 0.12 U Amperase UNG, 12.5 ng cDNA and 15 pmol of each primer (Supplementary materials: Table 1). The reaction conditions were an initial 2 min at 50 °C, followed by 10 min at 95 °C and 40 cycles of 15 s at 95 °C and 1 min at 59 °C. The mRNA expression levels were quantified relative to the level of the housekeeping gene glyceraldehyde-3-phosphate-dehydrogenase (GAPDH) using the following calculation: 2−(Threshold cycle of target mRNA − Threshold cycle of GAPDH) x 100.

TG2 ELISA

TG2 protein levels were measured in tissue homogenates using an enzyme-linked immunosorbent assay (ELISA) specific for TG2 as described previously [189]. Briefly, tissue samples were homogenized in ice-cold lysis buffer containing 50 mM Tris/HCl pH 7.5, 150 mM NaCl, 1 mM EDTA, 1 mM DTT, 100 µM PMSF, 10 µg/ml leupeptin, 10 µg/ml pepstatin and 10 µg/ml aprotinin. Homogenates were cleared by centrifugation (14,000 rpm for 30 min at 4 °C) and protein concentrations of supernatants were determined by the BCA method (Pierce Biotechnology, Perbio Science, Etten-Leur, NL). Of each sample, 10 g of protein was loaded in the assay.

Cell isolation, tissue homogenization and TG activity assay

cr-EAE animals were injected i.p. once daily, for 2 days (day 11–12 of disease), with KCC009 (40 mg/kg, Alvine Pharmaceuticals) in PBS/DMSO (1:1) or with vehicle (PBS/DMSO 1:1) from initial clinical symptoms (day 11) onwards (n = 6 per group). Two hours after the second i.p. injection (day 12), animals were sacrificed and lymph nodes, spleen and half of the spinal cords were collected for TG activity measurements. Furthermore, the other halves of the spinal cords were used to perform immunofluorescent stainings for monocytes and T cells. Blood was collected for T-cell and monocyte isolation. Peripheral blood mononuclear cells (PBMCs) were isolated as the interphase on a Ficoll-Paque (Amersham Pharmacia Biotech, Uppsala, Sweden) gradient as described [190]. The population consisted of >90% viable monocytes (ED9-positive cells as determined by FACS analysis) and <10% lymphocytes. T cells were collected by means of negative selection by incubating PBMCs fractions (containing B and T cells) with Dynal beads coated with anti-CD20 (OX-33) to remove B cells, resulting in a yield of about 1 × 106 T cells per rat. To measure TG activity in cell extracts and tissue homogenates, T cells, monocytes and tissue samples (spinal cord, spleen and cervical lymph nodes) were homogenized in ice-cold lysis buffer as used for TG2 ELISA. The activity was measured by using the TG Covtest TCMA (Transglutaminase Colorimetric Microassay; Covalab, Villeurbanne, France) following the manufacturer's protocol [191]. Equal cell numbers of T cells and monocytes (1 × 106 cells) were used in the assay.

Western blot

Tissue samples or NR8383 cells (rat alveolar macrophages, ATCC), treated with cytokines (50 ng/ml IL-1β + 50 ng/ml IFNγ) for 48 h and subsequently treated for 1 h with vehicle or 0.5 mM KCC009, were homogenized in ice-cold lysis buffer as used for TG2 ELISA.

Of each sample, 10 µg of protein was subjected to 10% SDS–polyacrylamide gel electrophoresis (SDS–PAGE) and transferred to a polyvinylidene difluoride (PVDF) membrane (Invitrogen). Membranes were incubated with primary antibodies: rabbit anti MMP9 (Serotec Ltd., 1:2000), rabbit anti Integrin-β1 (Chemicon, Millipore, Amsterdam, The Netherlands, 1:1000), mouse anti TNFα (BD Biosciences Pharmingen, San Diego, CA, USA, 1:200), rabbit anti iNOS (Santa Cruz, 1:200) and mouse anti FXIIIa (Abcam, 1:250)

overnight. For subsequent antigen detection, blots were incubated for 2 h with corresponding goat anti-mouse or goat anti-rabbit Immunoglobulins/HRP (Dako, Glostrup, Denmark, 1:10,000). Bands were visualized using the enhanced chemiluminescence (ECL) detection system SuperSignal West Dura (Pierce Biotechnology) and a Chemidoc image capture system (Bio-Rad, Veenendaal, The Netherlands). The ignal intensity of the bands was semi-quantified using Quantity One software (Bio-Rad).

Macrophage migration assay

Macrophage migration across monolayers of brain endothelial cells (EC) was assayed as described before [192]. NR8383 cells (6 × 105 cells/well) were added to 96-well plates containing cytokine-stimulated (50 ng/ml IL-1β + 50 ng/ml IFNγ for 48 h) brain EC monolayers (GP8 cells). Macrophages or ECs were preincubated with 0.5 mM KCC009 or 1% DMSO (vehicle) for 1 h before starting the migration assay. Macrophages were allowed to adhere and migrate for a 4 h period. To monitor macrophage migration, co-cultures were placed in an inverted phase-contrast microscope (Nikon Eclipse TE300) housed in a temperature-controlled (37 °C), 5% CO2 gassed chamber. A microscopic field (220 µm × 220 µm) was randomly selected and recorded for 9 min at 50 times normal speed by using a color video 3CCD camera (Sony, with a CMAD2). Migrated macrophages (phase-dark) could be readily distinguished from those remaining on the cell surface by their highly refractive (phase-bright) morphology. The level of migration was calculated as the percentage of migrated macrophages of the total macrophages within the microscopic field.

Cellular F-actin staining

The effect of KCC009 on the cytoskeletal organization of macrophages was visualized by the detection of F-actin using rhodamine phalloidin as described previously [134]. In short, NR8383 cells were plated on fibronectin-coated 8-well chamber slides (Labtek, Nalgene Nunc International) and left o/n at 37 °C in the presence of 10% FCS. The following day, the cells were pre-incubated with 0.5 mM KCC009 or 1% DMSO (control) for 1 h and subsequently fixed for 15 min with 4% paraformaldehyde, permeabilized with 0.1% Triton X-100 (Sigma–Aldrich) in PBS, blocked with 10% FCS in PBS, and stained for 1 h with rhodamine phalloidin in PBS (Molecular Probes, Invitrogen, 1:300). Slides were washed and embedded with Vectashield mounting medium (Vector Laboratories). Images were taken using a Leica Confocal microscope.

Rho activity assay

To determine the effect of KCC009 on RhoA activity, 5 × 106 NR8383 cells were treated with IFNγ and IL-1β (50 ng/ml each) for 48 h followed by a 1 h incubation with 0.5 mM KCC009 or 1% DMSO at 37 °C. Thereafter, cells were lysed with lysis buffer (50 mM Tris, pH 7.6, 500 mM NaCl, 0.1% SDS, 0.5% deoxycholate (DOC), 1% Triton X-100, 10 mM $MgCl_2$, 100 µM PMSF, 10 µg/ml leupeptin, 10 µg/ml pepstatin and 10 µg/ml aprotinin). Of the

cleared lysates, 20 µl was stored to determine the total amount of RhoA (total cell lysate). Remaining protein lysates were incubated with 60 µg bacterially produced GST-RBD (Rho Binding Domain of Rhotekin) [193] and bound to glutathione-agarose beads (Sigma–Aldrich). Beads were washed 4 times with lysis buffer, bound proteins were eluted in 30 µl SDS sample buffer and analyzed in parallel with 10 µl of the total cell lysate subjected to 15% SDS PAGE gel electrophoresis. Following blotting of the gel onto a PVDF membrane, the active form of RhoA and total RhoA could be detected with a mouse monoclonal antibody (Santa Cruz Biotechnology, Inc., 1:250).

Cell surface biotinylation and immunoprecipitation

To determine TG2 expression on the cell surface, NR8383 cells were incubated with or without cytokines (IFNγ and IL-1β, 50 ng/ml each) for 48 h and subsequently treated for 1 h with 0.5 mM KCC009 or vehicle. After washes with PBS to eliminate possible dead cells, cell surface proteins were biotinylated by incubating the macrophages for 30 min with 2 mg/ml Sulfo-NHS-LC-biotin (Pierce Biotechnology) in PBS at 4 °C. Subsequently, the cells were washed 3 times with 100 mM glycine in PBS (pH 8.0) and once with PBS at 4 °C and lysed in ice-cold lysis buffer as described for Western blot. Cell lysates were cleared by centrifugation (14,000 rpm for 30 min at 4 °C) and 100 µg of total cell protein was taken for each immunoprecipitation. Cell lysates were incubated with 50 µl 50% Neutravidin agarose beads (Pierce Biotechnology, pre-incubated for 30 min with TBS/10% BSA) for 1 h at RT. Beads were washed 3 times with lysis buffer and then with PBS. Beads were collected in 6× sample buffer containing 50 mM DTT and boiled for 10 min. Samples were centrifuged for 5 min at 12,000 rpm at 4 °C and levels of surface TG2 were detected using gel-electrophoresis and western blot as described above. A non-biotinylated cell sample was also run to ensure that the pulldown was specific only for cell surface biotinylated TG2 (Supplementary Fig. 3).

Cell viability measurements

The effect of KCC009 treatment on cell viability was determined by propidium iodide (PI) exclusion assay. Only PI that has been intercalated into DNA/RNA will result in an enhanced fluorescent signal indicative for cell death. NR8383 cells were plated in a 96-well plate (20,000 cells/well) and allowed to adhere for 24 h in serum-free medium. Medium was replaced with PBS containing 0.5 mM $MgCl_2$, 1.2 mM CaCl2, 0.1% glucose, 40 µg/ml PI (Sigma) and 0.5 mM KCC009 in 0.2% DMSO or 0.2% DMSO only (vehicle). During an incubation period of 16 h at 37 °C, PI fluorescence was measured at 30 min intervals, using a Fluostar OPTIMA microplate reader with an excitation wavelength of 544 nm and an emission of 612 nm. The average slope/min was measured per 30 min interval and averaged to a slope/min per 24 h (F-average). After 24 h, 160 µM digitonin was added for 20 min to permeabilize all cells and fluorescence measurements were performed to obtain a maximal fluorescent signal (Fmax). Percentage viability was calculated as 100 − (F-average/Fmax) × 100.

Statistical analysis

Where appropriate, data were analyzed by one-way or two-way ANOVA, followed by a t-test for independent measurements (Fisher's LSD test). For the area under the curve (AUC), a one-way ANOVA was performed followed by Tukey's multiple comparison test. Error bars represent standard error of the mean (S.E.M.). P-values represent *$p < 0.05$; **$p < 0.001$; ***$p < 0.0001$. The statistical evaluation was carried out by using the NCSS 2007 statistical program (NCSS, East Kaysville, Utah, USA).

RESULTS

TG immunoreactivity in human MS lesions

The observed presence of TG2 immunoreactivity in endothelial cells (Fig. 1A and B) is in line with previous studies [194, 195]. However, only in active MS lesions, TG2 positive cells appeared within parenchymal tissue located near blood vessels (Fig. 1B (arrowheads)), but most often in the perivascular space (Fig. 1B and C (arrow in B)). Pre-adsorption of the anti-TG2 antibody with recombinant TG2 abolished in TG2 immunoreactivity in these cells (Fig. 1D), indicating the specificity of the staining. Quantification of the number of TG2 positive cells in seventeen active MS lesion areas resulted in a mean of 5 TG2 positive cells per counted area (Fig. 1E). By co-localization studies, TG2 positive cells could largely be identified as MHC class II positive cells (Fig. 1F), which based on their rounded morphology and localization, likely reflected macrophages and not T cells (Fig. 1G). Although the number of B cells is rather limited in post-mortem MS tissue [16, 17] in comparison to macrophages, we cannot exclude TG2 being present in B cells.

Additionally, TG1 and TG3 immunoreactivity were studied in active MS lesions and control subjects. In our hands, TG1 immunoreactivity was not observed in either control (Fig. 1H) or MS tissue (Fig. 1I), whereas this antibody has shown TG1 in neurofibrillary tangles in brain material from Alzheimer patients [196]. TG3 immunoreactivity, like TG2, was located in blood vessels (Fig. 1J and K). Moreover, in white matter of control subjects (Fig. 1J) as well as in active MS lesions (Fig. 1K), TG3 immunopositive cells were found. However, the location of these cells was not specifically associated with lesions and no clear difference was seen in the amount of TG3 positive cells between control and MS tissue.

TG2 mRNA and protein levels are enhanced during chronic relapsing EAE in rats

TG2 expression was determined in the spinal cord of rats at different stages of cr-EAE, a model for relapsing-remitting MS (Fig. 2A). Notably, during the course of cr-EAE, TG2 mRNA and protein levels in the spinal cord increased to 2–3 times the levels present in control animals (Fig. 2B and C). The expression levels of some other members of the Transglutaminase family, including FXIIIa, TG1 and TG3 were low compared to TG2 and, more importantly, remained unaltered during the course of cr-EAE (Fig. 2B).

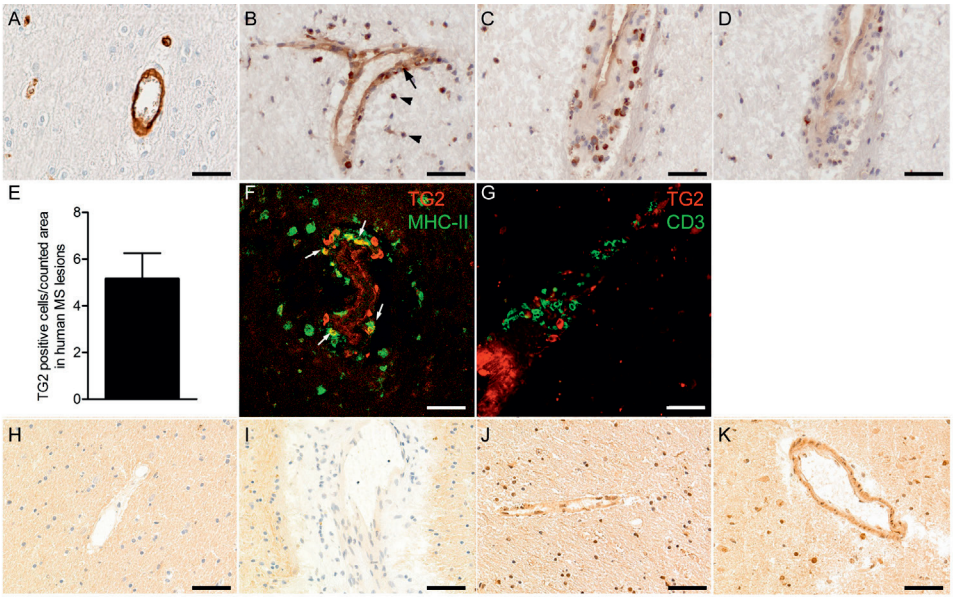


Figure 1. Expression of TG2, TG1 and TG3 in human active subcortical MS lesions compared to control subcortical white matter. (A) TG2 immunoreactivity is only present in blood vessels in subcortical white matter of a control subject. (B and C) TG2 immunoreactivity in perivascular space-located cells (arrow) and in tissue parenchyma (arrowhead) in MS lesions, which is almost absent (D) after pre-adsorption of the anti-TG2 antiserum with guinea pig TG2. (E) Quantification of TG2 positive infiltrating cells in MS lesion areas. (F) TG2 positive cells (red) can partly be identified as (G) MHC class II expressing cells (green) and thus likely represent infiltrated, activated monocytes (arrows in F). TG1 immunoreactivity is absent in subcortical white matter of (H) a control subject and in (I) an active MS lesion. TG3 immunoreactivity seems equally present in subcortical white matter of (J) a control subject and in (K) an active MS lesion. Scale bars indicate 50 µm in A–D and H–K, and 25 µm in F and G.

In IFA immunized (control) animals, TG2 immunoreactivity was observed in blood vessels only (Fig. 2D). In contrast, during the different stages of cr-EAE, TG2 immunoreactivity was, in addition to blood vessels, localized to perivascular cells in the rat spinal cord (Fig. 2D). Most of these TG2 immunoreactive cells were identified as Iba1 positive cells and morphologically appeared as amoeboid macrophages (Fig. 2E).

TG2 activity contributes to the clinical symptoms of EAE

To reveal that TG2 participates in the pathogenesis of EAE, $TG2^{-/-}$ mice and wild-type littermates were immunized with $MOG_{35–55}$. The induction of EAE in $TG2^{-/-}$ mice resulted in a significantly reduced mean clinical score as compared to their wild-type littermates (Suppl. Fig. 1A).

To determine whether pharmacological modulation of TG2 activity affects the disease process, cr-EAE rats were treated with KCC009, an irreversible inhibitor of TG2 activity. Daily treatment of cr-EAE rats with KCC009 did not result in additional weight loss or gross anatomical abnormalities in the gut (data not shown). Reduction of TG2 activity from the onset of clinical symptoms (Fig. 3A, arrow 1) or later stages of ongoing disease

(Fig. 3A, arrows 2 and 3) caused an immediate and marked attenuation in clinical deficits. Importantly, the administration of KCC009 from the first peak of clinical symptoms onwards (Fig. 3A, arrow 2) prevented relapsing disease. Of interest to note is that reduction of TG2 activity from early symptoms onwards did not alter TG2 protein levels at day 28 in spinal cord or liver (Fig. 3B), but it clearly reduced TG activity in the spinal cord, leaving TG activity in liver unaffected (Fig. 3C).

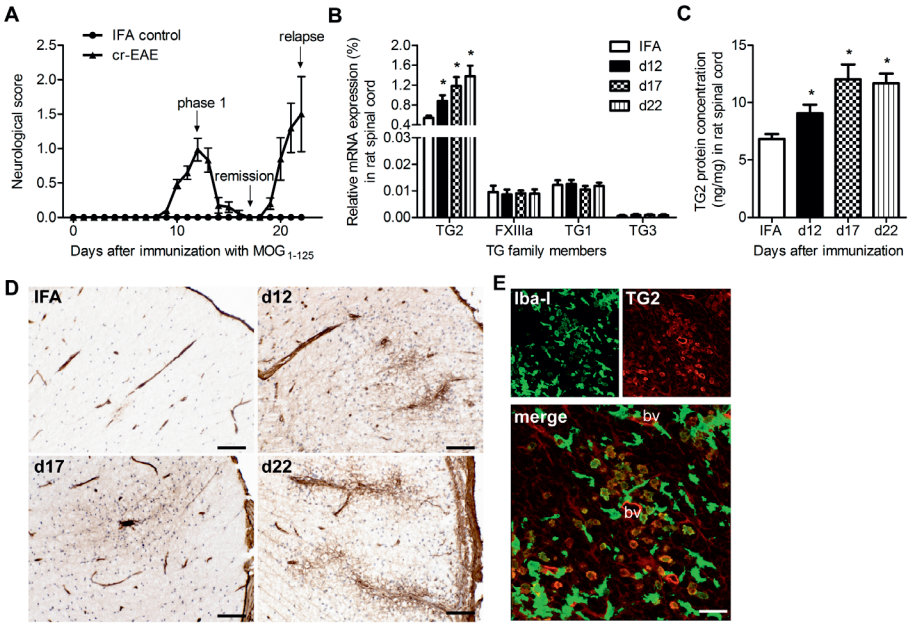


Figure 2. Enhanced TG2 expression in rat spinal cord during cr-EAE compared to IFA immunized control rats. (A) Clinical course of cr-EAE compared to IFA immunized rats. (B) mRNA levels of TG isoforms TG2, FXIIIa, TG1 and TG3 were measured with quantitative PCR and (C) TG2 protein levels measured with ELISA in the spinal cord during the different clinical phases of cr-EAE compared to IFA immunized rats. * $p < 0.05$ vs. IFA control. (D) TG2 immunoreactivity in the cervical spinal cord during phase 1 (d12), remission (d17) and relapse phase (d22) of cr-EAE compared to IFA control rats (IFA). (E and F) Immunofluorescent double labeling of Iba1 positive macrophages and TG2 positive cells in the spinal cord of cr-EAE animals during the relapse; bv = blood vessel. Scale bars indicate 100 µm in D, 25 µm in E (upper panels) and 10 µm in E (lower panel).

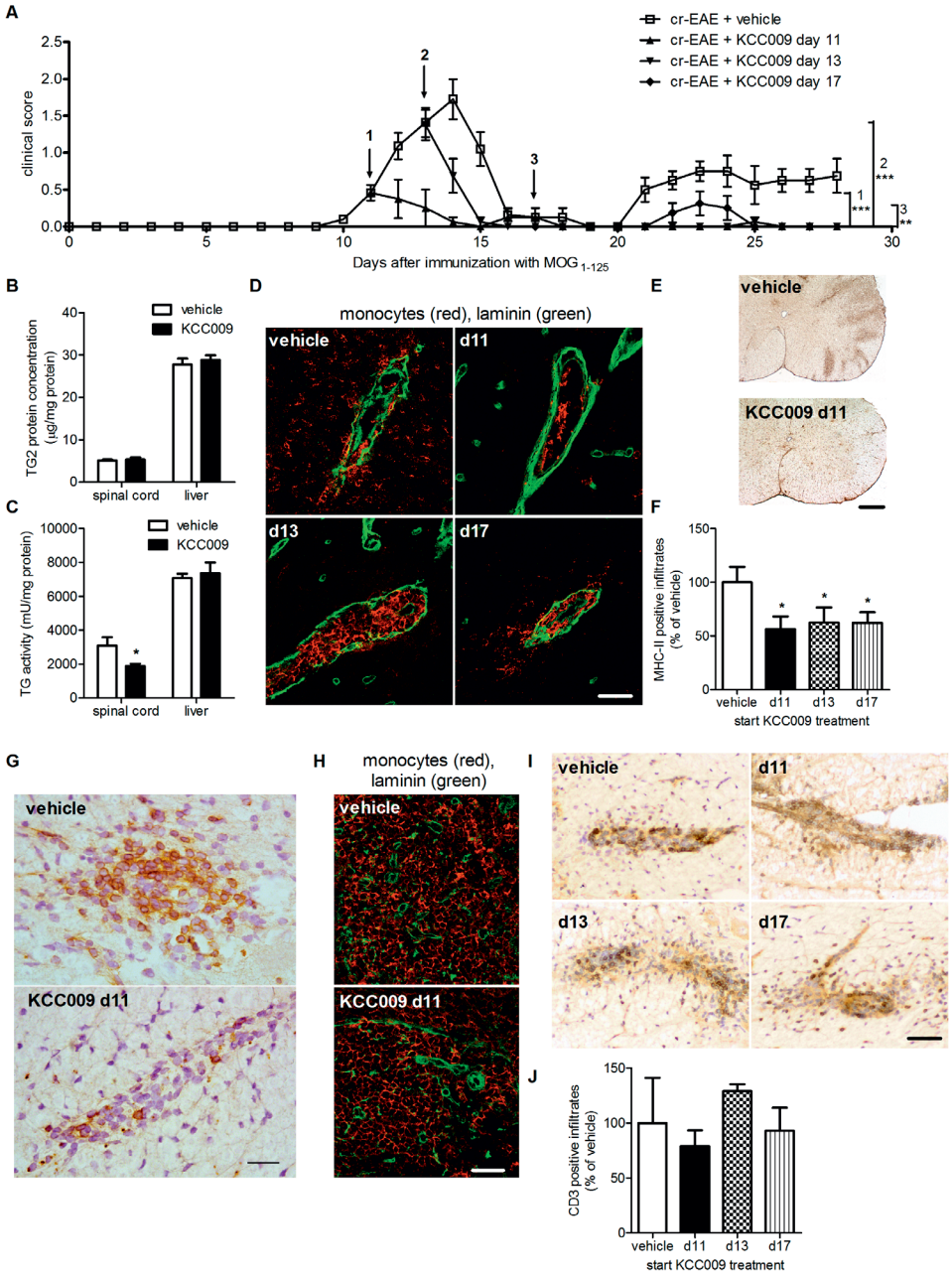


Figure 3: Beneficial effect of KCC009 treatment on clinical outcome of cr-EAE and effects on cellular TG activity. (A) Clinical scores of cr-EAE rats, treated i.p. daily with vehicle or KCC009 from first clinical signs onwards (day 11, arrow 1), from peak symptoms onwards (day 13, arrow 2) or remission onwards (day 17, arrow 3). To determine the effect of KCC009 treatment versus vehicle-treated animals, the area under the curve (AUC) was calculated from treatment at 1: first peak (day 11), 2: relapse (day 13) and 3: remission (day 17) and statistically compared

to the vehicle-treated animals from the same time-point onwards, i.e. day 11, day 13 or day 17, respectively. Data represent mean ± S.E.M, ** p< 0.01, ***p< 0.001 (B) TG2 protein levels measured using a TG2 ELISA and (C) TG2 activity levels measured using the TG Covtest in spinal cord and spleen. Cr-EAE rats were treated with vehicle or KCC009 daily starting from day 11 onwards and animals were sacrificed on day 28. Data represent mean + S.E.M., * p< 0.05. (D) Fluorescent double labeling of MHC class-II positive cells (red) and laminin (green) in the cervical part of the rat spinal cord of cr-EAE rats treated with vehicle from day 11 onwards or with KCC009 from day 11, day 13 or day 17 onwards. Animals were sacrificed on day 28. (E) Representative images of MHCII staining in the cervical spinal cord of a vehicle and KCC009 treated cr-EAE rat from d11 onwards and sacrificed at day 28. (F) Quantification of the spinal cord area containing MHC class-II positive cells in four representative animals from vehicle-treated and from KCC009-treated cr-EAE rats from day 11, day 13 or day 17 onwards and sacrificed on day 28. Data represent mean % compared to vehicle-treated rats + S.E.M., *p< 0.05. (G) Representative ED1 staining in the cervical spinal cord of a vehicle and KCC009-treated cr-EAE rat from d11 onwards and sacrificed on day 28. (H) Fluorescent double labeling of MHC class-II positive cells (red) and laminin (green) in the spleen of cr-EAE rats after treatment with vehicle or KCC009 from day 11 onwards and sacrificed on day 28. (I) Representative images of immunohistochemical staining of CD3 positive T cells in the cervical part of the rat spinal cord of cr-EAE rats treated with vehicle from day 11 or with KCC009 from day 11, day 13 or day 17 onwards. Animals were sacrificed at day 28. (J) Quantification of the spinal cord area containing CD3 positive cells in four representative animals from vehicle-treated and from KCC009-treated cr-EAE rats from day 11, day 13 and day 17 onwards and sacrificed at day 28. Data represent mean % compared to vehicle-treated rats + S.E.M. Scale bars indicate 25 µm in D, G, H and I and 200 µm in E.

Pharmacological modulation of TG2 activity using the reversible inhibitors cystamine or monodansylcadaverine (MDC) in cr-EAE rats or EAE mice, respectively, showed a reduction in clinical symptoms compared to vehicle-treated animals (Suppl. Figs. 2A and 1B). Moreover, less MHC II positive cells (Suppl. Fig. 2B) and a decrease in loss of MBP staining (Suppl. Fig. 2C) were observed in cystamine-treated cr-EAE rats.

KCC009 reduces MHCII positive cells in the spinal cord during cr-EAE

Post-mortem tissue of cr-EAE rats (obtained at day 28), which had been treated with KCC009 or vehicle from different time-points during disease onwards, was studied. In the spinal cord of vehicle-treated cr-EAE rats, MHC class II positive cells were detected in the perivascular space and surrounding blood vessels (Fig. 3D, vehicle). After the treatment of cr-EAE rats with KCC009 from the first clinical signs (day 11) onwards, most cells were present in the blood vessel lumen (Fig. 3D, d11). In cr-EAE rats treated with KCC009 from the first peak of clinical symptoms (day 13) onwards, numerous MHCII positive cells were present in the perivascular space (Fig. 3D, d13). Finally, in cr-EAE rats treated with KCC009 from remission (day 17) onwards, most cells were detected within the perivascular space, and to some extent surrounding the blood vessels (Fig. 3D, d17). Overall, we observed a reduction in MCH class II (Fig. 3E) as well as CD68 (Fig. 3G) positive cells in KCC009-treated versus vehicle-treated rats present in the spinal cord. Subsequent quantification confirmed a significant reduction in the spinal cord area containing MHC class-II positive cells in cr-EAE rats treated with KCC009 from day 11, day 13 and day 17 onwards versus vehicle-treated cr-EAE rats (Fig. 3F). Interestingly, in contrast to the observations in the spinal cord, MHC class II positive cells did not accumulate within blood vessels in the spleen of KCC009-treated cr-EAE rats but had a similar localization as in vehicle-treated cr-EAE rats (Fig. 3H).

KCC009 does not alter T-cell infiltration into the CNS

To determine if the reduction of TG2 activity selectively affected the infiltration of macrophages, we evaluated the infiltration of T cells upon KCC009 treatment. In both vehicle- and KCC009-treated cr-EAE rats, T-cell infiltrates are present in the perivascular space and around blood vessels in the spinal cord (Fig. 3I). Quantification of the spinal cord area containing CD3 positive T cells in KCC009-treated (starting at day 11, day 13 and day 17, respectively) versus vehicle-treated cr-EAE rats showed no significant alteration in the number of infiltrated T cells (Fig. 3J).

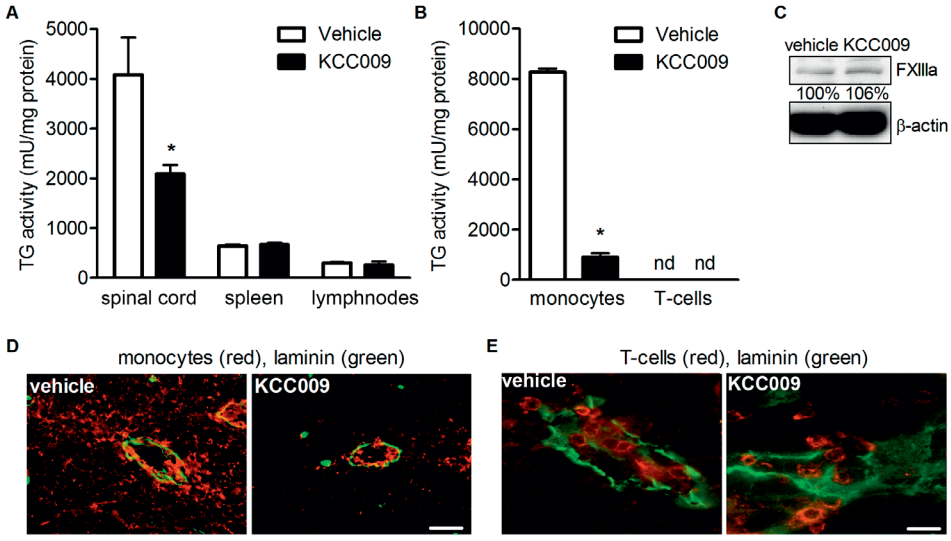


Figure 4: Short-term KCC009 treatment effect on TG activity and cell infiltration. (A) TG activity in the rat spinal cord, spleen and cervical lymph nodes of cr-EAE rats treated with KCC009 or vehicle from day 11 onwards and sacrificed at day 12. Data represent mean + S.E.M. *p< 0.01. (B) TG activity in blood-derived monocytes and T cells (collected at day 12 and treated with KCC009 from day 11). Data represent mean + S.E.M., *p< 0.01, nd = not detectable. (C) Effect of KCC009 treatment on the level of active FXIII = FXIIIa measured using western blot. Bands were quantified and corrected for β-actin. (D) Immunofluorescent staining for MHC class II positive cells (OX6) and (E) CD3 positive T cells together with laminin (to stain the basal lamina) after treatment of cr-EAE rats with vehicle or KCC009. Scale bars indicate 35 µm (D) and 20 µm (E).

Effect of short-term KCC009 treatment on monocyte infiltration

To study the effect of short-term KCC009 treatment on TG2 activity and cellular infiltration, cr-EAE rats were treated i.p. twice with KCC009, once on day 11 and once on day 12 of cr-EAE and sacrificed within 4 h after the i.p. injection on day 12. KCC009 treatment of cr-EAE rats selectively reduced TG activity in the spinal cord, but not in the spleen or cervical lymph nodes of cr-EAE rats (Fig. 4A). Moreover, monocytes isolated from cr-EAE rats showed reduced TG activity after KCC009 treatment of the animals, whereas TG activity was not detectable in isolated T-lymphocytes (Fig. 4B). However,

KCC009 treatment did not alter the expression level of active FXIIIa, which is structurally related to TG2, in primary isolated monocytes from the blood (Fig. 4C). Additionally, short-term TG2 activity reduction resulted in less infiltrating macrophages (Fig. 4D), but did not affect T-cell infiltration in the spinal cord of cr-EAE rats (Fig. 4E), similar to the observations after longer TG2 activity reduction as described in Section 3.5.

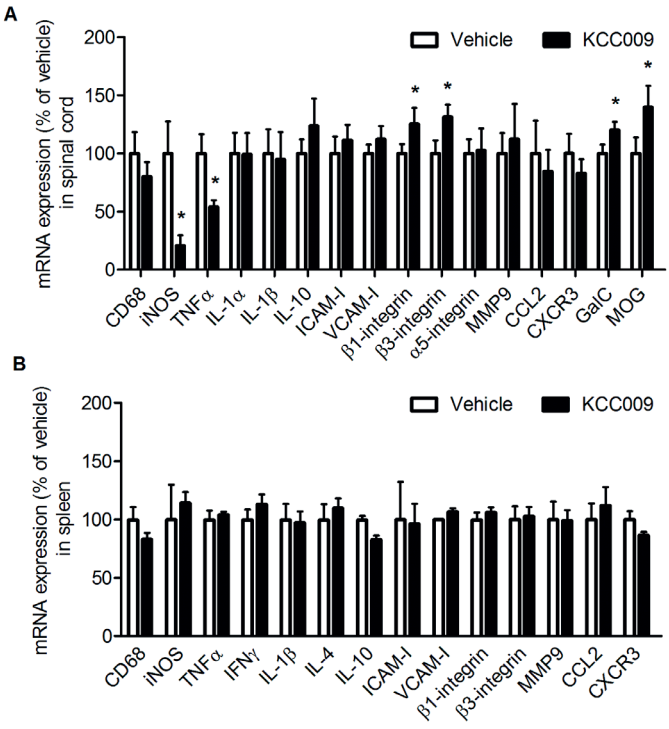
TG2 activity reduction affects mRNA and protein levels of specific inflammation-related mediators in the CNS, but not in the spleen of cr-EAE rats

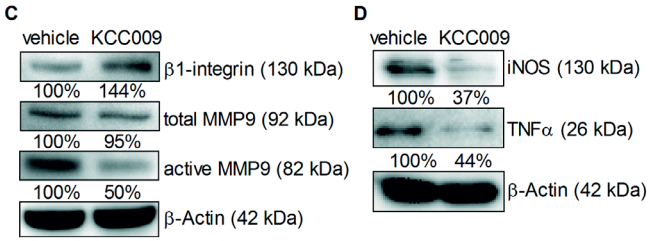
During cr-EAE, expression of various (inflammatory) genes involved in the pathological process were altered (Olsson, 1995). We determined whether the pharmacological reduction of TG2 activity affected gene expression levels in the CNS and spleen of cr-EAE rats. In the spinal cord of cr-EAE animals, treated with KCC009 from the initial clinical symptoms (day 11) onwards, significantly increased the mRNA levels of the integrins β1 and β3 by 25% and 31%, respectively, and reduced the expression of iNOS and TNFα by 80% and 46%, respectively (Fig. 5A). Expression levels of other inflammation-related genes remained unaltered. In the spleen of these animals, however, the expression levels of all relevant measured genes remained unaffected compared to vehicle-treated cr-EAE rats (Fig. 5B).

Lymphocyte adhesion to high endothelium is mediated by two β1 integrin receptors for fibronectin, α4β1 and α5β1 [197]. As β1-integrins are crucial to monocyte adhesion, its protein expression was studied and found to be increased by approximately 44% in the spinal cord of cr-EAE animals treated with KCC009 from initial clinical symptoms 9 (day 11) onwards as compared to vehicle-treated animals (Fig. 5C). Furthermore, the level of active MMP9, involved in macrophage migration, was reduced by 50% in the spinal cord of KCC009-treated cr-EAE animals, whereas full length MMP9 (pro-enzyme) protein levels remained unaffected (Fig. 5C). Since iNOS and TNFα are implicated in demyelination [166], their protein expression levels were determined and found to be decreased by 63% and 56%, respectively in KCC009-treated cr-EAE rats (Fig. 5D).

TG2 activity reduction alters the myelin status in cr-EAE rats

Luxol Fast Blue (LFB) staining on spinal cord material of cr-EAE rats sacrificed at day 28 showed that in vehicle-treated cr-EAE rats LFB staining was decreased surrounding blood vessels were infiltrates were present, indicating loss of myelin in the spinal cord. However, this decrease in LFB staining was largely prevented when cr-EAE rats were treated with KCC009 from day 11 onwards (Fig. 5E). Moreover, expression levels of the oligodendrocyte marker galactosylceramidase (GalC) and myelin oligodendrocyte glycoprotein (MOG) were increased by 20% and 40%, respectively (Fig. 5A) in KCC009-treated cr-EAE rats.





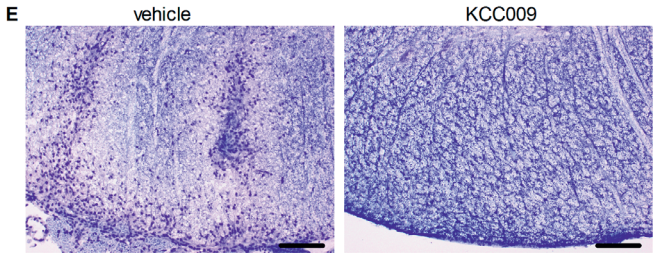


Figure 5: The effect of TG2 inhibition on mRNA expression levels of various genes involved in cr-EAE in rat spinal cord and spleen and demyelination in the rat spinal cord. (A) mRNA expression levels of CD68, various cytokines and genes involved in cell adhesion and migration related processes in the rat spinal cord, and (B) in the rat spleen, of cr-EAE rats after treatment with KCC009 or vehicle from day 11 onwards and sacrificed on day 28. Data represent mean + S.E.M., *p< 0.01. (C) Protein expression of total MMP9 and the active form of MMP9 and (D) protein expression of iNOS and TNFα in the spinal cord of vehicle and KCC009-treated rats started on day 11 after immunization onwards. Animals were sacrificed at day 28. Bands represent pooled protein from 6 animals per group. Semi-quantitative data represent % expression compared to vehicle-treated cr-EAE rats and are corrected for β-actin. (E) Demyelination was determined by LFB staining in the rat spinal cord of cr-EAE rats after treatment with vehicle or KCC009. Representative spinal cord sections are shown. Scale bars indicate 70 µm.

TG2 modulates macrophage migration through cytoskeletal rearrangements

To study which Transglutaminase family members were expressed in NR8383 cells, mRNA levels of TG2, FXIIIa, TG1 and TG3 were measured in KCC009-treated control and cytokine-stimulated cells. TG2 was expressed in NR8383 cells and increased upon cytokine treatment. FXIIIa and TG1 mRNA were detectable but at lower levels than TG2 and unaltered upon cytokine treatment. TG3, however, was not detectable in NR8383 cells (Fig. 6A). To study the levels of TG2 on the surface of macrophages, a biotin immunoprecipitation assay was performed. Upon cytokine treatment, TG2 expression on the surface of macrophages was clearly increased (Fig. 6A, lane 3; Suppl. Fig. 3). No effect of KCC009 treatment on the surface protein level was detected (Fig. 6A, lane 4; Suppl. Fig 3). Of note, treatment of macrophages with KCC009 did not affect cell viability (Fig. 6B).

To further explore the mechanism of KCC009 action in migration processes, we performed *in vitro* experiments using NR8383 cells that migrate through monolayers of brain endothelial cells (GP8 cells). Treatment of NR8383 cells with KCC009 to inhibit TG2 activity resulted in a marked reduction (75%) in transendothelial migration of KCC009-treated cells (Fig. 6C). In contrast, no effect on NR8383 cell migration was detected upon treatment of brain endothelial cells with KCC009 to inhibit TG2 activity (Fig. 6C). An additional observation was that KCC009 treatment attenuated the motility of NR8383 cells (Suppl. Videos 1A and B), suggestive for cytoskeletal rearrangements within the cells. Cellular staining for F-actin, using rhodamine phalloidin, showed a clear difference in the appearance of cellular extensions between vehicle-treated and KCC009-treated cells. Whereas cellular ramifications were extensively present in vehicle-treated cells, in KCC009-treated cells these ramifications were retracted (Fig. 6D). Furthermore, KCC009 treatment attenuated the level of active, GTP-bound RhoA in macrophages (79%) whereas the total RhoA level remained unaffected (Fig. 6E).

DISCUSSION

The present study demonstrates an important role for the enzyme TG2 and its activity in various models of experimental MS contributing to the appearance of clinical symptoms, enhanced macrophage migration and demyelination. Subsequent modulation of TG2 activity is therapeutically effective and acts by reducing macrophage infiltration into the spinal cord but not in the spleen, illustrating the potential of TG2 as a novel and more selective target for MS therapy.

This is the first time that TG2 is shown to be present in MHCII positive cells in active MS lesions and, a quite extensive appearance of amoeboid shaped TG2 positive Iba1 positive cells in lesions induced in cr-EAE rats. Other relevant TG isoforms, previously observed within the CNS [171] were either absent (TG1) or not differently expressed (TG3) in active human MS lesions compared to control subcortical white matter. Furthermore, there was no alteration in mRNA levels of TG1, TG3 and FXIIIa in cr-EAE rats compared to control rats. We therefore consider TG2 to be the most likely iso-enzyme to play a role in

the disease process of MS and cr-EAE. Indeed, the deletion of TG2 in mice reduced early clinical symptoms in MOG peptide-induced EAE supporting a role for TG2 in the pathogenesis of EAE as was also shown in an adoptive transfer EAE model [198]. Previously, we already showed that astrocytes are a source of TG2, most prominent in the rim of chronic active lesions when it comes to glial scar formation at a more distant site of the blood vessels [199]. Based on our present observations, we consider that in and around vascular cell infiltrates, macrophages, and not T cells, are the major source of TG2, although we cannot fully exclude that other infiltrating cell-types contribute as well.

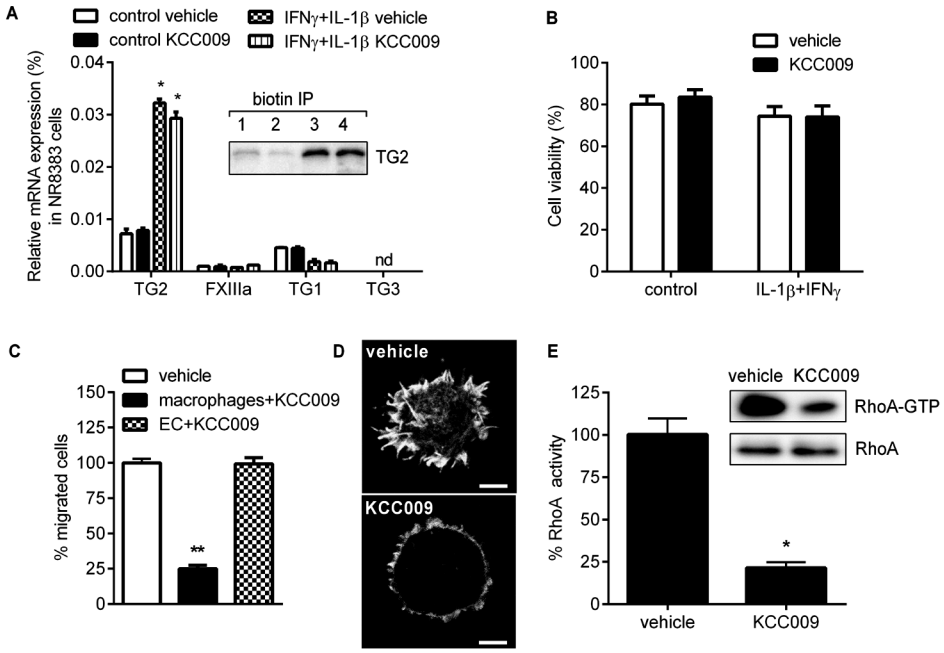


Figure 6: TG2 in macrophages in vitro. (A) mRNA expression levels of TG isoforms TG2, FXIIIa, TG1 and TG3 in macrophages and (insert) TG2 protein expression on the surface of macrophages that were treated with (1) vehicle, (2) KCC009, (3) IFNγ + IL-1β + vehicle or (4) IFNγ + IL-1β + KCC009. Data represent mean (n = 6) + S.E.M., *p< 0.01 compared to vehicle-treated control, nd = not detectable. (B) Cell viability of macrophages after treatment with KCC009 measured using the propidium Iodide exclusion assay. Data are expressed as mean + S.E.M. (n = 4). (C) Macrophage migration across confluent monolayers of brain ECs. Data represent mean (n = 4 wells) + S.E.M., **p< 0.001. (D) Cytoskeletal rearrangements of macrophages visualized with rhodamine phalloidin staining. Scale bars represent 15 µm. (E) Representative western blot illustrating RhoA GTPase activity in macrophages. Western blot quantification represents mean of 5 different active RhoA isolation experiments + S.E.M., *p< 0.01.

To determine the possible therapeutic potential of TG2 as a target, we aimed at pharmacologically modulating TG2 activity using three independent TG2 activity inhibitors. Cr-EAE rats were treated with KCC009, an irreversible inhibitor of TG2 activity [181]. We observed that the reduction of TG2 activity from different phases of cr-EAE onwards resulted in an immediate and dramatic reduction in clinical scores, indicating that

attenuation of TG2 activity has therapeutic potential. This notion is supported by a similar clinical improvement observed after i.p. treatment of cr-EAE rats with cystamine which is a competitive substrate for TG [200]. Furthermore, the clinical relevance of TG2 in EAE was substantiated across species by the observation that MDC, another competitive substrate for TG [154], also reduced clinical symptoms of EAE in mice. However, our data indicate that KCC009 given daily more effectively attenuates clinical symptoms of cr-EAE compared to cystamine or MDC treatment. Although we cannot exclude that pharmacokinetic characteristics of KCC009 favor its potent effect, it is more likely to be due to its pharmacodynamics, i.e., KCC009 is an irreversible inhibitor of TG2 activity, whereas cystamine and MDC are both competitive substrates for TG [201]. These inhibitor studies demonstrated that modulating TG2 activity is clearly effective in reducing experimental MS. We can, however, not conclude whether the observed effects are mediated solely via reduction of Ca2+-dependent cross-linking activity of TG2 or via reduction of Ca2+-independent TG2 mechanisms of action, e.g., co-receptor for β-integrins (reviewed in [93]). Moreover, even additional effects of the TG inhibitors, besides inhibiting TG2, cannot be fully excluded as a mechanism of action and are subject to research. The development of more, selective TG2 inhibitors that can be used *in vivo* is therefore of utmost importance.

It is of interest to note that β1- and β3-integrin expression in the spinal cord is enhanced when animals were treated with KCC009. Whether this is mechanistically due to a compensatory mechanism by which less TG2 activity is compensated by enhanced β-integrin expression remains to be established. It may, however, explain our neuropathological observations in the spinal cord of cr-EAE rats treated with KCC009 in which macrophages accumulate within the lumen of blood vessels and in the perivascular space with fewer cells migrating into the CNS parenchyma compared to vehicle-treated cr-EAE rats. Moreover, the observed reduced level of active MMP9, important for cell migration [165], found in the spinal cord of KCC009-treated cr-EAE rats further substantiates the role of TG2 in macrophage migration. However, no difference in macrophage localization within the spleen of vehicle- versus KCC009-treated cr-EAE rats was observed. Moreover, KCC009 treatment of cr-EAE rats selectively reduced TG activity in the spinal cord and not in cervical lymph nodes or spleen although recruitment of activated macrophages to these organs has been observed in EAE and MS [202]. This may be due to enhanced TG2 activity in the spinal cord produced by TG2 producing macrophages present locally during EAE, whereas in the lymph nodes and spleen little activity is present under these conditions, and not affected by the treatment.

It is worth noting that FXIIIa, which is present in monocytes and is structurally related to TG2 [126], remained low and unaltered during cr-EAE and in macrophages *in vitro*. Furthermore, *in vivo* KCC009 treatment affected FXIIIa expression neither in monocytes derived from cr-EAE animals nor in NR8383 cells treated with KCC009 *in vitro*. These data favor that TG2 activity, and not FXIIIa, is involved in macrophage migration during MS or cr-EAE. This conclusion is strengthened by the absence of bleeding in our animals treated long-term with KCC009, which would be expected if chronic inhibition of the activity of the coagulation factor FXIIIa by KCC009 played a significant role in the effect of the compound.

Another aspect of interest is that TG activity in T cells of cr-EAE rats is undetectable and no effect on T-cell migration into the spinal cord was observed after KCC009 treatment. This was unexpected as MS and EAE are classically considered as T-cell mediated diseases [203, 204]. It has been shown that TG2 is involved in T-cell mediated responses, e.g. altered cytokine expression [198, 205]. The present study demonstrates that TG2 protein and activity in activated macrophages, and not in T cells, is a key element in regulating macrophage migration into the CNS, thereby determining the clinical outcome of cr-EAE in rats. We can however not exclude that T cells or B cells present in lesions, alter their response due to TG2 produced by macrophages.

Our *in vitro* study demonstrated that reduction of TG2 activity by KCC009 in NR8383 cells, and not in brain endothelial cells, attenuates profoundly the transendothelial migration. Although TG2 seemed the most prominent TG produced by NR8383 macrophages, we cannot fully exclude a role for other TGs in these cells. Still, the influence of KCC009 treatment on macrophage migration *in vitro* supports our *in vivo* observation of a dramatically reduced migration of macrophages into the CNS in KCC009-treated cr-EAE rats. Thus, the observed *in vitro* effects are in agreement with our *in vivo* data, indicating that TG2 activity facilitates macrophages to pass the brain endothelium and probably stimulates migration into the tissue parenchyma by activating the extracellular matrix protein MMP9. While studying the effects of the reduction of TG2 activity on macrophage migration, we observed that KCC009 treatment attenuated the motility of macrophages. This observation suggests that the reduction of TG2 activity influences the cytoskeletal flexibility of macrophages. To better understand the down-stream mechanism(s) underlying this remarkable effect of KCC009, we examined polymerization of the cytoskeletal protein F-actin in KCC009-treated macrophages *in vitro*. It has been shown that macrophage migration over the blood-brain barrier requires a coordinated remodeling of the actin cytoskeleton [206]. We observed a clear reduction in F-actin containing cellular extensions of macrophages after treatment with KCC009, which is indicative of reduced cytoskeletal rearrangements in macrophages[134]. This effect may be due to reduced RhoA GTPase activity. Indeed, reduced RhoA activity was measured in macrophages upon KCC009 treatment, while leaving total RhoA levels unaffected. Since it is known that activation of RhoA is required for transendothelial migration of macrophages [207], and TG2 can activate RhoA GTPase [175], we suggest that TG2 activates RhoA resulting in cytoskeletal rearrangements essential for macrophage migration.

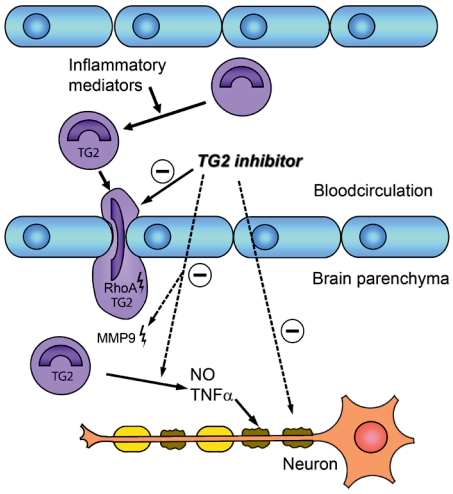


Figure 7: Schematic model representing a summary of the data obtained in the present study. During MS/EAE, inflammatory mediators (e.g., IL-1β, IFNγ, IL-4) induce TG2 production and activity in circulating monocytes/macrophages (purple icons). Upon activation, TG2 is involved in cytoskeletal remodeling and migration processes, leading to the passage of the brain endothelium and glia limitans (blue icons) by these cells into the CNS. Locally these macrophages contribute to demyelination by e.g., production of TNFα and nitric oxide. Inhibition of TG2 activity can contribute to less migration of monocytes/ macrophages into the CNS and ultimately less axonal demyelination. (For interpretation of the references to color in this figure legend, the reader is referred to the web version of this article.)

Of particular therapeutic interest is our observation that KCC009 treatment did not affect relevant cytokine or chemokine molecule expression levels in the spleen of cr-EAE rats. These findings indicate that, in contrast to other MS drugs currently used in patients (e.g., beta-interferon, natalizumab) [168, 169, 208], KCC009 leaves these immune-relevant responses intact likely resulting in fewer side effects. However, at the site of action within the CNS, in particular, the mRNA levels of iNOS and TNFα were reduced after treatment with KCC009. This observation is in line with observations in TG2-/- mice subjected to adoptive transfer EAE [198]. This suggests that infiltrated, activated macrophages contribute significantly to the local enhanced expression of iNOS and TNFα, whereas resident (glial) cells within the CNS are important producers of the other measured factors as shown previously by others in animals models for MS [209, 210]. Furthermore, the extent of demyelination in lesions around blood vessels was reduced after treatment of cr-EAE rats with KCC009 or with cystamine as shown by LFB or MBP staining, respectively. In fact, increased mRNA expression levels of GalC and MOG were found in KCC009-treated cr-EAE rats, suggestive of enhanced (re)myelination. It has previously been shown that TNFα and excess NO, produced by iNOS, in infiltrating macrophages and microglia contribute to myelin damage and subsequent impaired axonal conductivity [166, 209, 210]. Thus, the beneficial effect of reducing TG2 activity on myelination in cr-EAE rats may be due to the reduced presence of activated macrophages within the CNS and subsequent less production of iNOS and TNFα.

Overall, we conclude that the enzyme TG2 is an important new player in the pathogenesis of MS. Pharmacological modulation of TG2 activity results in clinical improvement together with selective blockade of macrophage migration into the CNS, less production of iNOS and TNFα, and diminished demyelination (see Fig. 7). These results provide a rationale for a therapeutic strategy that specifically targets TG2 activity, which might have potentially fewer side effects, i.e. disturbance of the peripheral cytokine response.

Conflict of interest

The authors declare that they have no financial conflict of interest.

Acknowledgements

We thank Alvine Pharmaceuticals (San Carlos, USA) for kindly providing KCC009, and Dr. I. Huitinga of the Netherlands Brain Bank for providing human brain material. Prof. Dr. Chris Linington (University of Aberdeen, UK) is thanked for his generous gift of the plasmid containing recombinant rat $MOG_{1–125}$. Wouter Gerritsen (Dept. Pathology, VU University Medical Center, Amsterdam, The Netherlands) is kindly acknowledged for his help with the Luxol Fast Blue staining. We thank Jan Bauer (Dept. Neuroimmunology, Medical University of Vienna, Austria) for his assistance with the MBP staining.

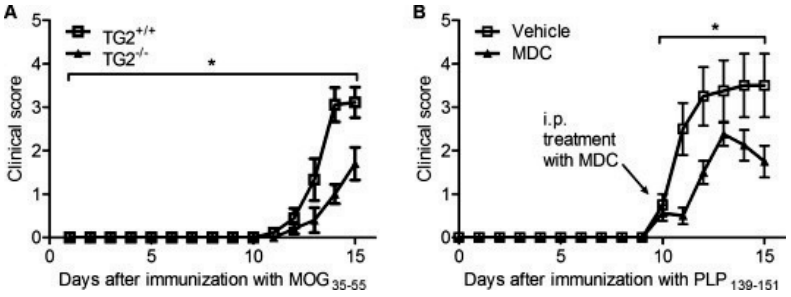
This work was financially supported by the Stichting MS Research [Grant number 08-635], EU Marie Curie ITN "TRANSPATH" [Grant number 289964], and the Netherlands Organization for Scientific Research (NWO-VIDI).

SUPPLEMENT

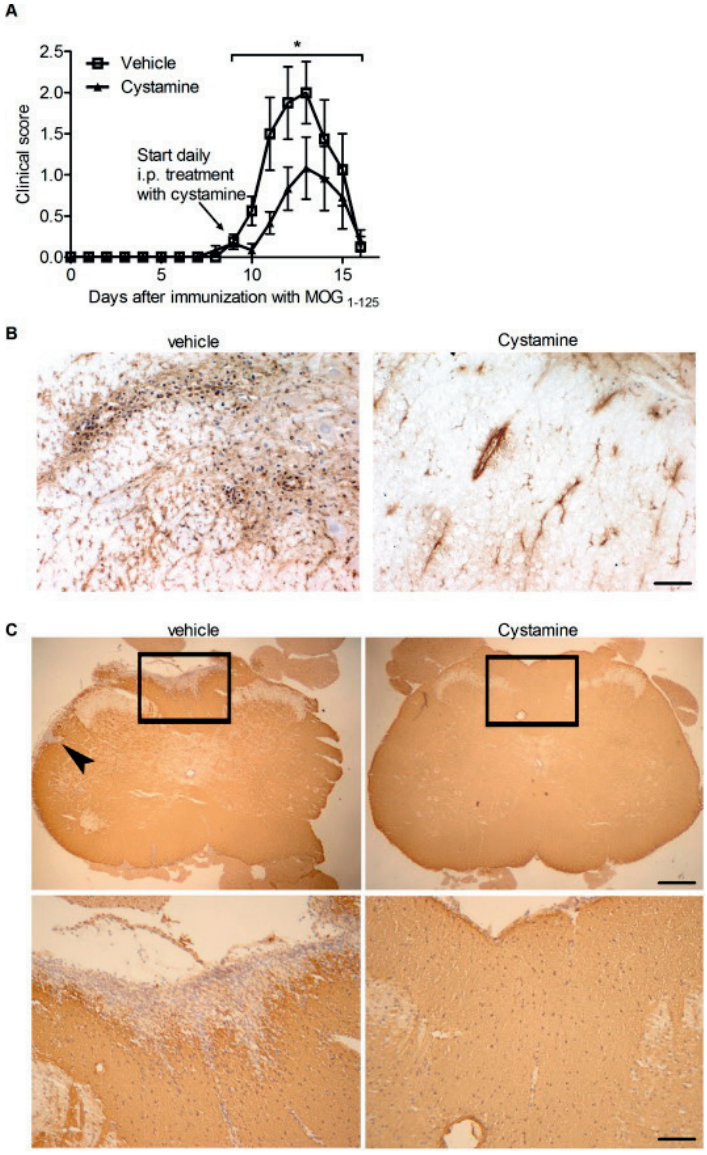
Online Resource Table 1: Oligonucleotide primers used for amplification of cDNAs[1]

rat cDNA	Sequence forward 5' to 3'	Sequence reverse 5' to 3'
GAPDH	TCAAGGGCATCCTGGGCTAC	CGTCAAGGTGGAGGAGTGG
CD68	CTCATCATTGGCCTGGTCCT	GTTGATTGTCGTCGTCTGCGGG
iNOS	AACTTGAGTGAGGAGCAGGTTGA	CGCACCGAAGATATCCTCATGA
TNFa	CCACACCGTCAGCCGATT	TCCTTAGGGCAAGGGCTCTT
TG1	ACCAGCAGTGGCATCTTC	AATGAAAGGTGTGTCATACTTC
TG2	AGAGGAGCGGCAGGAGTATG	AGGATCCCATCTTCAAACTGC
TG3	GAAGTCAAGGTGTGTTCC	AGATGAAGATCATGTCGAAG
FXIIIa	TCACTGCACGCATCAACGAGAC	TGCCTCGGACCTTGATGGTGAC
IL-1a	AGACAAGCCTGTGTG2CTGAAG	CAGAAGAAAATGAGGTCGGTCTC
IL-1b	AAAGAAGAAGATGGAAAAGCGGTT	GGAACTGTGCAGACTCAAACTC
IFNg	GTGTCATCGAATCGCACCTG	TCCCTGTTTTAGCTGCTGGC
IL-4	ACGTGATGTACCTCCGTGCTT	TCCCTCGTAGGATGCTTTTTAG
IL-10	AAAGCAAGGCAGTGGAGCAG	TCAAACTCATTCATGGCCTTGT
MMP9	TGTATGGTCGTGGCTCTAAAC	GTGGGACACATAGTGGGAG
α5-integrin	TGTATCCTGCATCAACCTTAG	TCCAGTTGGAGTTCCACC
β1-integrin	GAATGTAGCACAGATGAAGTG	CACACTCTCCATTGTTACTG
β3-integrin	AGAACTGACGGATACTGG	GAGTCTTCATAGTACTGGAATC
CCL2	ACGTGCTGTCTCAGCCAGATG	GACTCATTGGGATCATCTTGCC
CXCR3	GCCATGTACCTTGAGGTC	CCATAATCGTAGGGAGATG
GalC	ACGTTGAGTACCCATTATTTAG	TGCTCAAGGTCTTCGTTATTC
MOG	GCAGAAGTCGAGAATCTC	AACAGGGACAATAACAAAC

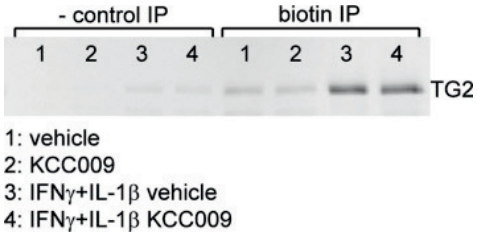
[1]Primers were designed using the Primer Express program (Applied Biosystems) and purchased from Eurogentec (Seraing, Belgium)



Supplementary Figure 1: Clinical scores of mouse EAE. (A) $MOG_{35–55}$-induced EAE in $TG2^{-/-}$ and $TG2^{+/+}$ mice resulted in an incidence of disease of 50% and 60%, respectively. The area under the curve (AUC) of the mean clinical scores was calculated from each group from the start till the end of the experiment and statistically compared. (B) $PLP_{139–151}$-induced EAE in mice treated i.p. with the TG inhibitor MDC or vehicle once on day 10. The area under the curve (AUC) of the mean clinical scores was calculated from each group from the start of treatment (day 10) onwards and statistically compared. Data represent mean + S.E.M. $^{*}P < 0.05$.



Supplementary Figure 2: Clinical scores of cr-EAE in rats and TG activity levels in the rat spinal cord after treatment with cystamine. (A) Clinical scores of cr-EAE after daily i.p. treatment with cystamine or vehicle started from first clinical symptoms onwards. The area under the curve (AUC) was calculated from the mean clinical score of each group from the start of treatment (day 9) onwards and statistically compared. Data represent mean ± S.E.M. $P < 0.05$. (B) Representative images of MHC class II (Ox-6) staining in the cervical spinal cord of a vehicle- and a cystamine-treated cr-EAE rat started at d9 onwards and sacrificed at d16. (C) MBP staining on the spinal cord on a vehicle and cystamine-treated cr-EAE rat started at d9 onwards and sacrificed at d25. Box and arrowhead show demyelinated areas in vehicle-treated cr-EAE rat. Boxes in vehicle- and cystamine-treated rats are further magnified in the lower panels. Scale bars represent 50 µm (B), 500 µm (C, upper panels) and 100 µm (C, lower panels).



Supplementary Figure 3: TG2 protein expression on the surface of NR8383 macrophages that were treated with (1) vehicle, (2) KCC009, (3) IFNγ+IL-1β + vehicle or (4) IFNγ+IL-1β + KCC009. A non-biotinylated cell sample (-biotin IP) was run aside a biotinylated cell sample (+biotin IP) to ensure that the pulldown was specific only for cell surface biotinylated TG2.



Chapter 3

TISSUE TRANSGLUTAMINASE APPEARS IN MONOCYTES AND MACROPHAGES BUT NOT IN LYMPHOCYTES IN WHITE MATTER MULTIPLE SCLEROSIS LESIONS

J Neuropathol Exp Neurol. 2019. Vol. 78, No. 6, June 2019, pp. 492–500

ABSTRACT

Leukocyte infiltration is an important pathological hallmark of Multiple Sclerosis (MS) and is therefore targeted by current MS therapies. The enzyme tissue Transglutaminase (TG2) contributes to monocyte/macrophage migration and is present in MS lesions and could be a potential therapeutic target. In the present study, we examined the cellular identity of TG2 expressing cells by immunohistochemistry in white matter lesions of 13 MS patients of which we analyzed 4 patients with 9 active and chronic active lesions in detail. In these active MS lesions, TG2 is predominantly expressed in leukocytes ($CD45^+$) but not in cells of the lymphocyte lineage, i.e. T cells ($CD3^+$) and B cells ($CD20^+$). In general, cells of the monocyte/macrophage lineage ($CD11b^+$ or $CD68^+$) are TG2 positive but no further distinction could be made regarding pro- or anti-inflammatory macrophage subtypes. In conclusion, TG2 is abundantly present in cells of the monocyte/macrophage lineage in active white matter MS lesions. We consider that TG2 can play a role in MS as it is associated with macrophage infiltration into the CNS. As such TG2 potentially presents a novel target for therapeutic intervention that can support available MS therapies targeting lymphocyte infiltration.

Chrobok NL, Bol JGJM, Wilhelmus MMM, Drukarch B, van Dam AM

Department of Anatomy and Neurosciences, Amsterdam Neuroscience, Amsterdam UMC, location VUmc, Amsterdam, The Netherlands

INTRODUCTION

Multiple sclerosis (MS) is a chronic inflammatory and neurodegenerative disease that is the most common cause of neurological disabilities in young adults [211]. MS clinical features can be diverse but include motor and sensory deficits, and cognitive impairment. MS pathology is characterized by the infiltration of leukocytes into the central nervous system (CNS) which results in inflammatory lesion formation concomitant with demyelination and axonal damage [179, 212-214]. The inflammatory active lesions in the CNS white matter consist mainly of leukocytes infiltrated from the blood and of resident CNS cells such as microglia and astrocytes that are activated by the local inflammatory response [20]. Cellular infiltration of the CNS is highly regulated and involves a complex adhesion and migration cascade. This cascade is tuned by many factors including chemokines and adhesion molecules which are upregulated during inflammation [24, 179, 215]. It is thought that auto-reactive T cells enter the CNS during MS pathogenesis. This is then followed by recruitment and influx of other leukocyte cell types including B cells and monocytes. B cells play a pathogenic role in MS development by prolonging and supporting inflammation by antibody and cytokine secretion as well as stimulating T cells [29-31, 216]. Infiltrating monocytes can differentiate into macrophages upon entering the CNS. Locally, they can diverge into macrophages exerting damage and promoting further inflammation or having anti-inflammatory properties and induce axonal regeneration and repair [217, 218].

Novel treatments for MS patients target mainly lymphocyte infiltration into the CNS [219, 220], which can be achieved either by the reduction in the number of circulating lymphocytes [43, 44] or by interference with mechanisms associated with cellular infiltration [221-223]. As it has been revealed that MS pathology is highly heterogeneous between lesions and patients [224], it is important to focus also on other cell types as potential (additional) targets to combat the disease. In this respect, we propose that monocytes and macrophages, whose detrimental roles have been established in MS and MS animal model pathogenesis [212, 225, 226], are of interest as potential targets.

The enzyme Tissue Transglutaminase (TG2) is involved in adhesion and migration of several cell types, including monocytes and macrophages [119, 227], which is observed in MS pathology [228]. The precise role of TG2 in MS has not been delineated yet, but its expression is confirmed in human leukocyte antigen-D related (HLA-DR)-positive cells in active white matter MS lesions [229]. Furthermore, TG2 is involved in inflammation and other MS-associated processes such as cell adhesion, migration and efferocytosis, as previously reviewed [230]. Additional data from MS rodent and primate models showed that TG2 is expressed in monocytes and macrophages and contributes to the development of MS-like disease symptoms [229, 231].

If monocyte and macrophage-derived TG2 contributes to MS pathology as indicated by animal model experiments, TG2 could hold promise as a potential target to reduce monocyte and macrophage infiltration and thus as add on therapy in MS. Considering the remaining uncertainty as to the cellular localization of TG2 in MS lesions and its potential impact on therapeutic approaches using modulation of TG2 activity, in the present study we questioned whether TG2 is expressed by monocytes and

macrophages or by lymphocytes present in (chronic) active white matter MS lesions. In addition, we studied if a macrophage subtype expressing TG2 can be established in these lesions.

MATERIALS AND METHODS

Brain tissue

Human post-mortem tissue from MS patients and non-neurological control subjects was obtained from the Pathology department of the Amsterdam University Medical Center and the Netherlands Brain Bank (Amsterdam, The Netherlands). The subcortical white matter tissue contained active or chronic active MS lesions as classified by and the presence of HLA-DR positive cells and loss of myelin [16, 177]. We studied post-mortem material of 13 clinically diagnosed and pathologically verified MS patients. All tissue samples contained TG2-immunopositive cells, although with a high variation in the number of immunoreactive cells. To be able to better characterize TG2 expressing cell type(s), we selected four of the 13 MS cases (Table 1, #1,2,3,7) with a total of 9 active/chronic active lesions and a relatively high number of TG2-immunopositive cells. In addition to these selected MS patients (average age 47 ± 5.7 years), six non-neurological control subjects (Table 1, average age 58.8 ± 2.9 years) were included. All subjects were matched for post-mortem delay. The clinicopathological data of the patients and control donors are summarized in Table 1. Informed consent was given by the donors for brain autopsy and the use of brain tissue for research purposes. The use of tissue in combination with the clinical information for scientific research was in compliance with the local ethical and legal guidelines.

Tissue processing

The snap-frozen brain tissue was cut in 10 µm thick cryo-sections. Sections were mounted on positively charged glass slides (SuperFrost Plus slides, Fisher Scientific, Pittsburgh, PA). After drying for 30 min at 37 °C, the dry slides were stored until use at -80 °C.

Lesion classification and selection

White matter MS lesions were classified by standard immunohistochemical stainings for myelin-specific proteolipid protein (PLP) and the major histocompatibility complex class II receptor HLA-DR, a marker for inflammatory cells, as described previously [232]. Active and chronic active lesions with ongoing demyelination were selected by the presence of foamy macrophages and neutral lipids by Oil Red-O staining.

Active (inflammatory) lesions were identified by the massive presence of HLA-DR and Oil Red-O positive cells throughout the lesion area. Chronic active lesions were characterized as lesions that had a broad active rim of HLA-DR and Oil Red-O positive cells combined with reduced cell numbers in the center of the lesion.

Immunohistochemistry

Sections were thawed, air-dried and fixed in acetone for 10 min (60 min for delipidation when used for PLP staining). In addition, sections were rinsed for 5 min with 50 mM Tris-buffered saline ([TBS]; pH 7.4), followed by incubation for 20 min with 0.3 % H_2O_2 in TBS including 0.1 % sodium azide to quench endogenous peroxidases. Non-specific binding of antibodies was blocked for 30 min with 3 % bovine serum albumin ([BSA] Sigma–Aldrich) in TBS containing 0.5 % TritonX-100 ([TBS-T] Sigma–Aldrich).

Single antigen detection

Single stainings were performed for HLA-DR, PLP and TG2 (see Table 2). Sections were incubated with primary antibodies overnight at 4°C in 3 % BSA in TBS-T) After washing with TBS, a 2-h incubation at room temperature followed with donkey anti-goat or goat anti-mouse biotinylated IgGs (dilution 1:400, 3 % BSA in TBS-T [Jackson ImmunoResearch Laboratories Inc., West Grove, PA]). After washing using TBS, the sections were incubated for 1 h at room temperature with HRP-labeled avidin-biotin complex ([ABC] 1:400 dilution, Vector Laboratories, Burlingame, CA). Detection of immunoreactivity was performed by adding chromogen 3,3-diaminobenzidine ([DAB] Sigma-Aldrich) and 0.01% hydrogen peroxide in Tris-HCl buffer (pH 7.6) to the sections. Nuclear counterstaining with hematoxylin was applied. Sections were dehydrated in graded ethanol solutions and cleared in xylene, before cover-slipping with Entellan mounting medium (Merck Millipore, Darmstadt, Germany). To ensure TG2 antibody specificity, the anti-TG2 antibody was pre-adsorbed with excess recombinant TG2 protein as follows. Recombinant guinea pig TG2 (2 units, Sigma-Aldrich) was mixed with 1.5 ml of a 1:10 000 dilution of the TG2 antibody and incubated at 4 °C for 6 h. Subsequent tissue staining was performed as described above, using this mixture as the primary antibody.

Co-labeling of antigens

To identify the cell type immunopositive for TG2, we co-labeled TG2 with immune markers for general leukocytes (CD45), pan-T cells (CD3), pan-B cells (CD20) and macrophages (CD11b, CD68, CD163, CD206, CX3CR1; Table 2). The fixed and pre-treated sections were incubated with primary antibody directed to one of the immune markers, diluted in TBS-T with 3 % BSA. Incubation was performed for 1 h at room temperature or overnight at 4 °C (no differences observed in the protocol used). After washes in TBS, ImmPRESS™ alkaline phosphatase (AP) reagent directed to mouse or rabbit IgGs (Vector Laboratories) was added to the sections for 30 min. Subsequently, slides were rinsed with TBS and Tris-HCl and then developed with liquid permanent red (LPR) as substrate (according to manufacturer, Dako, Glostrup, Denmark).

Table 1: Clinicopathological characteristics of MS patients and control subjects

#	Sex	Age	Type of tissue	MS disease duration (years)	PMD (h:min)	Cause of death
1	m	41	MS	14	7:20	Pneumonia, urosepsis
2	m	44	MS	22	10:15	General deterioration / infection
3	m	49	MS	25	8:00	Pneumonia
4	f	50	MS	17	7:35	Euthanasia
5	f	50	MS	12	9:05	Euthanasia
6	m	51	MS	>20	11:00	Unknown, infection 2 days prior to death
7	f	54	MS	13	9:25	Unclear, most likely respiratory failure
8	m	54	MS	21	8:15	Euthanasia
9	f	60	MS	7	10:40	Euthanasia
10	m	64	MS	35	7:30	Euthanasia
11	f	66	MS	22	6:00	Unknown
12	f	66	MS	23	9:35	Euthanasia
13	f	66	MS	17	10:45	Pulmonary hypertension
14	m	55	control	-	7:30	Euthanasia with oesophageal cancer
15	f	57	control	-	7:40	Euthanasia with metastatic urothelial cancer
16	m	57	control	-	9:45	Multi-system atrophy
17	f	60	control	-	7:30	Infection, fever of unknown origin
18	f	62	control	-	7:55	Unknown
19	m	62	control	-	7:20	Unknown

PMD: post-mortem delay

Oil Red-O staining

Neutral lipids, present in macrophages and indicative of myelin phagocytosis and degradation, were detected with Oil Red-O staining. An Oil Red-O stock solution of 0.5 g Oil Red-O (Sigma-Aldrich) in 100 ml isopropanol was prepared. After 3:2 dilution with distilled water and filtration, unfixed tissue sections were incubated for 10 min at room temperature. This was followed by a rinse with water, nuclear hematoxylin counterstaining and cover slipping with aquatex (Merck Millipore).

Table 2: Primary antibodies used in immunohistochemistry

Target	Origin	Dilution	Supplier	Article code
HLA-DR (LN3)	mouse	1:1,000	Pierce (Rockford, Illinois, USA)	MA5-11966
PLP	mouse	1:1,000	AbD Serotec (Oxford, UK)	MCA839G
TG2	goat	1:10,000	Upstate(via Merck Millipore, Darmstadt, Germany)	06-471
CD3	rabbit	1:3,000	Dako (Glostrup, Denmark)	A0452
CD11b	mouse	1:500	Abcam (Cambridge, UK)	ab34216
CD14	mouse	1:400	Dako (Glostrup, Denmark)	M0825
CD20	mouse	1:2,000	Dako (Glostrup, Denmark)	M0755
CD45	mouse	1:2,000	Dako (Glostrup, Denmark)	M0701
CD68	mouse	1:20,000	Dako (Glostrup, Denmark)	M0718
CD163	mouse	1:8,000	Gift, dept. Molecular Cell Biology and Immunology, VUmc, Amsterdam, The Netherlands	-
CD206	mouse	1:8,000	Abcam (Cambridge, UK)	ab8918
CX3CR1	rabbit	1:3,000	Abcam (Cambridge, UK)	ab8020

Subsequently, the sections were incubated with goat anti-TG2 antibody for 1 h at room temperature. Washing steps with TBS and Tris-HCl were followed by incubation with ImmPRESS™ horseradish peroxidase (HRP) anti-goat IgG reagent (Vector Laboratories) for 30 min at room temperature. The reagent was washed off with TBS and Tris-HCl and the signal developed with 3,3-diaminobenzidine (DAB, Sigma-Aldrich). Finally, slides were washed in Tris-HCl and tap water, counterstained with hematoxylin and mounted with an aqueous mounting medium containing mowiol (24 g glycerol, 24 ml distilled water, 48 ml 0.2 M Tris buffer, pH 8.5, 9.6 g mowiol 4-88 [Sigma-Aldrich]) and dried at 4 °C.

For all immunostainings, negative controls, the omission of the primary antibodies on several sections, served as the control for unspecific IgG binding and resulted in no staining (data not shown).

Image acquisition and semiquantitative analysis of immunopositive cells

Immunohistochemical images of 4-12 regions of interest ([ROI], 690 µm by 665 µm) per patient were acquired with Leica DM5000B microscope (Leica Microsystems, The Hague, The Netherlands) equipped with a spectral imaging camera (Nuance, PerkinElmer, Waltham, MA). Semiquantification of co-labeled cells was performed by assessment of the numbers of TG2-positive cells that were also immunopositive for one of the immune cell markers. For this purpose, the slides were imaged according to the Nuance user manual (provided by PerkinElmer, Waltham, Massachusetts, USA). In short, for each chromogen, that is DAB, LPR and hematoxylin, the specific emission spectrum was acquired and characterized with the Nuance software based on light absorbance/scattering. Acquired spectral images from the triple chromogen stainings were separated into the three individual channels using the predefined spectra. The manually counted number of TG2-

positive cells per patient varied from 45 to 295 cells, depending on the number of ROIs size and the numbers of available tissue blocks per patient. To handle variation in cell numbers, we determined the number of TG2 cells co-labeling with one of the immune cell markers as a percentage of total TG2-positive cells counted per patient. Images that were taken from bright field microscopy are shown pseudo-colored in the style of fluorescent stainings to increase visual contrast.

RESULTS

The 9 analyzed MS lesions were classified as active (n=1) or chronic active (n=8) by immunohistochemistry, using the above-described criteria. The general marker for antigen-expressing cells, HLA-DR, demonstrating lesion activity, was abundantly present in all MS lesions either in the center (active lesion) or in a broad rim surrounding the lesion (chronic active lesion; Fig A, B). Reduction in anti-PLP antibody immunoreactivity indicated demyelination which was partial or complete in all lesions (Fig 1D, E). To further classify the activity state of the lesions, Oil Red-O staining was performed. The intense red cellular staining specified myelin ingested by macrophages in all analyzed lesions, suggesting ongoing demyelination (Fig 1G, H). Brain tissue obtained from control patients showed very little HLA-DR expression (Fig 1C), no loss of anti-PLP immunoreactivity (Fig 1F), and no Oil Red-O staining signal (Fig 1I).

TG2 immunoreactivity in MS lesions

TG2 was commonly present in blood vessels in tissue from control subjects (Fig 2A, arrowhead) and in MS normal appearing white matter (NAWM, Fig 2B, arrowhead) and MS lesions (Fig 2C, arrowhead). In inflammatory active and chronic active MS lesions, additional TG2-positive ($TG2^+$) round cells were found in the perivascular cuff, the lesion area surrounding the blood vessels and in the parenchyma (Fig 2C, arrows). This cellular TG2 immunoreactivity was neither observed in inactive lesions (not shown), in normal appearing white matter of MS patients nor in control brain tissue, as shown previously by our group [229]. Pre-adsorption of the TG2 antibody with recombinant TG2 protein resulted in absence of cellular TG2 staining in MS lesions with only a slight residual vascular staining remaining (Fig 2D, arrowhead), indicating the specificity of the immunostaining.

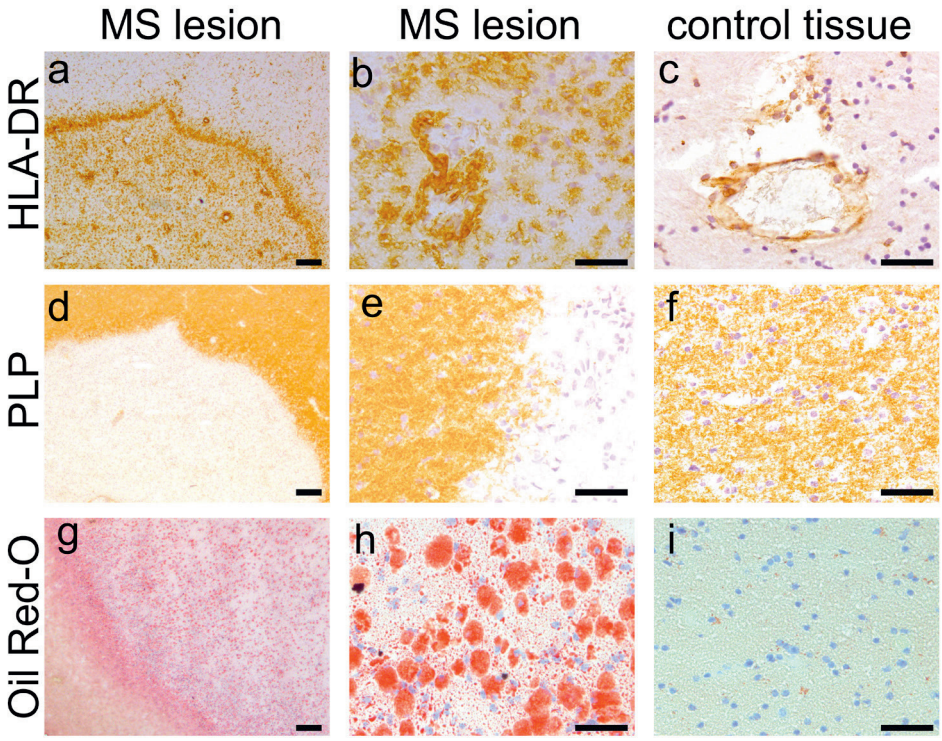


Figure 1: MS white matter lesion classification with PLP, HLA-DR, and ORO immunohistochemical staining. HLA-DR (A–C), PLP (D–F), and ORO (G–I) staining of postmortem MS lesion tissue (2 magnifications of 1 lesion each) and control tissue (C, F, I). Scale bars: B, C, E, F, H, I =50 µm; A, D, G = 200 µm. Abbreviations: HLA-DR, human leukocyte antigen-D related; PLP, myelin proteolipid protein; ORO, Oil Red O.

Characterization of $TG2^+$ cells in MS lesions

For cell type characterization of $TG2^+$ cells in MS lesions, we first stained post-mortem tissue with various immune cell markers, followed by co-labeling with TG2-antibodies and subsequent analysis.

TG2 immunoreactivity is present in leukocytes

The majority of $TG2^+$ cells found in active MS lesions appeared as round cells, characteristic of infiltrated leukocytes. Therefore, we performed a double labeling of the TG2 antibody (Fig 3A) with the general leukocyte marker CD45 (Fig 3B). We found numerous cells demonstrating both CD45 and TG2 immunoreactivity (Fig 3C arrow and inserts). After quantification of the amount of $TG2^+$ cells that are $CD45^+$, we observed that approximately 70 % of the $TG2^+$ cells were leukocytes (Fig 3D).

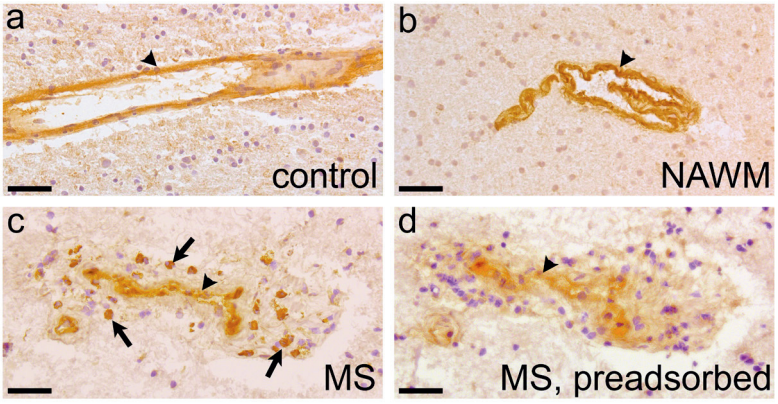


Figure 2: TG2 expression in white matter MS lesions and control tissue. (A–C) Vascular immunohistochemical TG2 staining (arrowhead) was observed in healthy control tissue (A), normal appearing white matter (NAWM) tissue of MS patients (B), and MS tissue (C). Additionally, cellular TG2 staining outside the vasculature (arrow) was not observed in control tissue (A) or NAWM (B), whereas in MS patient-derived tissue (C) some cells were strongly stained. (D) The antiTG2 immunoreactivity was strongly reduced after pre-adsorption of the TG2 antibody with recombinant TG2 protein. Scale bar: 50 µm.

TG2 immunoreactivity in lymphocytes

To further characterize $TG2^+$ leukocytes, we used markers that stain specific leukocytes subsets. First, we studied lymphocytes, i.e. T- and B cells, using CD3 and CD20 as pan-markers, respectively. In the MS lesions, especially around larger blood vessels, where also $TG2^+$ cells were present (Fig 4A, E), $CD3^+$ T cells (Fig 4B) and $CD20^+$ B cells (Fig 4eE were found. Although CD3 (Fig 4A-D) and CD20 immunoreactivity (Fig 4E-F) were present in numerous cells, these hardly co-localized with TG2 as shown in the overlay of both stainings (Fig4C, G). Quantification of the co-labeled cells indicated that of the $TG2^+$ cells only 3.8 % and 2.3 % were identified as T and B cells, respectively (Fig 4D, H).

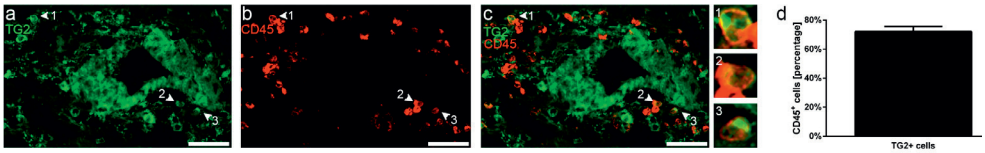


Figure 3: AntiTG2+ cells in MS lesions are positive for the leukocyte marker CD45. (A) $TG2^+$ cells (arrowheads) surrounding a blood vessel in a MS lesion. (B) Cells immunoreactive for the antiCD45 antibody (arrowheads). (C) Double staining of TG2 and CD45 indicates immunoreactivity for antiTG2 antibody in $antiCD45^+$cells (arrowheads, magnified inserts). (D) Quantification of $TG2^+$ cells immunoreactive for the antiCD45 antibody. Scale bar: 50 µm. Bar: standard error of the mean (SEM).

TG2 immunoreactivity in macrophage subtypes

Another subset of leukocytes found in MS lesions is of the monocyte and macrophage type. For their analysis as potential TG2 expressing cells, a broad panel of different cell markers was used. These markers are also known to be expressed by parenchymal microglia, depending on their activation status [233, 234]. Studying the MS lesions for

macrophages and $TG2^+$ cells (Fig 5A, E, I, M), many round cells representing monocytes and macrophages were present in these areas. First, we studied the population of $CD14^+$ cells in MS lesions (Fig 5B). We found numerous $CD14^+$ monocytes in close vicinity to blood vessels but also spread throughout the lesion. Most of them showed limited co-localization with TG2 staining (3.5 % co-labeling, Fig 5C, D). The two macrophage markers used were CD11b, a pan macrophage marker and CD68, a lysosomal marker for phagocytic active macrophages [235]. Both markers, i.e. CD11b (Fig 5F) and CD68 (Fig 5J), were present in cells in the lesion areas. Their co-labeling with TG2 staining resulted in 45 % of $TG2^+$ cells being $CD11b^+$ macrophages (Fig 5G,H) and 11 % were positive for CD68 (Fig 5K, L). Another cell surface macrophage marker, i.e. CX3CR1 [236], is expressed in MS lesions but also only showed limited co-localization (5.3 %) with TG2 staining (Fig 5N, O, P).

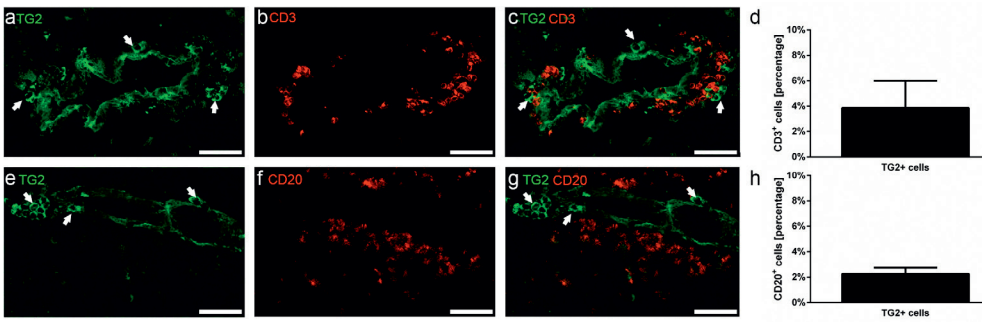


Figure 4: AntiTG2 antibody immunoreactivity in MS lesions was absent in lymphocytes. $TG2^+$ cells (arrows) surrounding a blood vessel in a MS lesion (A, E). (B) B cells present in MS lesions were detected using the B cell-specific marker CD20. (C) Double staining of antiCD20 antibody and anti$TG2^+$ cells showed (D) very little overlap of these 2 markers (arrows) and therefore limited expression of TG2 in B cells. (F) CD3 expression indicated the presence of T lymphocytes, but a merge of antiTG2 and antiCD3 antibody staining (G) revealed that both markers were expressed in different cell types (arrows), as quantified in (H). Scale bar: 50 µm. Bar: SEM.

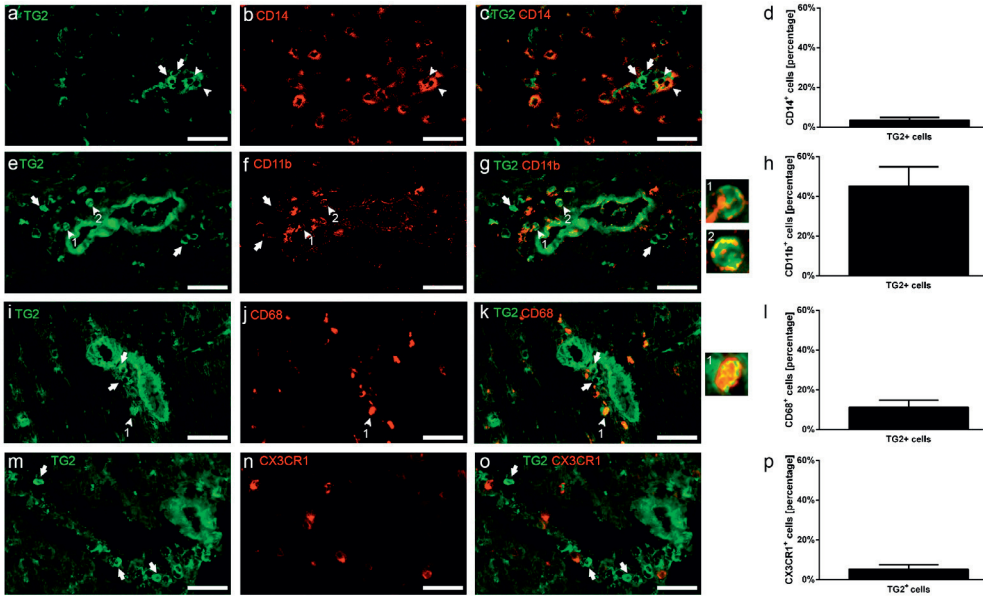


Figure 5: Abundant antiTG2 antibody immunoreactivity in monocyte/macrophages associated with MS lesions. (A, E, I, M) TG2$^+$ cells (arrows, arrowheads) surrounding blood vessels in MS lesions. (B) CD14$^+$-immunoreactive monocytes (arrowheads) were found in MS lesions. (C, D); however, few of the antiCD14$^+$ cells expressed TG2 (arrowheads), whereas the majority did not show immunoreactivity for antiTG2 antibody (arrows). (F) CD11b expression was found in lesions (arrowhead) and (G, H) approximately half of the CD11bþ$^+$cells expressed TG2$^+$ (arrowheads, magnified inserts). (J) CD68, a lysosomal macrophage marker, was present in MS lesions and (K, L) antiTG2 antibody immunoreactivity was present (arrowheads, magnified insert) in some but not all (arrows). (N). Another cell surface macrophage marker, CX3CR1, was expressed in MS lesions but (O, P) little co-localization with the antiTG2 antibody immunoreactivity was found (arrows). Arrows indicate TG2$^+$ cells that did not correspond to one of the monocyte or macrophage markers. Arrowheads indicate monocytes or macrophages showing immunoreactivity for the antiTG2 antibody. Scale bar: 50 µm. Bar: SEM.

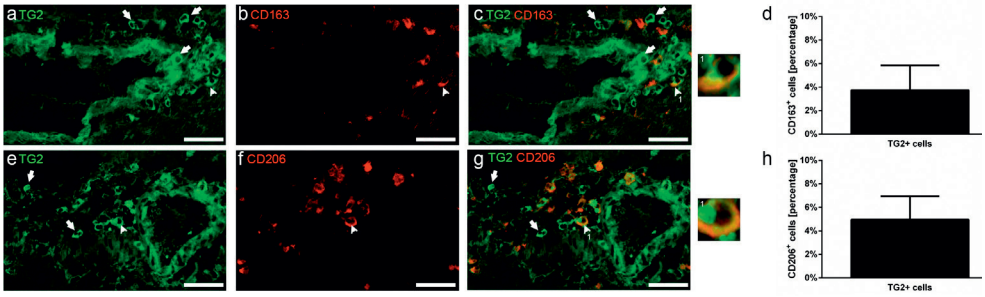


Figure 6: Expression of TG2 in alternatively activated (M2) type macrophages. (A, E) TG2$^+$ cells surrounding a blood vessel in a MS lesion (arrows, arrowheads). M2 macrophages were found in MS lesions as indicated by antiCD163 antibody (B) and antiCD206 antibody (F) immunoreactivity; however, only small proportions were found to be immunoreactive for the antiTG2 antibody in these M2 macrophages (C, D/G, H, arrowheads, magnified inserts) whereas TG2 staining was absent in the majority of M2 type cells (arrows). Scale bar: 50 µm. Bar: SEM.

As TG2 has been qualified as a marker for alternatively activated macrophages (M2) [237], we further characterized whether $TG2^+$ cells co-label with markers for alternatively activated macrophages, i.e. CD163 and CD206 [38]. In the area of $TG2^+$ cells in the lesions (Fig 6A, E) both CD163 (Fig 6B) and CD206 (Fig 6F) were present. Co-labeling of TG2 and the M2 markers (Fig 6C,G), however, resulted in only small numbers of double stained cells, i.e. CD163 was expressed in 3.8 % and CD206 in 5 % of the $TG2^+$ cells in the MS lesions (Fig 5P,T).

The results of the semi-quantification of $TG2^+$ cells co-labeling with immune cell markers in inflammatory MS lesions are summarized in Table 3.

Table 3: TG2 and Immune Cell Marker Co-localization in MS Lesions

Immune marker	% of TG2 cells positive for immune marker	Standard deviation (%)
CD45	72.16%	10.50%
CD3	3.85%	6.46%
CD20	2.27%	1.45%
CD14	3.52%	3.97%
CD11b	45.02%	29.06%
CD68	11.21%	9.89%
CX3CR1	5.29%	6.77%
CD163	3.74%	6.32%
CD206	4.96%	5.95%

DISCUSSION

Novel treatments of MS focus mainly on lymphocytes as a therapeutic target, but there is heterogeneity between MS lesions and patients with regard to the pathological features. Therefore, other cell types, in particular monocytes and macrophages, may be of interest as a potential target. TG2 plays a role in monocyte/macrophage migration and the aim of the present study was to examine TG2 expressing cell types in MS lesions in detail.

As the variation in the number of $TG2^+$ cells is high in different types of MS lesions, we included only active and chronic active lesions with still significant HLA-DR staining in the rim and a relatively high number of $TG2^+$ cells. The reason for the variation in TG2 expression between MS patients remains unsolved, but can potentially be related to e.g. disease duration and the clinical status of the patient. Since TG2 is upregulated under inflammatory conditions [230] it can be mostly seen in active or chronic active lesions with substantial leukocyte infiltration. With ongoing disease, the inflammation and cellular infiltration recede which in turn might reduce the expression of TG2 [238].

The main observation of our study is that the vast majority (~70 %) of $TG2^+$ cells are $CD45^+$ and display a round morphology, indicative of leukocytes infiltrated from the circulation. In our previous study, the $TG2^+$/HLA-DR-positive cells also had a round morphology [229] and thus likely represent a (sub)population of infiltrated leukocytes. To

further delineate the cell type(s) expressing TG2, we analyzed the two most abundant leukocyte cell types found in MS lesions, i.e. lymphocytes and monocytes/macrophages. Both $CD3^+$ T cells and $CD20^+$ B cells were hardly associated with $TG2^+$ cells, despite the fact that lymphocytes, together with monocytes and macrophages, migrate into the CNS as a part of MS pathology [216, 239]. We, therefore, propose that the migration process of lymphocytes into the CNS in MS may be independent of TG2 in lymphocytes, which is in line with previous rodent MS models in which lymphocyte migration was not affected by TG2 inhibition (29, 43). In addition, we determined the presence of TG2 in monocytes and macrophages. $CD14^+$ monocytes showed limited TG2 immunoreactivity. However, in circulating monocytes derived from MS patients, low but increased TG2 mRNA levels were present compared to control monocytes [240]. Still, these mRNA levels may not result in sufficient levels of protein to be detected by immunohistochemistry. It is also possible that the $TG2^+$ monocytes mostly remain in the circulation with a minority entering the CNS. TG2 immunoreactivity was clearly present in $CD11b^+$ cells. Although CD11b can also be expressed by natural killer cells and granulocytes in addition to macrophages, these cell types are rather scarce in MS lesions compared to macrophages [241-243]. Hence, we assume that the majority of the $TG2^+$ round $CD11b^+$ cells is of the macrophage lineage [119, 244].

Nowadays, macrophages are often subdivided into homeostatic (M0), classically activated (M1) and alternatively activated (M2) macrophages, based on a certain cell marker expression profile *in vitro* [245]. Depending on their phenotype they might adopt different functions that can be either beneficial or detrimental. Our data of TG2 immunoreactivity in a number of $CD68^+$ macrophages, i.e. macrophages with lysosomal activity may suggest that TG2 contributes to phagocytosis of, for example, myelin debris. Also, a role for TG2 in the process of efferocytosis, i.e. phagocytosis of apoptotic cells, has clearly been established [246-248]. However, CX3CR1, an important factor in the clearance of myelin debris [249], and TG2 co-expression proved limited in $CX3CR1^+$ cells in MS lesions. Together, these data suggest that if macrophage-derived TG2 contributes to the clearance of myelin debris, its impact may be limited. Generally, lysosomal active macrophages have been shown to have an anti-inflammatory signature [250] and it has been shown that TG2 expression is increased in M2 macrophages *in vitro* [237, 251]. In the MS lesions studied, we could not confirm that TG2 is only expressed by anti-inflammatory M2 macrophages. Still, the low number of $TG2^+$ cells that co-label with M2 markers may represent macrophages involved in phagocytosis and/or efferocytosis. We cannot rule out that also macrophages of the M1 type can be $TG2^+$ representing another subpopulation of the $CD11b^+$ or $CD68^+$ macrophages. Altogether, it is of importance to note that macrophages present in MS lesions are predominantly of an intermediate phenotype [38], which may explain our finding of relatively low numbers of $TG2^+$ anti-inflammatory macrophages in MS lesions.

With our analyses, we characterized the majority of the $TG2^+$ cells to be leukocytes of which the majority is of the monocyte/macrophage lineage. However, our analysis did not allow us to determine the lineage of the remaining 30 % of cells. One possibility is that their expression of our analyzed markers was too low to be detected in our immunohistochemical assays. For example, CD45 expression in microglia might be

below our detection limit [252]. In addition, we cannot exclude that certain subtypes of lymphocytes that are neither $CD3^+$ nor $CD20^+$ might be expressing TG2. Additional studies are needed to enlighten the identity of these cells and their potential effects when considering TG2 a potential target in the therapeutic treatment of MS patients.
Concluding, based on our observations we state that TG2 is largely expressed by cells of the monocyte/macrophage lineage in MS lesions. The $TG2^+$ macrophage phenotype cannot be clearly classified as M1 or M2 and hence a potential dual role of macrophage-derived TG2 in MS lesion pathology is possible. Our observations in animal models of MS supported a role for monocyte/macrophage-derived TG2 in cell adhesion and migration contributing to the disease process [229]. As we observed that TG2 contributes to human monocyte adhesion and migration *in vitro* [240], this could also hold true for the *in vivo* disease situation. Therefore, monocyte/macrophage-derived TG2 could be a potential target for intervention during MS that adds to the available lymphocyte focused therapies and broadens the spectrum of cells targeted in the heterogeneous MS lesions.

Acknowledgements

We thank Wouter H. Gerritsen, dept. of Pathology, Amsterdam UMC, for his assistance with the Oil Red-O staining. Furthermore, we thank the department of Molecular Cell Biology and Immunology, Amsterdam UMC, for the kind gift of the anti-CD163 antibody.



Chapter 4

MONOCYTE BEHAVIOR AND TISSUE TRANSGLUTAMINASE EXPRESSION DURING EXPERIMENTAL AUTOIMMUNE ENCEPHALOMYELITIS IN TRANSGENIC CX3CR1$^{GFP/GFP}$ MICE

Amino Acids. 2017 Mar;49(3):643-658

ABSTRACT

Leukocyte infiltration into the central nervous system (CNS) is a key pathological feature in multiple sclerosis (MS) and the MS animal model experimental autoimmune encephalomyelitis (EAE). Recently, preventing leukocyte influx into the CNS of MS patients is the main target of MS therapies and insight into cell behavior in the circulation is needed for further elucidation of such therapies. In this study, we aimed at *in vivo* visualization of monocytes in a time-dependent manner during EAE. Using intravital two-photon microscopy (IVM) we imaged CX3CR1$^{gfp/gfp}$ mice during EAE, visualizing CX3CR1-GFP^{+} monocytes and their dynamics in the spinal cord vasculature. Our observations showed that the intraluminal crawling of CX3CR1-GFP^{+} monocytes increased even before the clinical onset of EAE due to immunization of the animals. Furthermore, intraluminal crawling remained elevated during on-going clinical disease. Besides, the displacement of these cells was larger during the peak of EAE compared to control animals. In addition, we showed that the enzyme tissue Transglutaminase (TG2), which is present in CNS infiltrated cells in MS patients, is likewise found in CX3CR1-GFP^{+} monocytes in the spinal cord lesions and at the luminal side of the vasculature during EAE. It might thereby contribute to adhesion and crawling of monocytes, facilitating extravasation into the CNS.

Thus, we put forward that interference with monocyte adhesion, by e.g. inhibition of TG2, should be applied in a very early stage of EAE and possibly MS, to effectively combat subsequent pathology.

Navina L. Chrobok[1], Alexandre Jaouen[2], Keith K. Fenrich[2], John G.J.M. Bol[1], Micha M.M. Wilhelmus[1], Benjamin Drukarch[1], Franck Debarbieux[2] and Anne-Marie van Dam[1]

[1]VU University Medical Center, Amsterdam Neuroscience, Dept. Anatomy and Neurosciences, Amsterdam, The Netherlands; [2]Aix Marseille Université, Campus de la Timone, Developmental Biology Institute of Marseille, European Research Center for Medical Imaging, Marseille, France

INTRODUCTION

Multiple sclerosis (MS) is a chronic inflammatory and demyelinating disease of the central nervous system (CNS) that manifests in a wide range of clinical symptoms including sensory, motor and cognitive disabilities [212, 253]. About 85% of MS patients show a relapsing-remitting disease course with a pathological inflammatory phenotype characterized by a massive influx of leukocytes from the circulation into the CNS [254]. This cellular influx results in a local production of inflammatory mediators, activation of resident glial cells, demyelination, oligodendrocyte cell death and eventually axonal damage [254]. So far, preventing the influx of leukocytes is the main target of recently developed MS therapies. For instance, the drug natalizumab blocks α4β1-integrin and thereby largely prevents interaction of leukocytes with the endothelium [255].

Of the infiltrating leukocytes in MS, monocytes were shown to be essential for the development of clinical symptoms as investigated in experimental autoimmune encephalomyelitis (EAE), a well-known animal model of MS [225, 256]. Infiltration into the CNS requires an orchestrated collaboration of chemokines and adhesion molecules from the inflamed endothelium and their receptors on monocytes. Monocytes in the bloodstream first roll on the activated and inflamed endothelial lumen, before they strengthen their adherence and crawl along the lumen to find an extravasation site into the inflamed CNS or they detach and continue their journey in the vasculature [215, 257, 258].

The multifunctional enzyme tissue Transglutaminase (TG2) has been described to be involved in cell apoptosis and monocyte and macrophage adhesion and migration on fibronectin, a constituent of the extracellular matrix (ECM) *in vitro* [119, 121]. TG2 is up-regulated under inflammatory conditions and was shown to be present in monocytes in active CNS lesions during MS and EAE [108, 229]. Monocyte attachment to the endothelium and also differentiation into macrophages leads to a boost in TG2 expression [259, 260]. TG2 present on the surface of monocytes and macrophages can act as a co-receptor for β1- and β3-integrins, which are crucial for the adhesion of monocytes [119, 261]. This interaction with integrins enhances the affinity of the cells for extracellular matrix proteins, e.g. fibronectin, and therefore promotes monocyte adhesion and migration [119]. Recent studies from our and other groups have shown that knock-down of TG2 or pharmacological inhibition its activity in rodents suffering from EAE led to reduced disease symptoms [198, 229]. This could, at least partly, be explained by limited monocyte migration into the CNS [229], but no detailed information about cellular behavior *in vivo* in this context is known yet

Nowadays, the presence of demyelinating lesions in MS animal models can be visualized *in vivo* by magnetic resonance imaging (MRI) [262]. Furthermore, intravenous injection of a contrast enhancing agent reveals blood-brain barrier leakage in MRI, suggesting the presence of infiltrating cells but not providing information about the cell types being present [262]. Phagocytic cells in the lesions can be identified by MRI after injection of ultra-small super paramagnetic iron oxide (USPIO) particles or USPIO-labeled antibodies specific for cell surface receptors [262-264]. Although these techniques are non-invasive and provide relevant *in vivo* information on lesion formation, they lack

detailed analysis and high resolution of specific cell types present in the spinal cord vasculature before and during clinical symptoms.

As we consider monocytes as important players during the onset and development of clinical symptoms of MS and EAE [254], the aim of the present study is to investigate the interaction of monocytes with the spinal cord vasculature of EAE mice. For this purpose, we used transgenic CX3CR1$^{gfp/gfp}$ mice which express green fluorescent protein (GFP) instead of the chemokine receptor CX3CR1. This genetic modification results in green labeled monocytes and microglial cells. We imaged these CX3CR1-GFP^{+} cells with intravital two-photon microscopy (IVM), before and during symptomatic disease. Moreover, we analyzed the presence of immunoreactive TG2 and Caspase-3 in the spinal cord lesions previously analyzed by IVM.

MATERIALS AND METHODS

Animals

Adult homozygous CX3CR1$^{gfp/gfp}$ mice of 7 weeks of age and older were used in this study [265]. All animal experiments and surgical procedures were approved by the National Animal Studies Committee of France (authorization no. 13,300), as well as approved and authorized by the National Committee for Ethic in Animal Experimentation (Section N°14; project 86-04122012). The experimental setup of the presented study is depicted in Figure 1a.

Spinal cord surgery and window implantation

Microsurgical implantation of a spinal cord window was performed as described previously [266, 267]. Briefly, the mouse spinal cord was exposed from thoracic vertebra 13 (T13) to lumbar vertebra 1 (L1), and a piece of glass was fixed over the exposed spinal cord to provide permanent optical access to the exposed spinal cord (Figure 1b). A few hours past the window implantation, the animals were highly mobile and showed little or no signs of pain. Importantly, animals with implants groomed and behaved normally, did not show any signs of motor dysfunction, and continued to gain weight. After window implantation, a layer of vascular tissue can develop between the window and CNS tissue [266-268]. To limit the thickness and optical density of this vascular tissue and to provide post-operative analgesia and anti-inflammatory treatment, dexamethasone (0.2 mg/kg) and rimadyl (5 mg/kg) were injected subcutaneously every other day for 10 days.

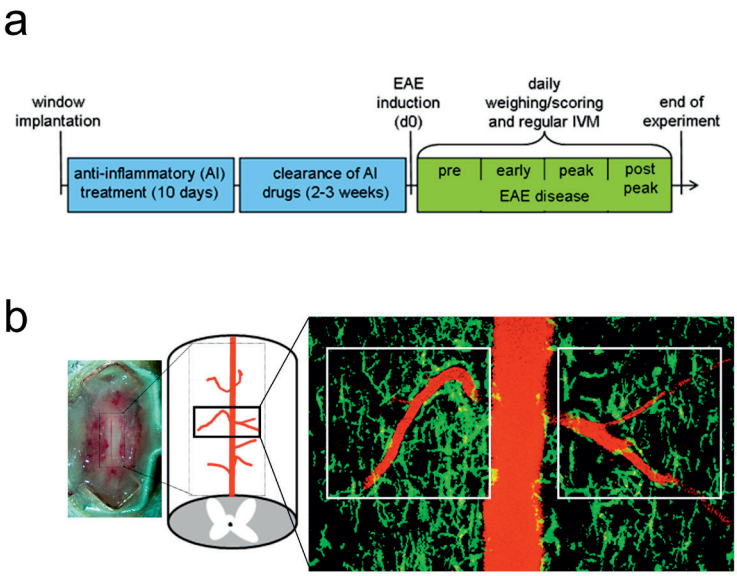


Figure 1: Setup of the experimental procedure. (a) Spinal cord window implantation is followed by anti-inflammatory treatment and a 2-3 week clearance period before EAE induction and IVM; (b) IVM imaged area of the spinal cord included the venules draining into the central dorsal vein around the vertebrae level T13 to L1.

Induction of EAE

EAE was induced 3-4 weeks after window implantation (i.e. 2-3 weeks after cessation of analgesic and anti-inflammatory treatment) when the window was clear and no fibrosis or signs of inflammation were visible. The entire experimental scheme is shown in Figure 8a. Mice were lightly anesthetized with isoflurane (Baxter, 1.75 % in air (v/v) for 1-2 min) to protect the spinal cord window from any strain due to mouse handling during EAE induction. Mice were injected subcutaneously in each flank and the base of the tail with a total of 75 µg myelin oligodendrocyte protein peptide ($MOG_{35–55}$, Tocris) in complete Freund's adjuvant (CFA), containing 800 µg mycobacterium tuberculosis (BD Biosciences). In addition, mice received 400 ng pertussis toxin in PBS (Sigma Aldrich) intraperitoneally on the day of immunization and two days later. Animals were weighed and clinical symptoms assessed daily, as described before [269]: 0: no detectable clinical signs, 0.5: partial tail weakness, 1: tail paralysis, 1.5: gait instability and/or impaired righting ability, 2: hind limb paresis, 2.5: hind limb paresis with partial dragging, 3: hind limb paralysis, 3.5: hind limb paralysis and forelimb paresis, 4: hind limb and forelimb paralysis, 5: moribund.

Two-photon intravital imaging

For each imaging session mice were anesthetized with 1.75 % isoflurane for 2 min, followed by intraperitoneal injection of ketamine (100 mg/kg) and xylazine (10 mg/kg). For sessions exceeding 1 hour, light anesthesia was maintained with 0.2–0.75 % isoflurane starting from about 45 min after the begin of the imaging session until completion. To acquire a visual contrast of blood vessels during imaging, mice were injected with either 2 µg of QDot-655 (Qtracker 655, non-targeted quantum dots; Invitrogen) or 2.4 mg

rhodamine B isothiocyanate-dextran 70 kDa (Sigma) in PBS, immediately before data acquisition via the tail vein or retrobulbal injection. A tunable femtosecond pulsed laser (Mai-Tai, Spectra-Physics) was used at 900 nm wavelength and coupled to an upright two-photon microscope (Zeiss, LSM 7MP) with a 20X water immersion objective lens (NA = 1.0) and five non-descanned detectors. The spinal cord window and the imaged area are shown in Figure 8b. The imaged vessels included the left and right venules draining into the central dorsal vein of the murine spinal cord. An area of 212.55x212.55 µm with a resolution of 0.41 µm per pixel and 5 µm distance between the individual planes of the stacks was scanned. 30 to 50 µm deep stacks were acquired with an acquisition rate of one plane per second. The imaging duration of the individual videos varied from 7:23 to 19:05 min and contained 35 to 80 stacks.

Analysis of CX3CR1-GFP$^+$ cells in the circulation

Videos and images were analyzed with the ZEN lite software (Zeiss) and Fiji with the MTrackJ plug-in [270, 271]. IVM analysis was performed on raw data, but IVM figures shown here were pseudo-colored as well as contrast enhanced.

To analyze the behavior of GFP$^+$ cells in the blood vessels of the spinal cord, the cells were separated into two groups: (1) fast moving cells, which shortly interact with the endothelium, and (2) crawling cells that interact extensively (>25 seconds) with the endothelium. The presented data reflect the quantification of cells of several blood vessels from one naïve animal, one CFA animal and two EAE animals per disease stage: (1) preclinical EAE when no symptoms are apparent yet, (2) early disease, (3) peak disease and (4) post-peak disease (Figure 8a). In addition, two mice, that were asymptomatic despite MOG immunization, were analyzed. Per disease stage a total of 80-340 cells present in 5-10 videos were examined. Besides the number of CX3CR1-GFP$^+$ cells, their intraluminal crawling movement along the endothelium was tracked and normalized to the same origin as well as medial and lateral crawling direction. All graphs were generated using GraphPad Prism 6 and microscopical image panels were created using Adobe Photoshop CS6.

Tissue processing and immunohistochemistry

At the end of IVM experiments, i.e. day 25-33 after EAE immunization (equivalent to post-peak disease), the mice were transcardially perfused with saline followed by 20-30 ml of 4 % paraformaldehyde in 0.1 M phosphate buffer (pH 7.4). Spinal cords and spleen were dissected and post-fixed for 2 h at 4 ºC. Tissue was cryo-protected with 10 % sucrose in PBS and embedded in OCT tissue tek (VWR Chemicals). Coronal sections (10 µm) were cut, dehydrated and stored at -80 ºC until immunostaining.

For single immunohistochemical stainings, sections were thawed, blocked in 3 % BSA in TBS containing 0.5 % Triton X-100 (TBS-T; Sigma), and incubated with primary antibodies for Iba1, CD68 (rat), CD3 or CD45 (Table 1). For double staining of CD45 and CD68 (rabbit), incubation of both primary antibodies was done at once. All sections were incubated with primary antibodies at 4 ºC overnight followed by three 5 min washes in

PBS. The sections were then incubated with appropriate AF594 or AF633-labeled IgG's (1/400, Molecular probes) in TBS-T for 2 h at room temperature. Before staining of NKp46 (Table 1) endogenous peroxidases were quenched (0.3 % H2O2, 0.1 % sodium azide in TBS) and sections incubated with primary antibody for 1.5 h at room temperature. After washing, ImmPRESS HRP anti-goat IgG polymer detection kit (Vector laboratories) was added for 30 min before slides were washed and incubated for 10 min with the TSA™ reagent Alexa Fluor 594® tyramide (1/100 in amplification buffer, Thermo Fisher Scientific). Immunohistochemical co-labeling of TG2 and the above used immune cell markers (Table 1), required pretreatment with a mouse on mouse blocking kit (M.O.M.; Vector Laboratories) according to the manufacturer's guidelines. Briefly, the sections were blocked for 1 h with blocking reagent and the staining was continued as described above with additional AF633-labeled donkey anti mouse IgG's (1/400, Molecular probes) to detect TG2. For double-labeling of TG2 and cleaved Caspase-3 fragments (17/19 kDa) (Table1), endogenous peroxidases were blocked, M.O.M blocking was applied and sections were incubated with antibodies as described above. ImmPRESS AP anti-rabbit IgG polymer detection kit (Vector laboratories) was added for 30 min, slides were washed and EnVision+ kit HRP anti-mouse (Dako) was applied for 30 min. After washing, the slides were first incubated with liquid permanent red (LPR, Dako) as AP substrate and then after a quick wash with DAB+ (Dako) as HRP substrate, both according to manufacturer guidelines. All slides were coverslipped with polyvinyl alcohol mounting medium with DABCO (Fluka) and all fluorescent slides were examined with a confocal laser-scanning microscope or a fluorescence microscope (Leica TSC-SP2-AOBS and Leica DM5000B, Leica Microsystems). The light-microscopical double staining for cleaved Caspase-3 fragments (17/19 kDa) and TG2 was analyzed with a Nuance spectral imaging camera (Nuance) and displayed in coolers representing fluorescent staining to increase the visual contrast. As negative staining control, primary antibodies were omitted, which resulted in minor or no background immunoreactivity (data not shown).

Table 1: Primary antibodies for immunohistochemistry

Target	Origin	Dilution	Supplier	Code
Iba1	Rabbit	1/1000	Wako chemicals	019-19741
CD68	Rat	1/300	Serotec	MCA1957
CD68	Rabbit	1/400	Abcam	ab125212
CD45	Rat	1-okt	Gift from dept. Molecular Cell Biology and Immunology, VUmc, Amsterdam	clone MP33
CD3	Rat	1/100	AbD Serotec	MCA500G
NKp46-biotin	Goat	1/100	R&D Systems	BAF2225
TG2	Mouse	1/100	Prof T. J. Johnson, Sheffield University, UK (gift)	Clone IA-12
Cleaved caspase-3 (Asp175); 17/19 kDa fragments	Rabbit	1/350	Cell Signaling Technology	#9661

Statistical analysis

IVM data were not normally distributed and therefore statistically analyzed using the non-parametric Kruskal-Wallis test followed by Dunn's multiple comparison test using GraphPad Prism 6. Differences were considered significant if $p<0.05$, and considered a trend if $p<0.06$.

RESULTS

Evaluation of EAE symptoms in CX3CR1$^{gfp/gfp}$ mice with a spinal cord window

The window implanted CX3CR1$^{gfp/gfp}$ mice developed a mild EAE disease course when immunized with myeloid oligodendrocyte glycoprotein peptide 35-55 (MOG_{35-55}). The average maximal clinical score was around 1.5 (Figure 2a) and the maximal loss of body weight was 8 % (Figure 2b). Naive and control animals (immunized with complete Freund's adjuvant, CFA) did not exhibit clinical deficits or loss of body weight at any time during the experiment.

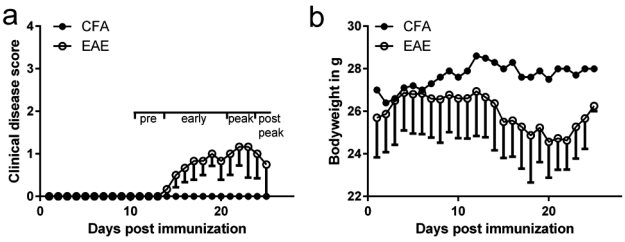


Figure 2: EAE in CX3CR1gfp/gfp mice. (a) Clinical disease scores and (b) body weight after immunization with MOG_{35-55} (○, n=3) or CFA (●, n=1) in CX3CR1$^{gfp/gfp}$ mice with spinal cord window implants. Data represent mean – SEM.

IVM of the spinal cord parenchyma of CX3CR1$^{gfp/gfp}$ mice

For *in vivo* imaging, we chose blood vessels draining into the central spinal cord vein on both left and right side of the central vein in the region of the vertebrae T13 to L1 (corresponding to spinal cord levels L4 to S1 [272]). Data from two-photon IVM (Figure 3) revealed two distinct CX3CR1-GFP$^+$ cell localization in the spinal cord: in the parenchyma (arrowheads) and within the vasculature (squares). CX3CR1-GFP$^+$ cells in the spinal cord tissue of the naïve animal (Figure 3a) were microglial-like cells with a ramified morphology and thin processes, as previously shown [265]. CFA immunization (Figure 3b) seemed to bring the CX3CR1-GFP$^+$ microglia in closer distance to the blood vessels. After MOG immunization, the mice in the pre-symptomatic stage showed slightly more GFP signal in the parenchyma than the CFA animal (Figure 3c). The parenchymal GFP signal further increased, especially in proximity to the blood vessel, coinciding with morphological changes of the CX3CR1-GFP$^+$ cells towards a more amoeboid shape when the mice entered the symptomatic stages of EAE (Figure 3d, e). During the post-peak disease stage, still, numerous amoeboid-shaped CX3CR1-GFP$^+$ microglia were present (Figure 3f). In EAE animals also CX3CR1-GFP$^+$ blood cells might have infiltrated the spinal cord, adding to the

numerous CX3CR1-GFP$^+$ amoeboid microglial cells, from which they cannot be distinguished, based on their morphology. Additionally, in the symptomatic stages of EAE (Figure 3d-f) some red-colored CX3CR1-GFP$^+$ cells in the parenchyma close to the blood vessels were observed (arrows). This was likely caused by cellular uptake of rhodamine B isothiocyanate-dextran leaked into the parenchyma. This was an EAE phenomenon and not detected in the naïve animal or the CFA animal (Figure 3a,b) and neither in asymptomatic animals (data not shown).

Cellular characterization of CX3CR1-GFP$^+$ cells

To confirm the monocyte/microglia identity of the CX3CR1-GFP$^+$ cells in the spinal cord of our CX3CR1$^{gfp/gfp}$ mice induced with EAE, we immunohistochemically characterized these cells in the spinal cord area that had previously been imaged by IVM and are hence from post-peak disease (n=3, Figure 4). Our observations revealed that CX3CR1-GFP$^+$ cells in the white matter lesions expressed markers for microglial cells and macrophages, i.e. Iba1 (Figure 4a, b) and the phagocyte marker for lysosomal activity, CD68 (Figure 3c, d). Furthermore, intense CD45 (Figure 4e, f) immunoreactivity was found in the lesion areas, mainly in amoeboid shaped cells (arrowheads and inserts). Moreover, co-localization of CD68 and CD45 in CX3CR1-GFP$^+$ cells was found (Figure 4g-i). We also observed ramified GFP$^+$ cells that were weakly immunoreactive for CD45 but not CD68, indicative of local microglia (arrows). This finding supports the hypothesis of an influx of CX3CR1-GFP$^+$ from the vasculature into the spinal cord, although this was not observed during IVM. In a CFA animal, fewer and mostly ramified CX3CR1-GFP$^+$ microglia were observed, uniformly distributed in the spinal cord (Supplement Figure 1). These cells were all positive for Iba1 (Supplement Figure 1a,b) but not for CD68 (Supplement Figure 1c, d), indicative of a microglial phenotype. It has been described that CX3CR1-GFP$^+$ cells can also comprise T and NK cells and therefore we stained for the presence of these cell types [265]. CD3 positive T cells (Figure 5a, b) appeared in the spinal cord lesions, although in low numbers compared to Iba1 and CD68 positive cells. Moreover, the CD3 positive T cells did not co-localize with GFP. NK cells were absent in the spinal cord lesions (Figure 5c, d), although spleen tissue of the same animals showed NKp46$^+$ cells that in small numbers co-localized with GFP$^+$ cells (Figure 5e, f).

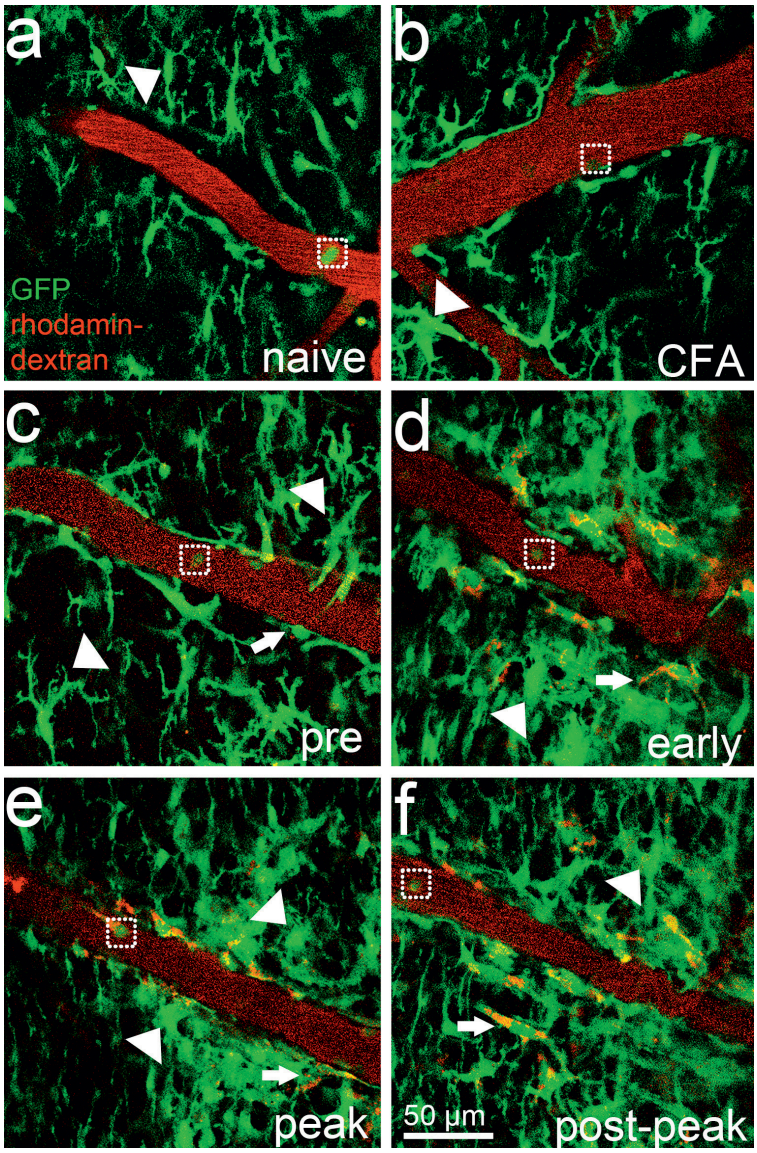


Figure 3: Representative two photon IVM of CX3CR1-GFP+ cells in the spinal cord of CX3CR1gfp/gfp mice. CX3CR1-GFP^{+} cells in the parenchyma (arrowheads) resemble microglial cells. They display a ramified phenotype in (a) naïve (n=1) and (b) the CFA animal (n=1). In MOG-induced EAE (n=3) animals (c-f), these cells morphologically change towards an amoeboid phenotype, with big cell clusters in symptomatic EAE (n=2) (d-f). Furthermore, during EAE (c-f), the red rhodamine B isothiocyanate-dextran (used to stain the blood vessels), leaks into the parenchyma where it is then taken up by cells resulting in red cellular staining (arrows). In addition to parenchymal locations, (a-f) CX3CR1-GFP^{+} cells were observed within the bloodstream, specified by squares.

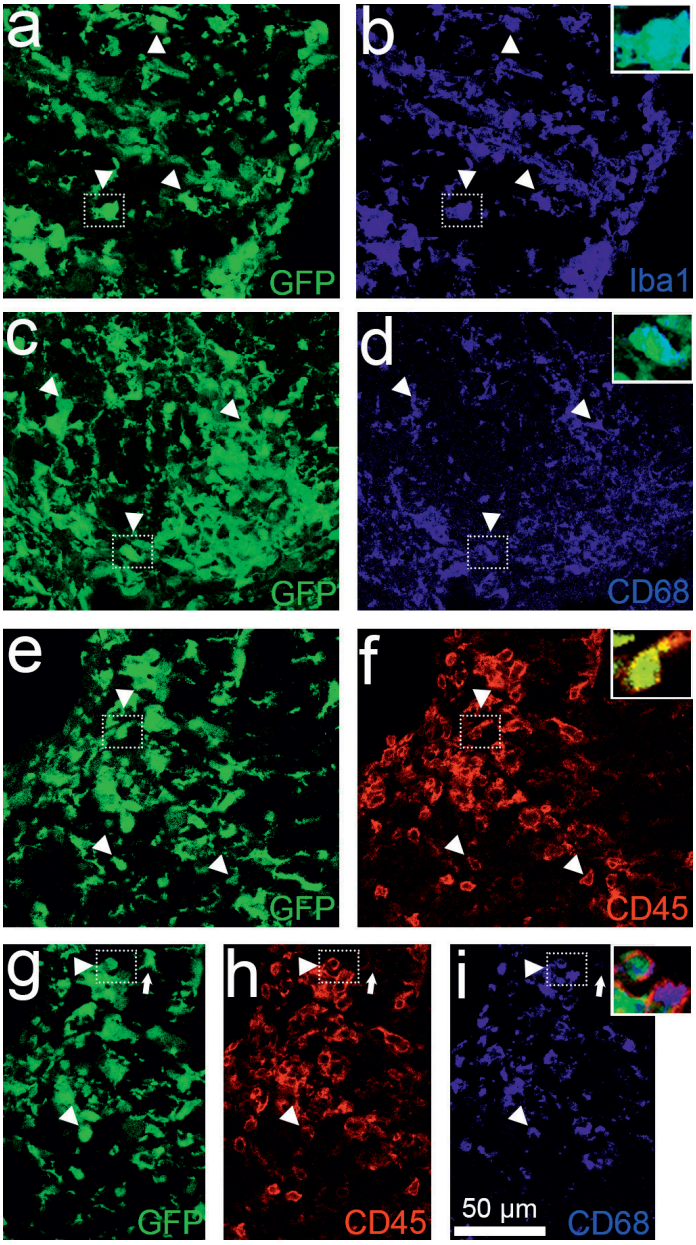


Figure 4: CX3CR1-GFP+ cells in EAE spinal cord tissue (n=3) stained post IVM are monocytes/macrophages and microglial cells. (a, c, e, g) Spinal cord EAE lesions in CX3CR1$^{gfp/gfp}$ mice show clusters of ramified and amoeboid CX3CR1-GFP^{+} cells with immunoreactivity for (b) Iba1, (d) CD68 and (f) CD45 (arrowheads). Triple positive cells for (g) GFP, (h) CD45 and (i) CD45 indicate that some GFP^{+} cells might have infiltrated from the bloodstream, while local ramified microglia (arrows) are GFP^{+} with low immunoreactivity for CD45 and none for CD68. Inserts provide higher magnification of double/triple positive cells.

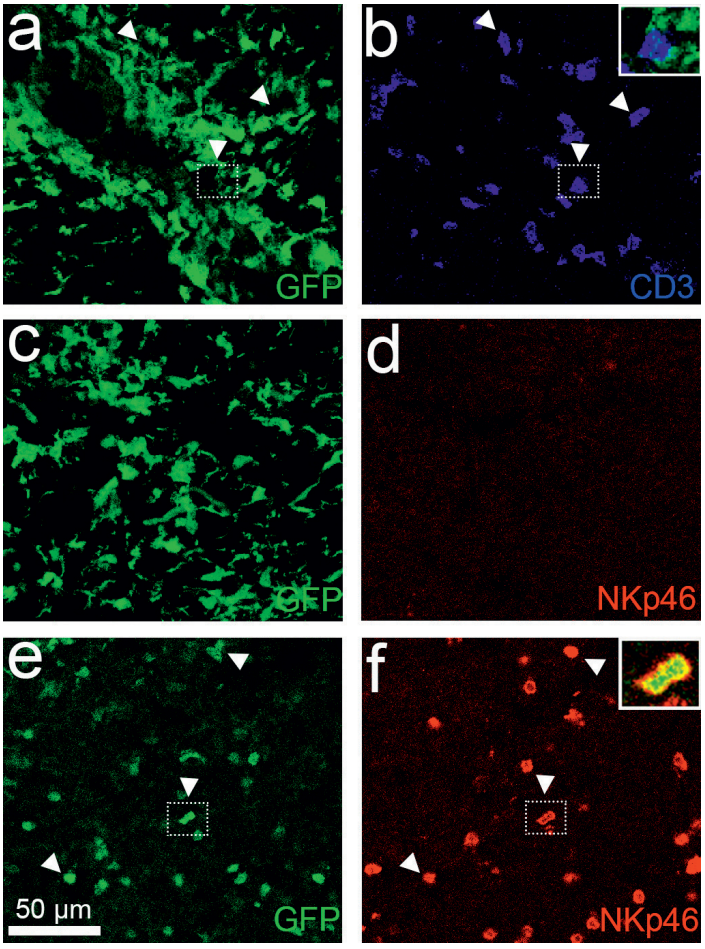


Figure 5: Neither T cells nor NK cells are amongst the CX3CR1-GFP+ cells in the EAE spinal cord tissue stained post IVM (n=3). (a, c) CX3CR1-GFP^{+} cells in spinal cord EAE lesions in CX3CR1$^{gfp/gfp}$ mice do not display immunoreactivity for (b) CD3 (arrowheads, higher magnification in the insert) and (d) NKp46. (e, f) show GFP^{+} and NKp46 co-labeled cells in the spleen (arrowheads, higher magnification in the insert), which served as a positive control for the NKp46 antibody.

IVM of GFP^{+} cells in the vasculature

Two photon imaging revealed that CX3CR1-GFP^{+} cells in the vasculature of the naïve mouse rarely interacted with or crawled along the luminal side of the blood vessel endothelium (~1 cell per 10 min) as depicted in Figure 6a. We termed these cells fast moving cells. An animal injected with CFA and subsequently imaged at a time point post injection comparable to the early disease phase in EAE animals, served as a control for the early stage of disease in EAE animals. The data showed a tendency of increased interaction of CX3CR1-GFP^{+} cells with the endothelium and around 15 cells per 10 minutes showed an extensive intraluminal crawling behavior for longer than 25 seconds, which were designated crawling cells. A comparable amount of cells was observed in MOG immunized animals during pre-symptomatic disease (Fig. 6a; pre). As EAE developed, the number of crawling cells was slightly reduced from pre-disease but remained elevated in all disease phases analyzed, including post-peak disease. As another control, we imaged

asymptomatic animals at a time point post-immunization that was comparable to post-peak disease. The number of crawling monocytes in asymptomatic mice was only half of the amount (~5 cells per 10 min) as found in post-peak EAE, indicating that the elevated crawling of monocytes is due to ongoing clinical EAE and not just due to the immunization as such.

A similar pattern of cell distribution was seen when the crawling cells were analyzed as a percentage of total CX3CR1-GFP$^+$ cells imaged within the circulation (Figure 6b). CFA immunization, as well as immunization with MOG, resulted in a significant increase in the percentage of CX3CR1-GFP$^+$ crawling cells within the mouse spinal cord vasculature of naïve to the presymptomatic EAE phase. The percentage of crawling cells progressively reduced significantly during the disease course from more than 80 % in presymptomatic disease to 46 % in the post-peak disease stage. In asymptomatic animals only 15 % of the cells were of a crawling phenotype, which was significantly different from the CFA injected control animal and the presymptomatic EAE animals

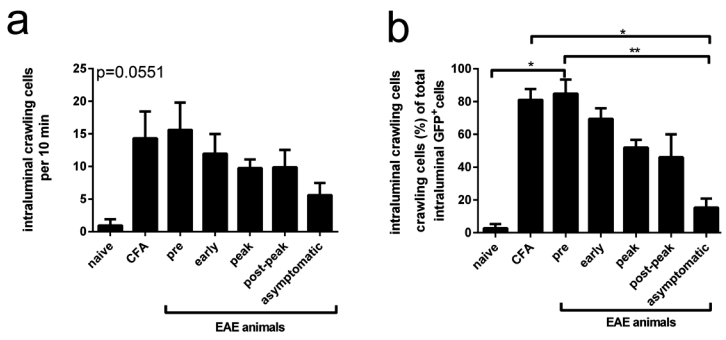


Figure 6: Quantification of the amount and percentage of intraluminal crawling CX3CR1-GFP+ monocytes during EAE. (a) The amount of crawling cells is expressed as the mean number of crawling cells counted per video in all available videos per disease stage or control and normalized to a timeframe of 10 minutes + SEM; p=0.0551, Kruskal-Wallis test. (b) The percentage of crawling cells of the total intraluminal CX3CR1-GFP$^+$ cells increased significantly during the pre-clinical phase of EAE and remained elevated during on-going EAE compared to asymptomatic animals. The percentage of crawling cells per total number of intraluminal CX3CR1-GFP$^+$ cells was calculated per video in all available videos per disease stage or control +SEM; *p< 0.05, **p<0.01. The results presented include data from naïve (n=1), CFA (n=1), EAE (n=2 per disease phase) and asymptomatic (n=2) animals.

Additionally, we examined the crawling movement of monocytes during their interactions with the endothelium. Plotting the individual crawling tracks revealed that the displacement and the direction of crawling changed over time of the EAE disease course (Figure 7). In the naive animal, as already shown in Figure 6, only few crawling monocytes were present with a very limited local displacement (Figure 7a). Consequently, they were excluded from further analysis. CFA immunization led to a displacement of monocytes up to about 100 µm (Figure 7b). In EAE induced animals (Figure 7c-e), the displacement of crawling CX3CR1-GFP$^+$ cells increased as the disease progressed with a maximum at peak disease, displaying with a displacement up to 200 µm. While the average track length presented little differences between CFA and EAE animals (Figure 7g), the distribution of the track length was altered within the different EAE phases (Figure 7h). Of all CX3CR1-GFP$^+$ crawling cells, 50-60 % displayed track lengths of less than 100 µm. Intermediate track lengths of 100-200 µm were similar during the different stages of EAE,

although there was a tendency that they were reduced compared to the CFA induced tracks (Kruskal-Wallis test, $p<0.05$, posthoc test not significant). Long distance displacement of crawling cells extending 200 µm distances was only observed in MOG immunized animals with a significant increase to around 20 % of total crawling CX3CR1-GFP$^+$ cells during peak disease. Furthermore, as already shown in Figure 7b-f, CX3CR1-GFP$^+$ cells did not only crawl in a medial direction with the bloodstream, but also in a lateral direction against the bloodstream (Figure 7i). In CFA and pre-disease EAE animals around 20 % of CX3CR1-GFP$^+$ crawling cells moved against the bloodstream. With on-going EAE, this cellular behavior reached around 35% of CX3CR1-GFP$^+$ crawling cells in peak disease.

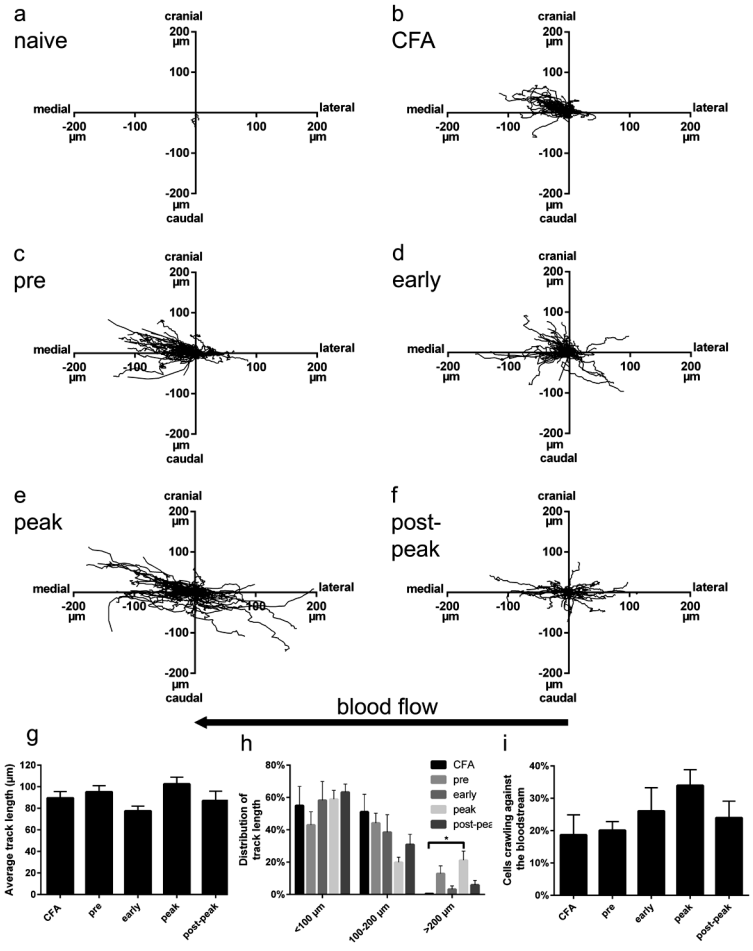


Figure 7: Tracks of intraluminal crawling CX3CR1-GFP+ cells. Monocyte crawling tracks are presented from (a) naïve (n=1), (b) CFA (n=1), and (c-f) EAE (n=2) animals per disease phase. (g) Average track length of crawling cells. (h) Distribution of track lengths per animal group. (i) Percentage of crawling cells moving against the bloodstream. Coordinates of each cell track were set to the same origin to determine medial (in direction of blood flow) or lateral crawling of CX3CR1-GFP$^+$ cells. The cranial and caudal direction of cell crawling depended on the orientation of the imaged blood vessel. All data are expressed as mean values +SEM.

GFP$^+$ cells in the spinal cord also express TG2

To study whether TG2 is present in our mouse EAE model, immunohistochemical analysis of spinal cord sections was performed. TG2 immunoreactivity was found in the blood vessels of all EAE animals (Figure 8a, d, g, arrows), and of the naïve and CFA control animals (as exemplified for the CFA animal in Supplementary Figure 2), as described before [229]. Additional cellular TG2 immunoreactivity was found in spinal cord lesions of EAE animals.

GFP$^+$cells, identified as Iba1 and CD68 positive microglia and monocytes/macrophages, but not CD3 positive T cells in EAE lesions showed TG2 immunoreactivity (Figure 8a-i). Most TG2 expressing cells exhibited an amoeboid morphology which could be monocytes and monocyte-derived macrophages. Furthermore, ramified microglial cells in and near the lesion area were somewhat TG2 positive. Intriguingly, we observed TG2 immunoreactivity in CX3CR1-GFP+ cells within the blood vessel attached to the lumen (Figure 8j, k). No extensive amounts of these cells were found due to perfusion of the animals, but particular cells attached to the endothelium were existent. As TG2 can contribute to immune cell apoptosis and is upregulated during this process [273], we studied the presence of active Caspase-3 in spinal cord EAE lesions. Only a few cells immunopositive for the cleaved Caspase-3 fragments (17/19 kDa) were found and single cells co-labeled with TG2, while others did not (Figure 8l,m). Overall, the presence of active Caspase-3 positive cells in the EAE affected spinal cord was limited.

DISCUSSION

The present study is one of the first to show *in vivo* behavior of circulating monocytes in the murine spinal cord at various time-points after EAE induction. We observed an increased crawling behavior of monocytes in CX3CR1-GFP$^+$ transgenic mice in EAE and CFA immunized animals compared to a naïve control. This increase was most pronounced early after immunization and was observed in all animals that received adjuvants with or without MOG_{35-55}. This indicates that this initial increase in monocyte crawling behavior is rather due to general activation of the immune system which is essential to induce EAE in MOG immunized mice. Indeed, recent observations showed an increase in blood-derived monocytes already in preclinical and early stage EAE [274]. We observed elevated intraluminal monocyte crawling during the early stages of EAE and despite subsequent reduction to intermediate levels at later disease stages, the amount of crawling cells remained elevated in EAE mice compared to naïve and also asymptomatic animals. Therefore an ongoing immune response as found in symptomatic EAE mice, which is absent in asymptomatic animals, seems needed to keep the crawling behavior of monocytes elevated. Moreover, the displacement length of individual crawling CX3CR1-GFP$^+$ monocytes was most extensive during peak disease. Furthermore, TG2 positive CX3CR1-GFP$^+$ cells could be identified in and near the blood vessels during EAE, indicating a role of TG2 in mouse EAE in these animals.

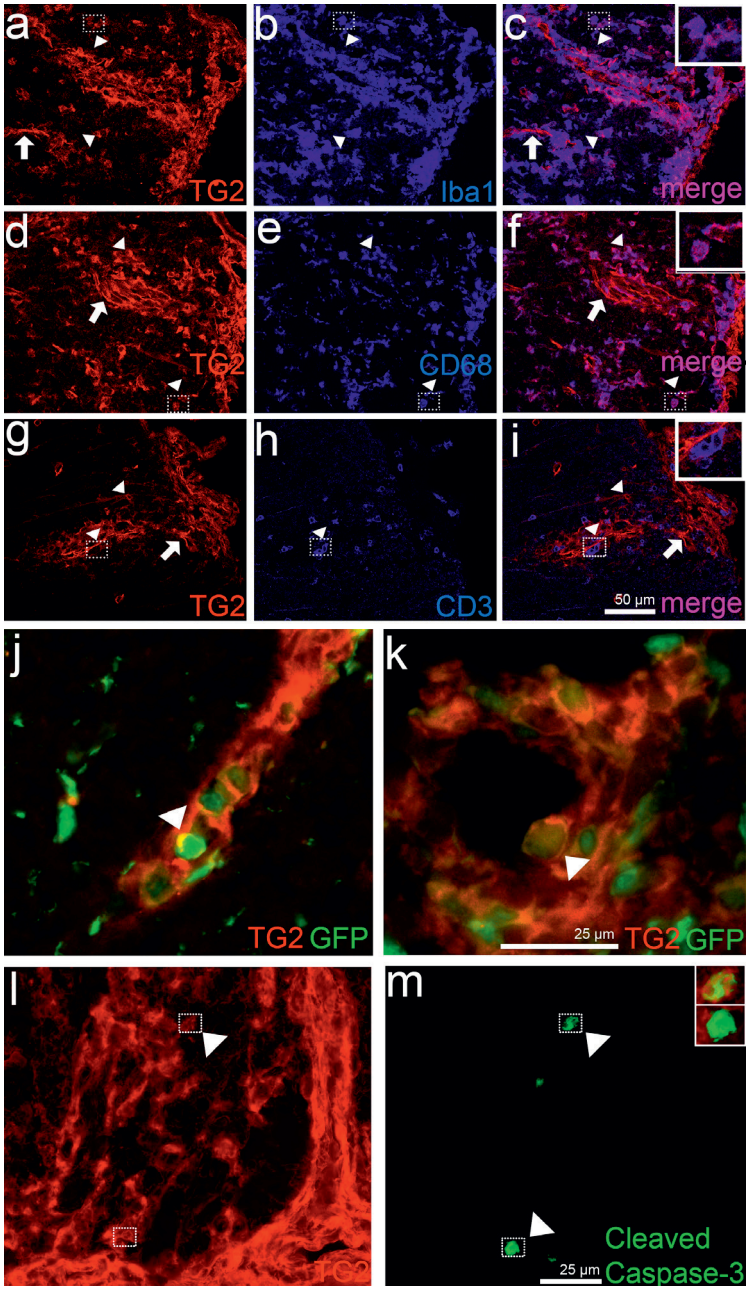


Figure 8: TG2 immunoreactivity in the post-mortem spinal cord of CX3CR1gfp/gfp EAE mice (n=3). (a, d, g) TG2 immunoreactivity is present in blood vessels (arrows) and cells (arrowheads) in spinal cord lesions of mice suffering from EAE. In these lesions (b) Iba1, (e) CD68 and (h) CD3 immunoreactivity is observed. TG2 is co-localized with (c) Iba1 and (d) CD68 and thus microglia and monocytes/macrophages but not (i) CD3 positive T cells. (j, k) GFP^+ and TG2 co-labeled monocytes can be found within the blood vessel (arrowheads). Blood vessels are presented in a sagittal (j) and coronal (k) direction. (l, m) Few cells in the EAE spinal cord lesions express cleaved Caspase-3, which can co-label with TG2 (arrowhead). Squares represent cells shown at higher magnifications in the inserts.

To perform *in vivo* IVM analysis of monocyte behavior, the spinal cord was made accessible by window implantation. Although such surgery could slightly delay EAE onset as described previously for the C57BL/6 strain, it does not alter overall progression or

disease score in this transgenic mouse strain [267]. The CX3CR1$^{gfp/gfp}$ transgenic mice used in this study express GFP instead of the chemokine receptor CX3CR1 and are henceforth CX3CR1 knockout animals. While this receptor was shown to be involved in leukocyte adhesion and migration, the CX3CR1$^{gfp/gfp}$ transgenic mice still develop EAE [275]. Of importance, experiments comparing of CX3CR1$^{gfp/gfp}$ with heterozygous CX3CR1$^{+/gfp}$ revealed that only the migratory properties of NK cells are affected during EAE in CX3CR1$^{gfp/gfp}$ animals leading to no NK cell recruitment to the EAE lesions [275]. Although we cannot completely exclude changed monocyte crawling behavior due to CX3CR1 depletion, the chemotaxis of monocytes and other leukocytes is not impaired as their recruitment to the site of inflammation is constant in homo-as well as heterozygous CX3CR1-GFP-expressing mice. We confirmed the impaired NK cell recruitment by the lack of NK cells in the spinal cord lesions, although NK cells expressing GFP were present in the spleen. For the first time, the described surgical approach of the spinal cord window implantation was used to access the spinal cord in the transgenic CX3CR1$^{gfp/gfp}$ mouse strain. Our observation of CD68, CD45 and/or Iba1 positive CX3CR1-GFP^{+}cells in the EAE spinal cord lesions, as well as the clearly developed clinical symptoms, support the notion that these mice can be used for IVM to analyze monocyte behavior during EAE.

Using IVM analysis, we found that CX3CR1-GFP^{+} are still able to crawl along the endothelial lumen, despite their loss of the CX3CR1 receptor and supporting previous data [275]. Although the number of experimental animals used in this study was very small, some interesting changes in the behavior of CX3CR1-GFP^{+} cells in the spinal cord vasculature were present between controls, EAE induced asymptomatic animals and EAE diseased animals and also within the different disease phases of EAE. Only a few of the CX3CR1-GFP^{+} cells were found in the spinal cord vasculature of a naïve animal which corresponds to previous observations [276, 277]. When compared to the total number of intraluminal CX3CR1-GFP^{+} cells, the data suggest that under control conditions, most monocytes are fast moving cells that are not interacting with the endothelium. However, upon treatment with CFA, more crawling monocytes were present at the luminal side of the blood vessel, likewise observed in the preclinical stage of EAE. This crawling monocyte behavior remained present during the early stage of EAE and had a tendency to recede partially during continuing disease. Nevertheless, it seemed higher throughout disease compared with asymptomatic animals. Thus, activation of the immune system stimulates CX3CR1-GFP^{+} cells in the mouse spinal cord vasculature to enhance their intraluminal crawling behavior, which remained present in EAE animals showing apparent disease symptoms. The observation that the percentage and number of monocytes interacting with the endothelium had a tendency to decrease as the clinical disease progressed might be unexpected, but may reflect the steady increase in monocyte migration into the CNS during disease progression, as shown by pathological studies [278, 279]. Of interest is, that a comparable disease-dependent behavior has been shown for T cells in the same EAE model. This suggests that T cells and monocytes behave in a related time-dependent way during EAE [24]. Moreover, asymptomatic animals showed a low amount of crawling cells, and also a low percentage of total CX3CR1-GFP^{+} cells in the vasculature, at a time point post immunization comparable to post-peak disease. This is in line with the idea that the

disease-induced change in monocyte intraluminal crawling behavior contributes to or is a consequence of on-going clinical EAE and not due to the immunization itself.

Subsequent analysis of the tracks of crawling monocytes showed that the average track length did not differ between control and EAE animals, but there is a clear change in maximum displacement of the crawling cells as well as crawling direction over the disease course. In particular, during peak disease, numerous monocytes showed extended crawling displacement along the endothelium, not only in the direction of the blood flow but also against it. Both of these observations could be a consequence of firmer interaction with the endothelium mediated by soluble factors, e.g. chemokines and cytokines, secreted by local cells to actively attract more cells to the CNS [280-282]. Additionally, up-regulation and activation of adhesion molecules on endothelial cells could be responsible for the extended crawling of monocytes in the lumen [283].

Along with CX3CR1-GFP$^+$ monocytes in the circulation, we observed CX3CR1-GFP$^+$ cells in the spinal cord parenchyma. Under normal conditions, they reflect ramified microglial cells but upon inflammatory conditions such as EAE, a clear increase in the amount of CX3CR1-GFP$^+$ cells around the blood vessels becomes evident. It is, however, not possible to distinguish infiltrating monocytes from amoeboid microglia based on their GFP expression. Nonetheless, extensive immunoreactivity of the blood leukocyte marker CD45 on CX3CR1-GFP$^+$ amoeboid shaped cells in the spinal cord parenchyma indicates that indeed cellular infiltration of blood-derived CX3CR1-GFP$^+$ cells had occurred. The density of ramified microglia around the blood vessels was increased since microglia migrate toward lesion sites, where the activated microglia can proliferate and enable phagocytizing properties such as taking up myelin and cell debris [256, 284, 285]. The phagocytic capacity of CX3CR1-GFP$^+$ cells is illustrated in the present study by rhodamine B isothiocyanate-dextran uptake that had leaked from the circulation in EAE animals but was negligible in control animals (naïve, CFA). The presence of the dextran in cells in the later stages of EAE can be either due to continuous uptake due to continuously damaged BBB integrity or slow intracellular degradation while the BBB had already been repaired.

Finally, we observed the multifunctional enzyme TG2 in GFP$^+$ microglial cells and monocytes/macrophages in the spinal cord lesions. Since TG2 immunoreactivity is only observed in or near lesion areas and not in ramified microglia in the non-affected spinal cord, it seems that TG2 is associated with inflammatory infiltrates and/or microglial activation in mouse EAE. Interestingly, also GFP$^+$ monocytes attached to the luminal side of the blood vessel were found to exhibit TG2 immunoreactivity. Although, due to transcardial perfusion, these cells were scarce. Since TG2 is, amongst other functions, known to be involved in monocyte adhesion and migration *in vitro* [119], we hypothesize that it might also be involved in the adhesion and migration processes *in vivo*. The presence of TG2 not only in the lesions but also at the luminal side of blood vessels, supports previous findings on the involvement of TG2 in monocytes in EAE.

Furthermore, TG2 is known to contribute to apoptotic processes [286]. During EAE, we observed very few cells in spinal cord lesions to express the apoptotic marker active caspase-3. This is in accordance with previous observations in mouse EAE [287]. Of the active caspase-3 immunopositive cells, single cells co-labeled with TG2 and others did

not. Thus, little apoptotic processes are ongoing in EAE, and there is probably a minor role for TG2 in these processes

Taken together, the observations in the present study showed that MOG immunization increased luminal monocyte crawling behavior, which remained elevated during EAE. Moreover, our results revealed that circulating monocytes in EAE animals produced TG2, which may contribute to monocyte crawling and adhesion. We put forward that selective interference with monocyte crawling and migration behavior should be applied in a very early stage of disease with the aim to counteract disease progression. By means of the here conducted experimental setup, future experiments on the effect of TG2 inhibition on monocyte behavior can be assessed *in vivo* which may lead to novel treatment options for MS patients.

Conflict of Interest

The authors declare that they have no conflict of interest.

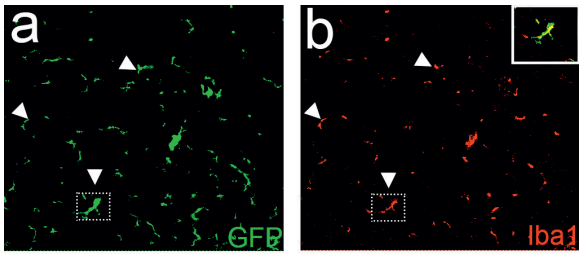
Ethical approval

All applicable international, national, and/or institutional guidelines for the care and use of animals were followed. All procedures performed in studies involving animals were in accordance with the ethical standards of the institution or practice at which the studies were conducted.

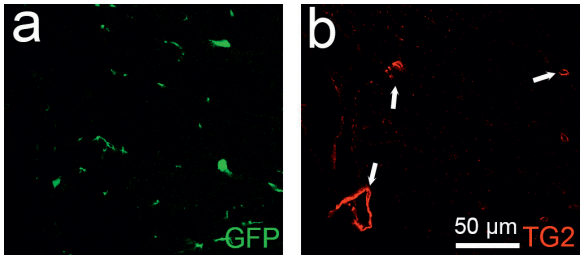
Acknowledgement

Prof T.J. Johnson (University of Sheffield, UK) is kindly acknowledged for his gift of the IA-12 antibody. This study was financially supported by EU Framework Programme 7 Marie Curie ITN 'TRANSPATH' (grant number 289964).

SUPPLEMENT



Supplementary Figure 1: (a, c) CX3CR1-GFP$^+$ cells in the spinal cord tissue of a CFA induced control animal (n=1) exhibit ramified microglial like morphology. These cells show immunoreactivity for (b) Iba1 but not (d) CD68, indicating a resting microglial phenotype. Arrowheads: co-labeled cells (higher magnification in the insert).



Supplementary Figure 2: (a) CX3CR1-GFP$^+$ cells in the spinal cord tissue of a CFA induced control animal (n=1) exhibit no immunoreactivity for (b) TG2. TG2 immunoreactivity is only found in blood vessels (arrows).



Chapter 5

CHARACTERIZATION OF TRANSGLUTAMINASE 2 ACTIVITY INHIBITORS IN MONOCYTES *IN VITRO* AND THEIR EFFECT IN A MOUSE MODEL FOR MULTIPLE SCLEROSIS

PLoS One. 2018 Apr 24;13(4):e0196433

ABSTRACT

The neurodegenerative disease multiple sclerosis (MS) is pathologically characterized by the massive influx of immune cells into the central nervous system. This contributes to demyelination and axonal damage which causes symptoms such as motor and cognitive dysfunctions. The migration of leukocytes from the blood vessel is orchestrated by a multitude of factors whose determination is essential in reducing cellular influx in MS patients and the experimental autoimmune encephalomyelitis (EAE) animal model. The here studied enzyme tissue Transglutaminase (TG2) is present intracellularly, on the cell surface and extracellularly. There it contributes to cellular adhesion and migration via its transamidation activity and possibly by facilitating cellular interaction with the extracellular matrix. Previous data from our group showed reduced motor symptoms and cellular infiltration after using a pharmacological TG2 transamidation activity inhibitor in a rat EAE model. However, it remained elusive if the cross-linking activity of the enzyme resulted in the observed effects. To follow-up, we now characterized two new small molecule TG2 activity inhibitors, BJJF078 and ERW1041E. Both compounds are potent inhibitors of recombinant human and mouse Transglutaminase enzyme activity, mainly TG2 and the close related enzyme TG1. In addition, they did not affect the binding of TG2 to the extracellular matrix substrate fibronectin, a process via which TG2 promotes cellular adhesion and migration. We found, that ERW1041E but not BJJF078 resulted in reduced EAE disease motor-symptoms while neither caused apparent changes in pathology (cellular influx), Transglutaminase activity or expression of inflammation related markers in the spinal cord, compared to vehicle-treated controls. Although we cannot exclude issues on bioavailability and *in vivo* efficacy of the used compounds, we hypothesize that extracellular TG1/TG2 activity is of greater importance than (intra-) cellular activity in mouse EAE pathology.

Navina L. Chrobok[1], John J. G. M. Bol[1], Cornelis A Jongenelen[1], John Brevé[1], Said El Alaoui[2], Javier Fidalgo-Lopez[2,3#], Guy Fournet[3#], Benoît Joseph [3#], Micha M. M. Wilhelmus[1], Benjamin Drukarch[1] and Anne-Marie van Dam[1*]

[#]These authors contributed equally to this work.

[1]Department of Anatomy and Neurosciences, Amsterdam Neuroscience, VU University Medical Center, Amsterdam, The Netherlands; [2]Covalab, Villeurbanne, France, [3]Institut de Chimie et Biochimie Moléculaires et Supramoléculaires, Université Claude Bernard—Lyon 1, Villeurbanne, France

INTRODUCTION

Multiple sclerosis (MS) is an inflammatory and demyelinating disease of the central nervous system (CNS) that displays a wide range of clinical symptoms, including sensory, motor and cognitive disabilities [4, 212, 253]. In most patients, MS is pathologically characterized by a massive influx of leukocytes into the CNS, which is also observed in the experimental autoimmune encephalomyelitis (EAE) animal model for MS [288]. The infiltrating leukocytes produce inflammatory mediators in the CNS that e.g. activate resident glial cells, induce oligodendrocyte cell death and cause axonal damage [254]. The underlying process of cell infiltration requires the collaboration of numerous factors whose presence is increased during inflammation and that are found within the cells and on their surface [162, 163]. Preventing the interaction of leukocytes with the brain blood vessel endothelium and thus inhibiting the influx of cells into the CNS is the target of recent MS therapies [255, 289].

A novel factor of interest involved in the migration of cells is the enzyme tissue Transglutaminase (TG2) [119]. TG2 is a calcium-dependent protein crosslinking enzyme whose expression and activity can be increased by inflammatory mediators, due to the presence of inflammatory responsive elements in its promotor region [290]. Of interest is that TG2 contributes to cell adhesion and migration via its fibronectin binding domain [119]. In this manner, it can act as a co-receptor for β1- and β3-integrins, which are crucial for the adhesion of cells [261]. The interaction of TG2 and integrins on the cell surface enhances the binding affinity for the extracellular matrix protein fibronectin and promotes cell migration, including that of monocytes [119, 261]. A recent study from our group demonstrated TG2 immunoreactivity in infiltrating leukocytes in MS active lesions. Moreover, we observed that TG2 is present in infiltrating monocytes and contributes to pathology by promoting monocyte migration into the CNS in an experimental MS rat model [229]. In addition, the cross-linking activity of TG2 and possibly other Transglutaminases may contribute to such processes by affecting extracellular matrix deposition and modifications as well as rearrangement of the cytoskeleton [126, 229, 291].

Thus, TG2 seems an interesting target in MS, by selectively modulating its enzymatic and/or non-enzymatic activities. The enzymatic transamidating activity of TG2 can be inhibited with chemical compounds to elucidate the contribution of TG2 activity in particular, but also other Transglutaminases, to various cellular processes *in vitro* and *in vivo* and study their link with disease processes.

Due to TG2's role in cellular adhesion and migration and together with its increased presence during inflammation, we hypothesize that TG2 activity contributes to the clinical outcome of experimental MS. Recent studies from our lab and other groups have shown that TG2 knock-out mice and likewise rats treated with TG2 enzymatic activity inhibiting compounds, showed reduced clinical disease symptoms during EAE [198, 229]. This could, at least partially, be explained by diminished monocyte migration into the CNS [229]. Still, it remains unclear if just TG2 transamidating activity inhibition or also other properties of the used TG2 inhibitor (KCC009), i.e. disturbed fibronectin assembly and therefore the interaction of cells with the ECM, resulted in the observed effects [182].

Therefore, the present study is a follow-up to determine whether the administration of two different TG2 inhibitors affect the clinical outcome of the most commonly used EAE mouse model. For this purpose we chose two different pharmacological compounds; BJJF078 and ERW1041E to inhibit TG2 transamidating activity. The dihydroisoxazol derivative ERW1041E was chosen for its success to inhibit TG2 activity in a mouse celiac disease and mouse hypoxia experimental model *in vivo*, even though it was known that this inhibitor also inhibits TG1 with a similar potency [152, 153]. The new aminopiperidine derivative BJJF078 has not been extensively characterized yet but showed very promising TG2 inhibitory capacity over other commonly used TG2 inhibitors in a test tube setting. In the present study, we first characterized the inhibitory capacity of the two TG2 activity inhibitors using various recombinant Transglutaminase proteins. In addition, we measured their ability to inhibit cellular TG2 activity and determined their effect on TG2-fibronectin binding. Ultimately, we studied the expression of various Transglutaminases during mouse EAE and the effect of BJJF078 and ERW1041E treatment on the clinical and pathological outcome of mouse EAE. Overall, we observed that ERW1041E, but not BJJF078 reduced disease symptoms in mouse EAE. As ERW1041E neither inhibits cellular TG2 nor affects the interaction between TG2 and fibronectin, we conclude that extracellular TG2- and possibly TG1-derived transamidating activity contributes to EAE disease.

MATERIALS AND METHODS

Inhibition of recombinant Transglutaminase activity

The potency and specificity of TG2 inhibitors were assessed with various recombinant TGs, as previously described [292, 293]. The reaction buffer (50 mM Tris, 100 mM NaCl, 10 mM $CaCl_2$, 5 mM H-Gly-OMe*HCl (glycinemethylestherhydrochloride, Sigma), 5 mM hexadimethinbromide (Sigma), 9.1 mM DTT, pH 7.5) was heated to 37 °C in a 96 well plate. Then 50 µM of the TG substrate Abz-NE(CAD-DNP)EQVSPLTLLK-OH (Zedira) was added. 1 µg/ml recombinant TG (human TG1, human (hTG2) / mouse TG2 (mTG2) or human Factor XIII (FXIII); Zedira) were added.

The two lyophilized TG2 inhibitors (see Fig 1 for chemical structure) BJJF078 (3,4-Dimethoxy-N(5-[4-(acryloylamino)piperidine-1-sulfonyl]-naphthalen-1-yl)-benzamide, see S1 Appendix, synthetized and provided by Covalab, Villeurbanne, France and Institut de Chimie et Biochimie Moléculaires et Supramoléculaires, Villeurbanne, France) and ERW1041E (2-[(3-Bromo4,5-dihydro-isoxazol-5-ylmethyl)-carbamoyl]-pyrrolidine-1—carboxylic acid quinolin3-ylmethyl ester, kindly provided by Prof C. Khosla, Stanford University, USA)[153, 294, 295] were dissolved in DMSO (stock solution: 54 mM) and stored at -80 ºC. These stocks were further diluted and various concentrations of the TG2 inhibitors (0.3 nM to 100 µM), were added to the wells (final DMSO concentration per well: 0.06 %). The relative increase in fluorescence emission, correlating with enzymatic activity, was measured over 4 h with a fluorimeter (Excitation: 320nm, emission: 405 nm; Fluostar, GMB).

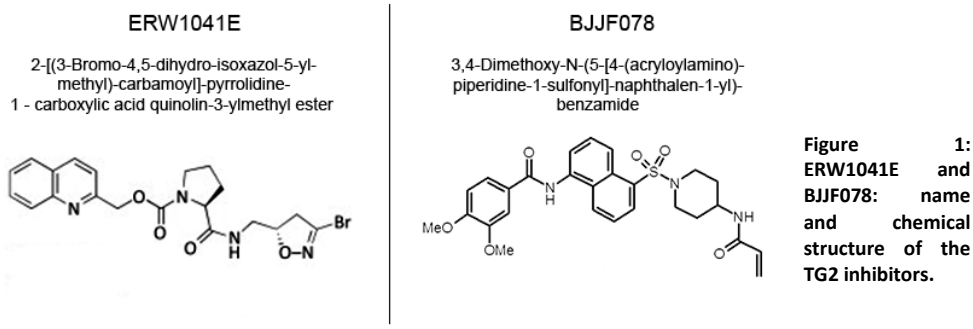


Figure 1: ERW1041E and BJJF078: name and chemical structure of the TG2 inhibitors.

Cellular inhibition of TG activity in THP1-cells

Human monocytic THP-1 cells (TIB-202, ATCC) were transduced with a lentiviral vector (pCDH-hTG2, gift from Prof K. Mehta, University of Texas, USA) to overexpress human TG2, to ensure high protein levels in addition to their constitutive expression that can be inhibited. To obtain a stable TG2 overexpressing cell line, transduced cells (THP-1/pCDH-hTG2 (THP-1/TG2)) were positively selected with puromycin and cultured at 37 °C and 5 % CO2 in air in RPMI-1640 medium (Gibco) supplemented with 10 % fetal calf serum (FCS; Gibco), and 50 Units/ml of penicillin and 50 µg/ml streptomycin (Gibco).

THP-1/TG2 cells cultured with 3 % FCS were differentiated into macrophages with 250 nM phorbol-12-myristate-13-acetate (Sigma) for 48 h hours. Simultaneously, the cells were stimulated with 1 µM retinoic acid (Fluka) as TG2 expression inducer to ensure maximal TG2 expression and activity. The *in vitro* TG activity inhibition assay was performed as previously described [296]. In detail, the cells were washed with serum-free medium and incubated for 4 h (37 °C, 5 % CO2) with 1 mM of the TG substrate 5-(biotinamido) pentylamine (BAP, Pierce) in serum free medium. A range of concentrations (0.03 to 100 µM) of the TG2 inhibitors BJJF078 and ERW1041E dissolved in DMSO (final DMSO concentration per well: 0.06 %). were added into the wells for 15 min (37 °C, 5 % CO2). As a positive control for this assay similar concentrations of the well characterized TG2 inhibitor Z006 (Zedira) were added to separate wells. Subsequently, 8 µM of the calcium ionophor A23187 was added for 1 h to allow cellular calcium influx which activates (intra-)cellular TG. After washing with cold PBS (supplemented with 1.2 mM calcium and 0.5 mM magnesium), the cells were harvested in ice-cold homogenizing-buffer (50 mM Tris, 150 mM NaCl, 1 mM EDTA, pH 7.5) supplemented with protease inhibitors (100 µM phenylmethylsulfonyl fluoride 1 µg/ml pepstatin, 10 µg/ml aprotinin, 10 µg/ml leupeptin, all Sigma). The total protein concentration was determined with the BCA method (Pierce, according to protocol) and adjusted to the same concentration in all samples. Subsequently, 96-well Maxisorp plates were filled with coating buffer (50 mM Tris, 150 mM NaCl, 5 mM EGTA, 5 mM EDTA, pH 7.4) and 1 µg of protein sample added and incubated on a shaker (overnight, 4 °C). After equilibration to room temperature, 200 µl of incubation-buffer (50 mM Tris, 80 mM NaCl, 2.5 % bovine serum albumin, 0.01 % SDS, 0.01 % Tween20, pH7.4) was added to each well. The plate was incubated for 5 min

on a shaker at room temperature, followed by 2 hours on a shaker at 37 °C. After washing with wash-buffer (50 mM Tris, 80mM NaCl, 0.5 % bovine serum albumin, 0.01 % Tween20, pH 7.4), 100 µl streptavidin conjugated horseradish peroxidase (HRP) (1/5000 in wash-buffer) was added per well and incubated for 1 hour at room temperature on a shaker. This step was followed by a washing step and incubation with the HRP-substrate o-phenylenediamine dihydrochloride (OPD, 0.6 mg/ml in substrate buffer with 38 uM citric acid, 88 uM Na_2HPO_4, 4.9 mM H_2O_2, pH 5.0). Adding 100 µl OPD-solution starts the color reaction, which is developed within 30 min and then stopped by adding 100 µl/well 1 M H2SO4 . The optical density at 492 nm was measured.

Inhibition of TG2 interaction with fibronectin

To determine the potential effect of BJJF078 and ERW1041E on the interaction of TG2 with fibronectin, ELISA experiments were performed as described previously [157]. Briefly, 96 well ELISA plates (Nunc, Maxisorp) were coated with 100 µg/ml mouse anti his-tag monoclonal antibody (Roche) in PBS at 4 ºC overnight. This was followed by simultaneous washing and blocking with 0.5% BSA in PBS (3x 10 min). Per well 50 µl of a 10 nM human recombinant TG2 (his-tagged, Zedira) solution in PBS was added. Into each well (triplicates) either DMSO (control, 1 % final concentration) or TG2 inhibitors (BJJF078, ERW1041E, final concentration 5 and 15 µM in 1 % DMSO) were added. As a positive control similar concentrations of TG53, a small molecule that inhibits the interaction between TG2 and fibronectin was added (kindly provided by Prof D. Matei, Northwestern University, Chicago, USA) [157]. To determine possible consequences of the active and inactive enzymatic state of TG2, experiments were performed calcium-free and after the addition of 1 mM $CaCl_2$. After 1 h incubation at RT, 50 µl of 10 nM FN42-biotin solution (kindly provided by Prof D. Matei) was added to the wells. After an additional 1 h incubation at RT and washing steps (3x 10 min) with 0.5% BSA in PBS, 100 µl streptavidin-HRPO conjugate (from kit opr001, Covalab) was added and incubated for 1 h at RT. This was followed by another series of washes and the color reaction started with 100 µl of 3,3',5,5' tetramethylbenzidine substrate (TMB, from kit opr001, Covalab). After sufficient color development (15 min), the reaction was stopped with 1M HCl and absorbance was measured at 450 nm.

Induction of EAE and treatment with TG2 inhibitors

All animal experiments were approved by the animal ethical committee of the VU University Medical Center and carried out within the animal facility of the Vrije Universiteit Amsterdam (protocol number ANW14-02). C57BL/6 (C57BL/6JOlaHsd) mice were purchased from Harlan (The Netherlands) at an age of 10 weeks and acclimatized to the new environment with water and food access ad libitum for 2 weeks before EAE induction. Humane endpoints were taken into account to prevent unnecessary suffering of the animals.

Active EAE was induced with the myelin oligodendrocyte glycoprotein peptide amino acids 35-55 (MOG_{35-55}) from a EAE induction kit (Hooke laboratories), according to

the provided protocol. In short, mice were injected subcutaneously in the upper and lower back with 100 µl of an emulsion of MOG_{35-55} in complete Freund's adjuvant (CFA, containing heat inactivated Mycobacterium tuberculosis) each. At 3 hours and 26 hours after the subcutaneous injection of the emulsion, mice received an intraperitoneal injection of 150 ng pertussis toxin dissolved in PBS (volume: 0.1 ml). Disease symptoms and body weight were assessed daily starting from day 7 after immunization according to the following scale: 0 no disease, 0.5: partial tail weakness, 1: tail paralysis, 2: hind limb weakness, 3: partial hind limb paralysis, 4: complete hind limb paralysis, 5: moribund, dead [297].

The mice were injected twice daily with BJJF078 (n=11) or ERW1041 (n=12), starting from the onset of EAE symptoms until the end of the experiment (day 21/day 28 after immunization). The EAE animals were injected intraperitoneally with an inhibitor dose of 25 mg/kg body weight (i.e. ~100 µl) containing 20 % DMSO, while the corresponding control groups (n=12 and n=10) were injected with PBS in 20% DMSO.

Tissue processing

Animals were sacrificed between day 21 and day 28 post EAE induction. Mice were anesthetized by intraperitoneal injection of ketamine and xylazine and sacrificed by decapitation. Liver, spleen and spinal cord tissue were carefully dissected and snap-frozen in liquid nitrogen and stored at -80 C until use. Coronal cryo-sections (10 µm) were cut from the cervical, thoracic and lumbar spinal cord tissue (embedded in OCT tissue tek, VWR Chemicals), dehydrated and stored at -80 ºC until use.

***In situ* TG activity in tissue sections**

In situ TG activity detection in post-mortem tissue from EAE mice was performed as described previously [298]. Thawed unfixed cryo-sections of the cervical, thoracic and lumbar spinal cord were incubated in buffer (100 mM Tris-HCl, pH 7.4, 5 mM $CaCl_2$, 1 mM DTT, pH 7.4) for 20 min at room temperature. The incubation was continued for 30 min at 37°C in buffer supplemented with 50 µM of the TG substrate BAP (Pierce). Some sections had 100 µM of the TG2 inhibitor Z006 (Zedira) added to the buffer in both incubation steps to determine TG2 specificity of the derived signal in the assay. Sections were subsequently washed with MilliQ water, air-dried and fixed for 10 min with acetone. After washes in TBS, endogenous peroxidase activity was blocked for 15 min with 0.3 % hydrogen peroxide and 0.1 % sodium azide in TBS. Subsequently, sections were blocked with 3 % bovine serum albumin in TBS containing 0.5 % TritonX-100 (TBS-T). This step was followed by incubation with HRP-labeled avidin-biotin complex (ABC complex 1:400; Vector Laboratories) for 1 h at RT and detection with the chromogen 3,3-diaminobenzidine (DAB, Sigma) and nuclear counterstaining with hematoxylin, if applicable. Sections were dehydrated in graded ethanol solutions and cleared in xylene before coverslipping with Entellan mounting medium (Merck Millipore).

Immunohistochemistry

Immunohistochemical staining was performed on cervical, thoracic and lumbar spinal cord sections from EAE mice treated with vehicle, BJJF078 or ERW1041E. The sections were brought back to room temperature and fixed with acetone for 10 min.

Single immunohistochemical staining

For single immunohistochemical stainings (CD3, CD45, CD68), endogenous peroxidase activity was blocked for 15 min with 0.3 % hydrogen peroxide and 0.1% sodium azide in TBS. Sections were subsequently blocked with 3 % bovine serum albumin in TBS containing 0.5 % TritonX-100 (TBS-T). The sections were incubated with primary antibodies (Table 1) at 4 ºC overnight. After subsequent 2 h incubation with appropriate biotinylated IgGs (1/400, Jackson), the procedure was continued with a 1 h incubation with HRP-labeled avidin-biotin complex (ABC complex 1:400, Vector ABC elite kit, Vector laboratories) and the protocol was followed as described for the *in situ* TG activity staining above. Semi-quantitative analysis of cellular infiltrates per cell type was performed by unbiased manual evaluation of stained lesion areas per spinal cord section.

Table 1. Primary antibodies used for immunohistochemistry.

Target	Host	Dilution	Supplier	Code/Clone
CD3	Rat	1/200 (DAB) 1/100 (FL)	Serotec	MCA500G
CD45	Rat	1/10	Dept. MCBI, VUmc, Amsterdam, Netherlands [299] (gift)	MP33
CD68	Rat	1/500 (DAB) 1/1000 (FL)	Serotec	MCA1957
TG1	Goat	1/100	Santa Cruz	sc-18129
TG2	Mouse	1/100	Prof T. J. Johnson, Sheffield University, UK (gift)	Clone IA-12

FL: fluorescent; DAB: 3,3-diaminobenzidine

Bright field immunohistochemical double labeling

Co-labeling of TG1 and CD45 was performed for bright field microscopy. After the blocking of endogenous peroxidase activity blocked with 0.3 % hydrogen peroxide and 0.1% sodium azide in TBS for 15 min, the sections were subsequently blocked with 3 % bovine serum albumin in TBS-T. The sections were incubated with both primary antibodies (Table 1) at 4 ºC overnight. After 30 min incubation with ImmPRESS alkaline phosphatase coupled anti goat IgGs (Vector laboratories), a 2 h incubation with biotinylated mouse anti rat IgGs followed (1/400, Jackson). Subsequently, the sections were incubated for 1 h incubation with HRP-labeled avidin-biotin complex (ABC complex 1:400, Vector ABC elite kit, Vector laboratories). Ultimately, color reaction was performed first with liquid permanent red (LPR, Dako) and then with DAB. Images acquired with a spectral imaging camera (Nuance) are shown pseudo-colored in the style of fluorescent staining to increase visual contrast.

Fluorescent immunohistochemical double labeling

Immunohistochemical fluorescent co-labeling of the immune cell markers CD3, CD45 and CD68 with TG2 (Table 1) required pre-treatment with a mouse on mouse blocking kit (M.O.M.; Vector Laboratories) according to the manufacturer's guidelines. Briefly, the sections were blocked for 1 h with blocking reagent. This was followed with incubation with primary antibody (TG2 and either CD3, CD45 or CD68) at 4 ºC overnight. After 2 h incubation with AF594 or AF488 labeled appropriate IgGs (1/400, Molecular Probes), the sections were coverslipped with Vectashield hard containing DAPI (Vector laboratories).

RNA isolation and semi-quantitative RT-PCR

Total RNA from snap-frozen spinal cord (pooled cervical, thoracic and lumbar region) was isolated using Trizol (Invitrogen) according to the manufacturer's protocol. RNA concentration and purity were determined with a NanoDrop 2000 spectrophotometer (Thermo Fisher Scientific). Purity was accepted with a 260/230 nm absorbance ratio of 2.00-2.20 and a 260/280 ratio of 1.90.-2.00. For reverse transcription into cDNA, 1 µg of RNA was used with the High-Capacity cDNA Reverse Transcription kit (Life Technologies), using 50 pmol oligo-dT16 primers, according to the manufacturer's instructions. For quantitative real-time PCR (qPCR), Power SYBR Green Master Mix (Applied Biosystems) was used according to manufacturer's protocol. Intron-spanning primers (Table 2) were designed with Primer-BLAST [299], purchased from Eurogentec and used at 3.75 pmol per 12.5 ng cDNA in each reaction. Subsequently, qPCR was performed according to the previously published MIQE guidelines [300]. The qPCR reaction was performed in a total volume of 20 µl in MicroAmp Optical 96-well Reaction Plates on a StepOnePlus Real-Time PCR system (Applied Biosystems). The thermal cycling conditions were an initial 10 min at 95 °C followed by 50 cycles of 15 s at 95 °C and 1 min at 60 °C. The reaction specificity was verified by a melt curve analysis. The relative expression level of the target genes was determined by the LinRegPCR software (http://www.hfrc.nl, downloads, applications, lin reg PCR, version 2017) using the following calculation N0 = Nq/ECq (N0 = target quantity, Nq = fluorescence threshold value, E = mean PCR efficiency per amplicon, Cq = threshold cycle [301]. The obtained values were normalized to glyceraldehyde-3-phosphate-dehydrogenase expression (GAPDH) [302, 303].

Table 2. Oligonucleotide primers used for cDNA amplification.

Protein /gene	Reference sequence NCBI	Sequences forward (fwd) and reverse (rev)	Amplicon length (base pairs)
FXIII / F13A1	NM_028784.3	fwd: 5'-CAGCAATGGTGAATGCCAAGGA-3' rev: 5'-GCTGATGGAGGGATGCCGTA-3'	85
GAPDH	NM_008084.2	fwd: 5'-GGAGAAACCTGCCAAGTATG-3' rev: 5'-TCCTCAGTGTAGCCCAAGATG-3'	90
IFNγ /	NM_008337.4	fwd: 5'-GTTTGAGGTCAACAACCCAC-3'	116

IFNG		rev: 5'-ATCAGCAGCGACTCCTTTTC-3'	
IL-1β / IL1b	NM_008361.4	fwd: 5'-GCCACCTTTTGACAGTGATG-3' rev: 5'- CTTCTCCACAGCCACAATGA-3'	184
IL-1ra / IL1RA	M57525.1	fwd: 5'-TGACAGTGGAACGGAATGAC-3' rev: 5'-GTATCCCAGATTCTGAAGGCT-3'	98
iNOS / NOS2	NM_010927.3	fwd: 5'-ACATCGACCCGTCCACAGTAT-3' rev: 5'-CAGAGGGGTAGGCTTGTCTC-3'	177
TG1 / Tgm1	NM_001161715.1	fwd: 5'-ACCAGCAGTGGCATCTTC-3' rev: 5'-ATGAAAGGTGTGTCATACTTC-3'	88
TG2 / Tgm2	NM_009373.3	fwd: 5'-GGGCCTTCTCATCGAACCAG-3' rev: 5'-CAGGACCCGGATCTTGATTTC-3'	91
TG3 / Tgm3	NM_009374.3	fwd: 5'- ACATCAGCACCAAGGCAGTAGG -3' rev: 5'- CCTCGAAGATGTTGCGCCGAAA-3'	152
TG6 / Tgm6	NM_001289747.1	fwd: 5'- CAGCAGTGGTAGGAGTGACAG -3' rev: 5'- CTCTTGGAAGGGGTTATGTTG-3'	187
TNFα / TNFa	NM_013693.2	fwd: 5'-GTAGCCCACGTCGTAGCAAAC-3' rev: 5'-GGCACCACTAGTTGGTTGTCTT-3'	116

Statistical analysis

The normal distribution of the data was determined with the Shapiro-Wilk test (GraphPad Prism, Version 6). If normally distributed, subsequent student T-test or, if not normally distributed, Mann-Whitney U test or generalized linear model analysis was applied (GraphPad Prism or IBM SPSS Statistics, Version 22). Significant differences were considered to be present if p-values were below 0.05.

RESULTS

BJJF078 and ERW1041E inhibited recombinant Transglutaminase activity

Test tube measurements were performed to determine the inhibitory potency and specificity of BJJF078 and ERW1041E towards TG1, TG2, and FXIII enzymatic activity. Although the homology of human and mouse TG enzymes is high (84 %, protein BLAST, NCBI), these TG2 inhibitors were specifically designed to inhibit human TG2 activity. As the present study intended to use them in a mouse model, we compared the inhibitory effect of the compounds on recombinant mouse and human TG2 activity (Fig 2a). IC50 values of BJJF078 were 41 and 54 nM, for human and mouse TG2, respectively. ERW1041E proved less potent and required µM concentrations to inhibit TG2 activity. Furthermore, it was slightly more potent to inhibit human than mouse TG2 activity (IC50 of 1.6 µM vs 6.8 µM, respectively). Other members of the TG family tested included human TG1 and Factor XIII. The IC50 of BJJF078 to inhibit TG1 was 0.16 µM and it was 0.44 µM for ERW1041E (Fig 2b). Furthermore, the IC50 values of BJJF078 and ERW1041E to inhibit FXIII activity were 22 µM and 52 µM, respectively (Fig 2c).

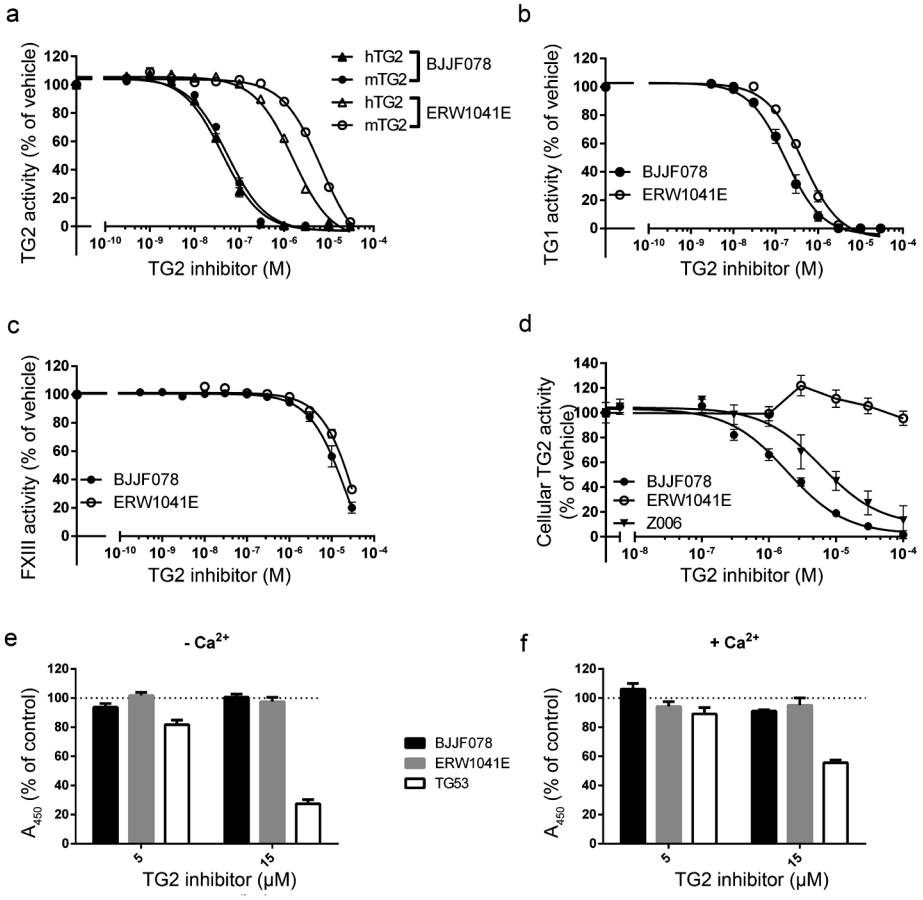


Figure 2: Inhibition of TG activity and TG2-fibronectin interaction by BJJF078 and ERW1041E in solution and in vitro. (a) BJFF078 and ERW1041E dose-dependently inhibited human (hTG2) and mouse (mTG2) recombinant TG2 activity. BJJF078 and ERW1041E inhibited also (b) human recombinant TG1 and (c) human recombinant FXIII. (d) Cellular activity of human TG2 in THP1 cells was dose-dependently inhibited by BJJF078 and Z006 but not by ERW1041E. (e,f) Effect of BJJF078 and ERW1041E on TG2 binding to fibronectin without (e) or with added calcium (f). n=1-3 independent experiments with triplicates each.

BJJF078 and not ERW1041E inhibited cellular TG2 activity *in vitro*

We determined if BJJF078 and ERW1041E were able to inhibit cellular TG activity. TG2 overexpressing THP-1 macrophages were stimulated to ensure high amounts of the active enzyme that can be pharmacologically inhibited. BJJF078 effectively reduced TG2 transamidating activity in this setup, with an IC50 of 1.8 µM (Fig 2d, closed circles). ERW1041E instead proved to have no effect on TG2 activity in this experimental setup (Fig 2d, open circles). The well-established TG2 inhibitor Z006 was used as a positive control (Fig 2d, triangles) and showed an IC50 of 6 µM, which is in a similar range as BJJF078.

BJJF078 and ERW1041E did not interfere with TG2 binding to fibronectin

To measure the effects of the TG2 activity inhibitors on the interaction between TG2 and fibronectin (fragment FN42), an ELISA experiment was conducted. Neither BJJF078 nor ERW1041E interfered with the binding of TG2 to FN42, whereas TG53, a small molecule inhibitor designed to interrupt TG2-fibronectin binding resulted in a dose-dependent reduction of TG2-fibronectin binding irrespective of the presence of calcium (Fig 2e,f).

ERW1041E modestly reduced EAE disease symptoms

We determined the effect of BJJF078 and ERW1041E on the outcome of EAE in C57BL/6 mice *in vivo* when treated from the first signs of disease motor symptoms onward. BJJF078-treated mice showed no differences in the severity of motor symptoms compared to the vehicle-treated control group (Fig 3a). Furthermore, no differences in the loss of body weight were observed (Fig 3b). In contrast, treatment with ERW1041E resulted in a modest but significant reduction in the severity of motor symptoms compared to vehicle-treated mice (Fig 3c). During disease development the progress of motor symptoms is alike, but the average maximal disease score reached in the ERW1041E (score 3.4) treated animals was lower than in the vehicle control group (score 3.9). The loss of body weight was similar in both groups and thus not affected by ERW1041E treatment (Fig 3d). No obvious adverse effects of the compound injections were observed *in vivo* or by post-mortem analysis of the abdomen.

TGs mRNA and protein in the spinal cord of EAE mice

The mRNA levels of various TG family members were measured in the spinal cord of vehicle-treated EAE animals as their presence could, in addition to TG2, contribute to EAE pathology. Tgm1 and Tgm2 were equally expressed, while Tgm3 and F13A1 showed lower mRNA levels and Tgm6 expression was below the detection limit (Fig. 4a). Additionally, we identified TG1 and TG2 protein in the spinal cord using immunohistochemical staining. At first, the infiltrated leukocytes in the spinal cord lesions were visualized with the general leukocyte marker CD45, indicating EAE lesion formation. TG2 immunoreactivity was present in all inflammatory lesions of the spinal cord and closely associated with $CD45^+$ cells (Fig 4b). Whereas TG1 immunoreactivity was less associated with $CD45^+$ cells (Fig 4c,d). Furthermore, about half of the spinal cord lesions show the presence of TG1 immunoreactivity (Fig 4c) while the other lesions are almost devoid of TG1 (Fig 4d).

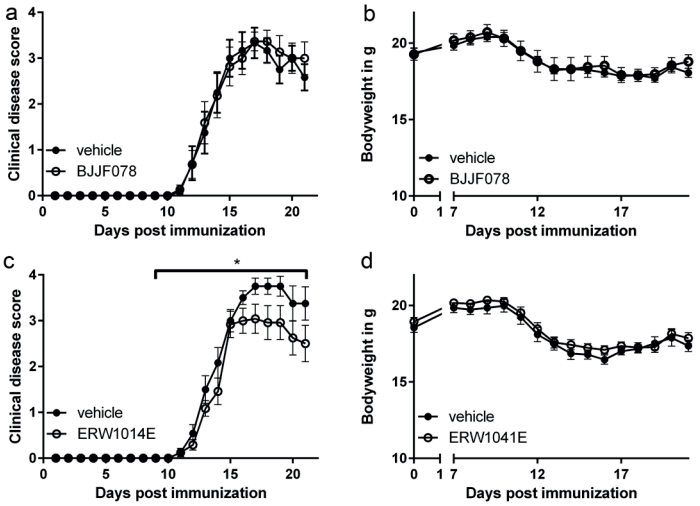


Figure 3: Disease scores and body weight of EAE animals treated with BJJF078 or ERW1041E. (a) BJJF078 did not affect motor symptoms or (b) body weight of EAE affected mice compared to vehicle treated animals. (c) ERW1041E reduced motor symptoms significantly without (d) affecting the loss of body weight of EAE affected mice. n=11-12 animals per treatment group. Statistics: generalized linear model, *P<0.05.

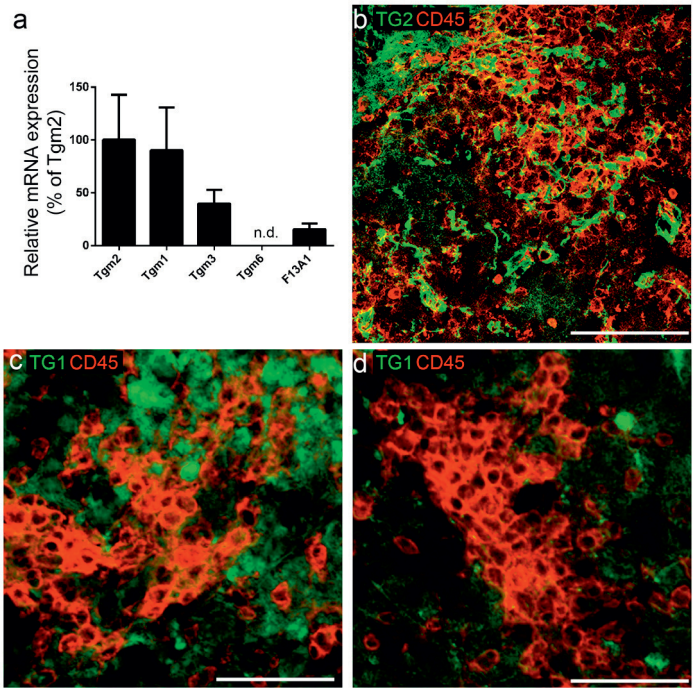


Figure 4: Transglutaminases mRNA, and TG1 and TG2 immunoreactivity in post-mortem spinal cord tissue of EAE animals. (a) EAE spinal cord mRNA levels for Tgm1, Tgm2, Tgm3, Tgm6 (n.d.=not detectable) and F13A1, (b) TG2 immunoreactivity (green) associates with CD45 (red) stained EAE lesions whereas TG1 immunoreactivity (green) is found in some lesions (d) but not in others (d). Scale bar: 25 µm. n= 9 animals/group.

TG activity in spinal cord sections of EAE mice was not affected by ERW1041E or BJJF078

In addition to the presence of TGs, also their activity was analyzed. *In situ* incorporation of the general TG substrate BAP in spinal cord sections of EAE mice allowed us to determine the level of TG enzymatic activity. To take a possible short *in vivo* half-life of BJJF078 into account which is unknown, the animals received the last injection 30-60 min before they were sacrificed. Some inter-individual variation of TG activity signal was found in the animals, which correlated to the number of lesions per section. However, the TG substrate BAP was readily incorporated in similar amounts in spinal cord sections from vehicle, BJJF078 and ERW1041E treated mice, independent of treatment (Fig 5a-c). This TG related signal, that is associated with the inflammatory lesions, was clearly reduced when the highly specific TG2 inhibitor Z006 was co-applied to the sections, indicating the source of the signal to be mainly TG2 (Fig 5d-f).

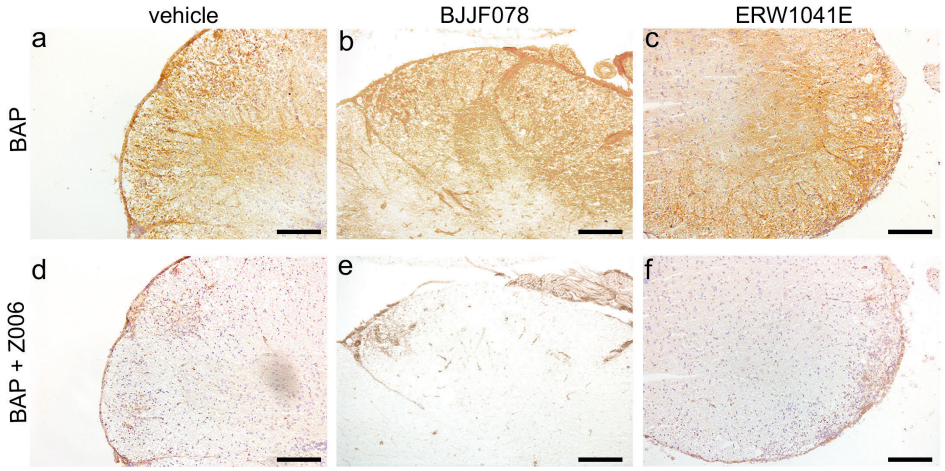


Figure 5: TG activity in spinal cord post-mortem tissue derived from EAE animals treated with vehicle, BJJF078 or ERW1041E. (a-f) *In situ* TG activity was detected in spinal cord sections derived from (a, d) vehicle, (b, e) BJJF078 and (c, f) ERW1041E treated mice. (d-f) Co-incubation of the sections with the TG2 inhibitor Z006 diminished TG activity. Scale bar: 50 µm. n= 11 or 12 animals/group.

Inflammatory cell marker and TG2 expression in the spinal cord

Inflammatory lesions in the spinal cord of EAE mice were identified by detection of CD45 positive leukocytes (Fig 6a-d), CD68 positive macrophages (Fig 6e-h) and CD3 positive T cells (Fig 6i-l). The relative amount of these inflammatory cells was not affected by treatment with BJJF078 or ERW1041E upon visual inspection (Fig 6c, d, g, h, k, l) or after semi-quantification (Table 3). Co-labeling of the CD markers (red) with TG2 (green) revealed that CD45 presence (Fig 6b) was closely associated with that of TG2. The immunoreactivity of CD68 (Fig 6f) was associated with TG2 to a lesser extent whereas CD3 immunoreactivity seemed to be found in patches with no TG2 expression (Fig 6j).

Table 3: Semi-quantitative analysis of CD45, CD68 and CD3 expression in the spinal cord of EAE mice treated with vehicle or TG2 activity inhibitors.

	CD45, range (average)	CD68, range (average)	CD3, range (average)
vehicle (control)	+ to +++ (++)	- to +++ (++)	- to + (-/+)
BJJF078	+ to +++ (++)	- to +++ (++)	- to + (-/+)
ERW1041E	+ to +++ (++)	- to +++ (++)	- to + (-/+)

-: no positive cells, + few positive cells, ++: intermediate amounts of positive cells, +++: high amounts of cells/ cellular clusters, in 3 sections per animal (cervical, lumbar and thoracic spinal cord) of 9-12 animals/group

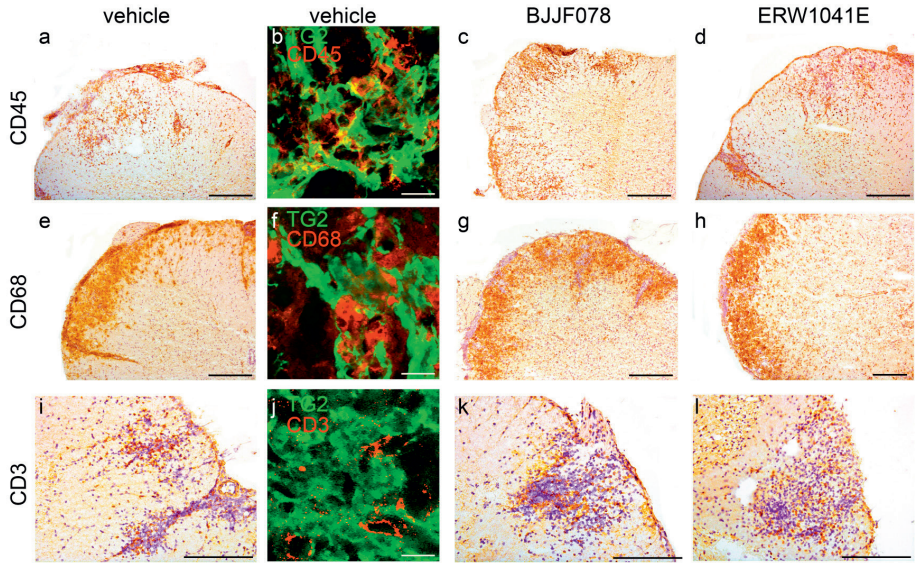


Figure 6: Cell infiltrates and TG2 expression in the spinal cord of BJJF078 or ERW1041E treated EAE mice. (a-d) BJJF078 and ERW1041E did not affect the infiltration of CD45 positive leukocytes into the spinal cord. Also (e-h), CD68 positive phagocytic cells and (i-l) CD3 positive T cells were observed in similar amount in vehicle- and TG2 inhibitor-treated animals. (b, f, j) show co-labeling of TG2 (green) with the immune cells makers (red) (b) CD45, (f) CD68 and (j) CD3. Scale bar: 100 µm, except for b, f, j: 50 µm. n=9-12 animals/group.

Expression of inflammatory mediators in the spinal cord of ERW1041E-treated EAE mice

ERW1041E treated EAE mice showed fewer motor symptoms than vehicle-treated mice, which was not corroborated by an altered leukocyte pathology in the spinal cord as shown by immunohistochemistry. We therefore analyzed the mRNA levels of inflammation-related genes which could be affected by TG2 inhibition in this model. RNA levels of the

following factors were measured: IL-1ra, IL-1β, IFNγ, TNFα and iNOS. Whereas most mRNA levels were not affected by ERW1041E treatment, TNFα and iNOS mRNA levels were slightly but not significantly enhanced after ERW1041E treatment (Fig 7a-e).

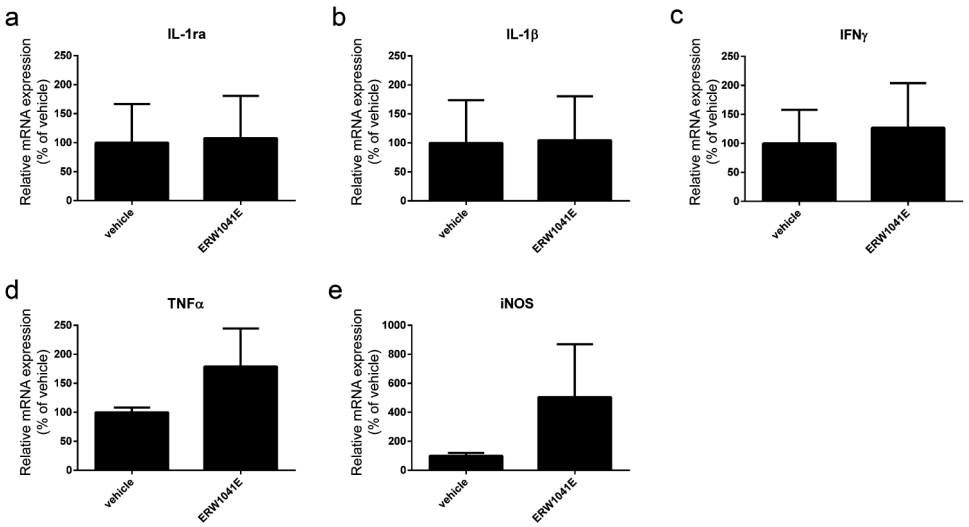


Figure 7: qPCR analysis of gene ex-pression associated with in-flammation in the spinal cord of ERW1041E and vehicle only treated EAE mice. mRNA levels of in-flammatory markers (a) IL-1ra, (b) IL-1β, (c) IFNγ, (d) TNFα and (e) iNOS were not significantly changed in the spinal cord of ERW1041E animals compared to the vehicle-treated group. n= 9-12 animals/group. Statistical analysis: student T-test or, if not normally distributed: Mann-Whitney U test.

DISCUSSION

In the present study, we used two irreversible TG2 activity inhibitors to measure their effect on disease symptoms, severity and pathology in a mouse EAE model for multiple sclerosis. Our previous studies identified TG2 as a possible therapeutical target in a rat chronic relapsing EAE model in which TG2 inhibition reduced cellular infiltration as well as disease symptoms [229, 304]. Moreover, EAE induced in C57BL/6 mice has previously been shown to be, at least partly, mediated by TG2 [229]. The present work extends these observations of TG2 inhibition using new pharmacological compounds in mouse EAE, to determine whether Transglutaminase activity is of relevance in the commonly used mouse MS model in the C57BL/6 strain. The treatment of the animals with the compound ERW1041E led to a significant reduction in motor symptom severity compared to vehicle-treated animals, while this was not observed after treatment with the compound BJJF078.

Although many TG2 inhibitors have been presented over the years, their use in animal models is scarce. The dihydroisoxazol derivate ERW1041E was chosen in this study for its previous proven efficacy *in vivo* [152, 153] and the new aminopiperidine derivative

BJJF078 showed very promising TG2 inhibitory ability with recombinant proteins (data not published) and the inhibition of cellular TG2 activity. The characterization of both compounds using recombinant human and mouse TG2 revealed a similar inhibitory capacity of recombinant TG2 and is reflecting the 84 % protein sequence homology of TG2 in both species (protein BLAST, NCBI).

Despite the previous *in vivo* results with ERW1041E that are presumably TG2 mediated [152], this inhibitor is not specific for TG2 alone but shows equipotency for TG1, as we showed to be the case for BJJF078 as well, while another TG member of the TG family, i.e. FXIII, is inhibited to a lower degree. However, it has to be pointed out that the affinities of the tested recombinant Transglutaminase enzymes for the substrate used in the assay vary and consequently it is not possible to make a direct comparison of the IC50 values between the Transglutaminase isotypes.

Subsequently, we studied the expression of various Transglutaminases in murine EAE spinal cord and found equal levels of Tgm1 and Tgm2 and lower levels of Tgm3, Tgm6 and F13A1 mRNA. Although we could hardly detect Tgm6 mRNA, other recent data showed TG6 protein expression in human MS and mouse EAE spinal cord lesions [305], which could indicate a low turn-over of the protein. By studying the *in situ* Transglutaminase activity in the spinal cord sections of EAE mice, we observed that most of the measured TG activity is derived from TG2. This is supported by the observation that the spinal cord lesions are consistently associated with TG2 but not necessarily with TG1 expression. Furthermore, we observed that TG2 is more associated with infiltrated CD45+ leukocytes than TG1 in the lesions. Concluding, it is likely that the reduction in mouse EAE symptoms after treatment with ERW1041E is due to inhibition of TG2 activity. Nevertheless, we cannot fully exclude that off-target effects and/or inhibition of TG1 and other Transglutaminases activity are involved as well.

So far very little is known about the mode of action of TG2 and possibly other TGs during EAE. It remained unknown if extracellularly and/or (intra-)cellularly located TGs contribute to EAE disease and which function(s) of the enzymes are of importance. We observed that BJJF078, in contrast to ERW1041E [94], can inhibit cellular TG2 activity although in EAE mice no measurable effect was found. These observations suggest that extracellular TG2 activity seemed to be more relevant than (intra-)cellular TG2 activity to mediate EAE motor symptom development.

Surprisingly, ERW1041E treatment did neither affect the leukocyte influx nor the production of inflammatory mediators in the murine EAE spinal cord. This is in contrast to the previously observed results of pharmacological TG2 activity inhibition with the TG2 inhibitor KCC009 in rat EAE, although both inhibitors are structurally related and belong to the dihydroisoxazol type [229]. Of interest in this respect is that KCC009 can interfere with fibronectin assembly [182, 229], whereas the interaction of TG2 and fibronectin was not affected by either BJJF078 or ERW1041E. This may at least partly explain why no change in leukocyte infiltration was observed in the present study. Another explanation of the different outcomes of ERW1041E and the previously used KCC009, is the use of a mouse EAE model instead of the rat chronic relapsing EAE model. The pathogenesis of this mouse model in C57BL/6 mice is more depended on lymphocytes than monocytes [67, 68], the suspected main source for TG2 [229]. Moreover, the non-cellular site of action of

ERW1041E might suggest a different mechanism than purely cellular TG and especially TG2 activity inhibition aiding cell migration. A possible mechanism of action could lie in TG activity affecting extracellular matrix deposition and stiffness [126, 306]. This process might be altered by the inhibition of TGs *in vivo*, irrespective of the effect on cell migration or the production of inflammatory mediators [291]. This could also explain why BJJF078 and thus cellular TG inhibition did not exert any effect in this model.

An additional explanation for the lack of effect of BJJF078 could be its limited bioavailability. A previous successful *in vivo* dose and treatment scheme of ERW1041E was used [153], but no *in vivo* bioavailability information on BJJF078 is available yet. Hence, it might be possible that BJJF078 is (1) not distributed to the site of interest or (2) has a much shorter half-life compared to the proposed 12 h inhibitory *in vivo* half-life of ERW1041E. Therefore we cannot exclude that BJJF078 might be useful as an *in vivo* TG activity inhibitor once its pharmacokinetic properties are revealed and optimized. We can thus not eliminate that cellular TG1 and TG2, in addition to extracellular TG enzymes, may contribute to EAE.

To summarize, our data indicate that BJJF078 and ERW1041E are both potent inhibitors of human and mouse TG2 and TG1 activity but do not interfere with TG2-fibronectin binding. Interestingly, in mouse EAE, ERW1041E and not BJJF078 treatment is able to reduce motor symptoms. Although we cannot exclude issues on bioavailability and *in vivo* efficacy of the inhibitors used, we hypothesize that surface/extracellular TG1/TG2 activity is of greater importance than (intra-)cellular TG1/TG2 activity to mediate mouse EAE pathogenesis. Furthermore, this effect is independent of TG2-fibronectin binding which is neither affected by ERW1041E nor by BJJF078, but the potential side and mechanism of action of ERW1041E remain elusive. Subsequent studies could focus on delineating the process of surface or extracellular TG1/TG2 transamidating activity in this EAE model, which might be of interest to reduce cellular infiltration in EAE and MS.

Acknowledgements

We would like to thank B. Palanski and Prof C. Khosla (Stanford University, USA) for providing us with ERW1041E. We thank Prof K. Mehta (University of Texas, USA) for providing the pCDH-hTG2 vector and Prof D. Matei (Northwestern University, Chicago, USA) for providing FN42 and TG53. Furthermore, the help of the staff from the UPC animal facility of the VU was highly appreciated. The assistance of Prof Jos Twisk (VUmc, Amsterdam) for the statistical analysis of the EAE experiments was highly valued.

SUPPLEMENT

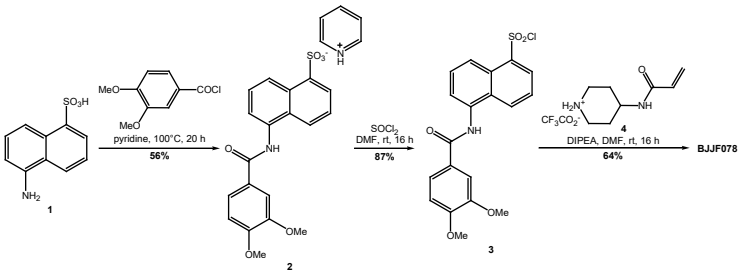
S1 Appendix: Synthesis of BJJF078

Step 1: to a solution of the commercially available 5-amino-1-naphthalenesulfonic acid (1) (CAS: 84-89-9) (1 equivalent) in pyridine (0.67 M) was added 3,4-dimethoxybenzoyl chloride (1.2 equivalents) and the resultant solution was stirred at 100ºC for 20 h. The solvent was removed under vacuum and the crude material was taken up in methanol (twice) to obtain a

precipitate. The latter was filtered to give 5-[(3,4-dimethoxybenzoyl)amino]naphthalene-1-sulfonate pyridinium salt (2) as a solid. Yield: 56%; mp: > 210ºC (washing MeOH); ^{1}H NMR (300 MHz, DMSO-*d*$_6$) δ (ppm): 3.85 (s, 3H, CH_3), 3.86 (s, 3H, CH_3), 7.11 (d, *J* = 8.5 Hz, 1H, H_{Ar}), 7.45 (dd, *J* = 7.2, 8.5 Hz, 1H, H_{Ar}), 7.48-7.57 (m, 2H, H_{Ar}), 7.68 (d, *J* = 2.0 Hz, 1H, H_{Ar}), 7.75 (dd, *J* = 2.0, 8.4 Hz, 1H, H_{Ar}), 7.89-8.01 (m, 4H, H_{Ar}), 8.41-8.51 (m, 1H, H_{Ar}), 8.81 (dd, *J* = 1.5, 7.7 Hz, 1H, H_{Ar}), 8.87 (d, *J* = 5.2 Hz, 2H, H_{Ar}), 10.30 (s, 1H, NH, NH); ^{13}C NMR (75 MHz, DMSO-*d*$_6$) δ (ppm): 55.6 (CH_3), 55.7 (CH_3), 111.0 (CH), 111.1 (CH), 121.2 (CH), 124.1 (CH), 124.4 (CH), 124.5 (CH), 124.9 (CH), 125.1 (CH), 126.2 (CH), 126.5 (C), 127.1 (2 CH), 129.8 (C), 130.2 (C), 133.9 (C), 142.5 (2 CH), 144.2 (C), 145.9 (CH), 148.4 (C), 151.6 (C), 165.6 (C=O); MS (ESI): m/z = 386.3 $[M\text{-}PyrH]^-$.

Step 2: to a suspension of the pyridinium salt 2 (1 equivalent) in DMF (0.59 M) was added dropwise thionyl-chloride (1.5 equivalents). The reaction was stirred at room temperature for 16 h. The reaction mixture was poured into ice-water. The resulting solid was quickly filtered, washed twice by cold water and dried over P_2O_5 under vacuum. The freshly moisture sensitive crude 5-[(3,4-dimethoxybenzoyl)amino]naphthalene-1-sulfonyl chloride (3) was not further purified and was used directly in the next step. Yield: 87%.

Step 3: to a solution of the ammonium salt 4 (1 equivalent) in DMF (0.1 M) was added *N*,*N*-diisopropylethylamine (DIPEA, 3 equivalents) at room temperature, followed by the addition of 3 (1,1 equivalents) at 0ºC. The reaction mixture was stirred at room temperature for 16 h. The mixture was poured dropwise into water and the resulting precipitate was filtered, washed with 1N HCl and washed again with water (twice). The crude solid was dried over P_2O_5 under vacuum then purified by column chromatography on silica gel (solvent: MeOH/CH_2Cl_2 5:95) to give 3,4-dimethoxy-*N*-(5-[4-(acryloylamino)piperidin-1-sulfonyl]naphthalen-1-yl)benzamide (BJJF078). Yield: 64%; mp: 125-128ºC (washing EtOH); ^{1}H NMR (300 MHz, DMSO-*d*$_6$) δ (ppm): 1.31-1.48 (m, 2H, CH_2), 1.76-1.88 (m, 2H, CH_2), 2.83-2.95 (m, 2H, CH_2), 3.59-3.79 (m, 3H, CH + CH_2), 3.87 (s, 6H, 2 x CH_3), 5.55 (dd, *J* = 2.7, 9.7 Hz, 1H, =CH_2), 6.04 (dd, *J* = 2.7, 17.1 Hz, 1H, =CH_2), 6.16 (dd, *J* = 9.7, 17.1 Hz, 1H, -CH=), 7.14 (d, *J* = 8.6 Hz, 1H, H_{Ar}), 7.63-7.83 (m, 5H, H_{Ar}), 8.06 (d, *J* = 7.6 Hz, 1H, NH), 8.20 (d, *J* = 6.4 Hz, 1H, H_{Ar}), 8.32 (d, *J* = 8.3 Hz, 1H, H_{Ar}), 8.56 (d, *J* = 8.5 Hz, 1H, H_{Ar}), 10.45 (s, 1H, NH); ^{13}C NMR (101 MHz, DMSO-*d*$_6$) δ (ppm): 30.9 (2 x CH_2), 44.0 (2 x CH_2), 44.8 (CH), 55.6 (CH_3), 55.7 (CH_3), 111.0 (CH), 111.1 (CH), 121.3 (CH), 122.9 (CH), 124.6 (CH), 125.2 (CH=), 125.3 (=CH_2), 126.2 (C), 127.8 (CH), 128.8 (C), 129.9 (CH), 130.0 (CH), 130.5 (C), 131.7 (CH), 133.5 (C), 135.1 (C), 148.4 (C), 151.8 (C), 163.8 (C=O), 165.7 (C=O); MS (ESI): m/z = 524.2 $[M+H]^+$; HRMS (ESI): calcd for $C_{27}H_{30}N_3O_6S$ $[M+H]^+$, 524.1850; found, 524.1835.



Schematic representation of BJJF078 synthesis.



Chapter 6

SUMMARIZING DISCUSSION



SUMMARIZING DISCUSSION

MS is a seriously incapacitating progressive neuroinflammatory disorder for which potent and tailored pharmacological treatments are needed. One of these treatments is Natalizumab, which is very effective in blocking T-lymphocyte infiltration into the CNS and reducing clinical symptoms. Unfortunately, it can also cause serious side effects [307, 308]. This example of a very effective treatment demonstrates that drugs that reduce the influx of leukocytes or specific subsets thereof, but with fewer side effects, are of significant interest in MS research. With this goal in mind, a detailed understanding of the type of cells and mechanisms involved in the disease process of MS is of crucial importance to develop new therapeutic agents to halt or dampen disease progression. Based on the outcome of previous research, we believe that especially monocytes and/or macrophages are an interesting target. They are known to have a detrimental influence in the early stage of MS pathogenesis and in matching inflammatory animal MS models (experimental autoimmune encephalomyelitis, EAE) and constitute the majority of infiltrated immune cells in the CNS lesions [212, 225, 226, 254, 309]. Thus, monocytes and macrophages are of special interest as loci of targets for the development of tailored treatments for MS.

Within this context, we focused on the enzyme TG2 and its potential role in MS and EAE. The increased presence and activity of TG2 during inflammation *in vivo* is known to contribute to many fundamental and pathology related processes, including cell adhesion and migration, ECM deposition, cytoskeletal rearrangement, cell differentiation, apoptosis and phagocytic processes such as efferocytosis. The involvement of TG2 in at least some of these processes, also relevant in MS, makes it an interesting protein to study.

The aims of this thesis were therefore to

1) identify the presence of TG2 and the cell types expressing it in post-mortem CNS material of MS patients and of relevant MS animal models, i.e. EAE in rats and mice.

2) determine the contribution of TG2 to EAE symptoms and pathology and its potential as a druggable target.

TG2 expression in MS and EAE lesions

Our studies demonstrated the cellular expression pattern of TG2 in inflammatory active white matter of both post-mortem MS and EAE CNS tissue (**chapters 2, 3, 4 and 5)**. We first confirmed TG2's constitutive expression in endothelial cells in the human and murine CNS tissue, irrespective of the disease state. In post-mortem MS patient-derived brain material, we observed additional cellular TG2 expression, distinct from that of healthy control subjects (**chapters 2 and 3**). Cells with a round morphology present in the perivascular cuff and the surrounding parenchyma of (chronic) active MS white matter

lesions express TG2. These cells are not observed in healthy control tissue or in inactive MS lesions in which inflammatory activity is not detectable anymore. The appearance of TG2 in cells with a round morphology in lesions with inflammatory activity is in line with observations that TG2 expression can be regulated by various inflammatory mediators [310, 311]. The presence of these inflammatory mediators in the CNS is highest during active disease and recedes over time when blood brain-barrier functions are restored and thus less immune cells and inflammatory mediators appear in the brain [238]. We identified these TG2 expressing cells in MS lesions as MHC-II positive cells (**chapter 2**) and further characterized them as leukocytes (i.e. CD45 expressing cells, **chapter 3**). Consequently, we believe that these cells are predominantly immune cells extravasated from the bloodstream [312]. Our more detailed analysis exposed their identity primarily as monocytes and macrophages (**chapter 3**). Although a large portion of cellular infiltrates in MS lesions consists of lymphocytes [216], no TG2 immunoreactivity was found in lymphocytes, indicating that involvement of TG2 in MS is probably exclusively mediated by monocyte- and macrophage-derived TG2.

To further extend our knowledge on TG2 expression in MS pathology, we studied tissue from EAE animal models, which are models commonly used for MS research [313]. Corresponding to the expression of TG2 in macrophages in (chronic) active MS lesions, TG2 appears in macrophages and/or microglial cell in the spinal cord of dark agouti rats suffering from chronic relapsing EAE (cr-EAE, **chapter 2**) and in C57BL/6 mice suffering from monophasic EAE (**chapters 4 and 5**). Interestingly, in both rodent species, the number of TG2 expressing cells in the lesions seems to correlate with lesion size and disability symptoms, supporting a connection between TG2 and inflammation. In addition, we not only observed TG2 expression in affected spinal cord tissue but also in round cells adhered to the luminal wall of the spinal cord vasculature potentially on their way to infiltrate the CNS tissue (**chapter 5**). This indicates that TG2 upregulation in monocytes in EAE might already occur previous to their extravasation into the CNS parenchyma. Circulating monocytes have a relatively low TG2 expression, but upon adhesion to the endothelium, TG2 expression in monocytes immediately increases as they differentiate into macrophages [244]. However, we cannot exclude that TG2 expression is already increased in circulating monocytes in EAE affected animals. An option that is supported by MS patient-derived data, which showed that TG2 expression is higher in circulating monocytes of MS patients compared to those of healthy control subjects [240].

The MS and EAE-related TG2 upregulation in peripheral monocytes might then very well be a prelude to further involvement of TG2 in MS and EAE pathology in the CNS. Indeed, we found that TG2 in CNS lesions in MS and EAE seems to be predominantly expressed in macrophages with lysosomal and therefore phagocytic activity (CD68 expressing macrophages), suggesting that TG2 might be involved in phagocytosis of myelin debris or apoptotic cells [246], an important process for clearance of MS lesions. Unfortunately, further analysis into macrophage phenotypes subsets did not reveal a predilection for any cellular subset in MS lesions (**chapter 3**). Generally, lysosomal active macrophages have an anti-inflammatory signature [248], and there is an increase of TG2 expression in such cells *in vitro* [237, 251]. However, we could not confirm that TG2 expression is limited to an anti-inflammatory macrophage phenotype *in vivo*. These

observations are supported by previous data on the presence of intermediate phenotypes in MS lesions as a substitute for clear distinct cellular macrophage subtypes [38].

We demonstrated that TG2 in rodent EAE and human MS lesions is predominantly expressed in leukocytes and more specifically in macrophages, which are abundantly present in MS lesions and are involved in disease pathology following infiltration of the CNS [179]. Additionally, in another EAE model in marmoset (i.e. non-human primates), showed a similar TG2 expression pattern in monocytes/macrophages [231]. The constraint of TG2 expression to cells associated with lesions that show inflammatory activity in MS and EAE is in line with its upregulation during inflammation. It also supports our hypothesis that TG2 is involved in both disease pathologies, possibly via a contribution to cellular migration and CNS infiltration, a well-known role of TG2 [119], and is involved in the myelin phagocytosis process. The restriction of TG2 expression to specific cell types that are major players in disease pathology of MS and EAE, makes TG2 an interesting therapeutic target with a restricted range of action and potentially limited side effects.

A contribution of TG2 to EAE development in rodents

To investigate a potential causal contribution of TG2 to EAE motor symptom development and pathology, we pharmacologically manipulated TG2 activity in rodent EAE models (**chapters 2 and 5**). For this purpose we used three small molecule compounds that have been developed as irreversible TG2 inhibitors, i.e. KCC009 [181], ERW1041E [153] and BJJF078. In addition, we included two reversible acting competitive substrates, cystamine [200] and monodansylcadaverine [181]. We treated rat and/or mice suffering from experimentally induced EAE with these compounds and assessed the consequence(s) of these interventions on motor symptoms and spinal cord pathology which we supported with additional data derived from an *in vitro* blood-brain-barrier model (**chapter 2**). Surprisingly, the effect of treatment is vastly dependent on the combination of compound and EAE model, which we believe depends not only on the compound used but also on the variation in pathology in different EAE models and/or species. Overall, the pharmacological blockade of TG2 activity in rat and mouse models showed that it can drastically reduce EAE motor symptoms and pathology. The administration of TG2 inhibiting compounds, i.e. KCC009, ERW1041E, cystamine and monodansylcadaverine, resulted in a reduction of motor symptoms, confirming a role for TG2 in EAE. These data on the contribution of TG2 to EAE motor symptom development were supported with data derived from TG2 knockout mice, which similarly to the drug-treated animals, developed less paralysis compared to wildtype littermates (**chapter 2**). Our findings therefore suggest that TG2 is indeed contributing to the development of EAE symptoms in our rodent models. In contrast, the compound BJJF078, did not result in any measurable effects, which we believe might be due to limited bioavailability under our experimental conditions, which has not been tested yet.

The effect of reversible and irreversible compounds was comparable, albeit, on average, irreversible inhibitor treatment seemed slightly more effective. This could be due to their general pharmacological characteristics. Irreversible inhibitors bind covalently to

their target, whereas reversible inhibitors bind non-covalently and therefore may dissociate off the active enzyme and therefore result in less inhibitory action.

In some of our animal experiments, the reduction in motor symptoms was accompanied by a massive reduction in CNS infiltration of leukocytes and lesion formation (**chapter 2**). The animals treated with TG2 inhibitors showed considerably fewer and smaller spinal cord lesions compared to untreated animals suffering from EAE. The cells whose CNS infiltration was hampered by TG2 inhibition were exclusively MHC-II positive cells, presumably monocytes/macrophages. This effect was strongest in KCC009 treated cr-EAE rats and was manifested as a selective reduction in macrophages found in spinal cord lesions. The reduction of specifically this cell type is in agreement with our previous data on their TG2 expression status in EAE. We did not observe any change in lymphocyte infiltration, as we already expected from their lack in TG2 expression (**chapter 2, 3**). Although EAE and MS are considered T cell-driven diseases [203] and TG2 is known to be involved in T cell-mediated cytokine expression [198, 314], our data propose that the effect of TG2 inhibition on EAE motor symptoms is due to monocyte- and macrophage-derived TG2. The effective inhibition of macrophage CNS infiltration in spinal cord lesions after KCC009 treatment may, in turn, explain the observed decrease in demyelination and reduced disability scores of the animals (**chapter 2**). Similarly, complete depletion of macrophages in another rat EAE model did not affect CNS T cell recruitment [225]. However, demyelination was highly reduced [225], which indicates that monocytes/macrophages are indeed important effector cells involved in demyelination in EAE. Our combined data on TG2 expression in monocytes and macrophages (**chapter 2, 3, 4 and 5**) and from the treatment of cr-EAE rats with KCC009 (**chapter 2**) hint towards monocyte- and macrophage-derived TG2 as an important factor involved in their infiltration into the CNS during EAE/MS. However, ERW1041E, a compound that did not clearly inhibit cellular CNS infiltration, still resulted in a reduction of motor impairment in mice (**chapter 5**), but is more modest than found in the cr-EAE model in rats. The mechanism of action behind the reduced symptoms in the mouse model has not been unraveled yet. We consider that the lack of effect of TG2 inhibition on cellular infiltration might be due to a reduced macrophage dependence of the mouse models compared to rat cr-EAE. Comparing the pathology of our EAE models reveals that the cr-EAE model is mainly macrophage driven [67], whereas the mouse models are more T cell driven [68]. Our observations of pharmacological TG2 inhibition in rats versus mice are in line with these described differences in pathology. Nevertheless, we still observe reduced motor symptomatology in mice lacking TG2 or after pharmacological inhibition of TG2 activity. We propose this might be due to a similar effect as the clinic-radiological paradox in MS patients: formation of new lesions and disability scores do not necessarily correlate [315], a paradox that has also been discussed in an EAE animal model [316]. Our observation on the clinical versus lack of histological effect of TG2 inhibition might therefore not only rely on the inhibition of monocyte or macrophage infiltration. One such potential effect could be that TG2 inhibition results in a different composition of cellular subsets of leukocytes or other cell types present in the lesions or a changed activation states and subsequently changed functions of the cells in the lesions. This might directly affect the development of pathology and result in reduced motor symptoms. Other possibilities are not influenced by

reduced cellular migration but could rely on changed signaling pathways by TG2 inhibition, influencing symptom development such as secretion of inflammatory modulators.

Our data suggest that TG2 can contribute to clinical EAE development via not yet unraveled mechanisms. Promising is that our effective therapeutic treatment approach after the onset of disease symptoms resembles the treatment of RRMS patients. Therefore we conclude that the administration of TG2 inhibitors can reduce ongoing inflammation and motor impairment in EAE and hence TG2 could be a potential target of interest in MS patients.

(sub)cellular localization and function of TG2 in EAE

When focusing on TG2 as a target it is essential to consider that it is a multi-functional protein present in several (sub)cellular compartments and that it shows localization-dependent activities [85, 93, 317]. TG2 is constitutively expressed in many cells, including monocytes/macrophages and CNS resident cells. Various stimuli such as lipopolysaccharide and several cytokines including IFNγ and IL-4 [310, 311, 318, 319] lead to a quick upregulation of TG2 expression in monocytes and macrophages which can usually be detected at both the mRNA- and protein level and by measuring enzymatic transamidation (a.k.a. cross-linking) activity which is often observed to be increased under inflammatory conditions [108]. As such, the restriction of TG2 expression to active and chronic active MS and EAE lesions (**chapters 2, 3, 5**) underlines the inflammation related expression of TG2 in active MS and EAE. In general, the predominant (sub)cellular localization of TG2 is in the cytoplasm but its presence has also been confirmed in virtually every other cellular compartment, including the nucleus, mitochondria, endoplasmic reticulum and cell membrane. In addition, an excreted form of TG2 can be found in the ECM [101-104, 106, 107, 320].

Although the reduction in TG2 activity demonstrated clear beneficial effects in our animal models, it remained uncertain which cellular localization of TG2 instigated the observed *in vivo* effects. There are also several possibilities on how this effect was mediated. One of them is that this was due to the actual inhibition of the transamidation activity of TG2 (and/or other TGs) or that it was the result of the down-tuning of other, non-enzymatic functions of TG2. Furthermore, the inhibition might affect the conformation of TG2 and keep it in its open, enzymatically active conformation and therefore affect its (trans-)location and interaction with potential binding partners. We addressed some of these questions by studying several of the above described TG2 inhibitors *in vivo* and *in vitro*. With an *in vitro* blood-brain-barrier model, we confirmed that rat monocyte/macrophage adhesion and migration across rat brain endothelial cells is TG2-dependent (**chapter 2**). In this set-up, we stimulated monocytes with pro-inflammatory cytokines, which are also present in MS and EAE, and observed increased TG2 expression on the cell surface, which then, in turn, could be pharmacologically inhibited by KCC009, resulting in reduced transendothelial migration, a process that might be similar *in vivo*. We subsequently analyzed the specificity of other TG2 inhibitors and observed that they all preferentially inhibited TG2 activity over the other members of the transglutaminase enzyme family (**chapter 5**). Our *in vitro* assays moreover revealed that

the inhibitory compounds vary in their cell permeability, with KCC009 [321] and ERW1041E [181] being the most cell-impermeable TG2 inhibitors. Using the cell-permeable and impermeable TG2 activity inhibitors in our *in vivo* EAE experiments (**chapters 2 and 5**), the cell-impermeable TG2 inhibitory compounds (KCC009 and ERW1041E) were more effective than a cell-permeable one (BJFF078) in reducing EAE motor symptom development and in cell migration *in vitro* (only KCC009), which suggests a potentially important role of extracellular TG2 activity in these processes.

Even though it seems that extracellular TG2 activity is of importance for the here studied processes of cellular migration and development of EAE symptoms, we cannot rule out that intracellular TG2 is involved in the observed effects of TG2 inhibition. Likewise, TG2 is known to also mediate so-called outside-in signaling which means that extracellular TG2 can affect intracellular processes [122, 322], which can be affected by TG2 inhibition. We showed, that KCC009 treatment of *in vitro* macrophages reduced the F-actin stained cellular protrusions, an intracellular process necessary for the regulation of cytoskeletal flexibility. This flexibility is essential for adhesion, migration and extravasation of monocytes and macrophages [206]. The small GTPase RhoA is a major player in this process [134], whose activation is mediated by TG2 transamidation **(chapter 2)**. RhoA activation is only one example that shows how the enzymatic transamidation activity of TG2 can affect cellular motility and migration. How this intracellular process is blocked when KCC009 cannot permeate the cell remains unclear at this point but is presumably due to the above mentioned outside-in signaling. A potential mode of action of extracellular TG2 to affect the cellular protrusions in a similar way as RhoA is focal adhesion kinase (FAK). FAK is a kinase that is activated by the clustering of integrins on the cell surface. This clustering is facilitated by cell-surface TG2 that engages with integrins and direct association of FAK activity regulated by TG2 was shown in pancreatic cancer cells [323]. Accordingly, increased expression of TG2 results in increased integrin clustering and hence FAK activation which itself is associated with a pro-migratory profile of (cancer) cells [324, 325]. Although our study focused mostly on inhibiting TG2 transamidation activity, this process described above is independent of the cross-linking activity of TG2 [325].

Next to its enzymatic activities, some of TG2's actions are non-enzymatically mediated. These enzymatic activity-independent mechanisms can thus be potentially affected by TG2 inhibitory compounds used in this thesis. Of particular interest is the interaction of TG2's fibronectin-binding domain with extracellular fibronectin. The interaction of cells with this extracellular matrix protein is also of relevance for the adhesion and migration of cells [182]. The likely extracellularly mediated effect on macrophage adhesion and migration by KCC009 may thus be, at least partly, due to inhibition of the interaction of TG2 with fibronectin. Although not tested for this compound, the chemically similar compound ERW1041E did not affect TG2-fibronectin binding *in vitro* (**chapter 5**) but still reduced EAE motor impairment *in vivo*. These data suggest that an interplay of TG2's transamidation function and possibly other functions of TG2, that have not been studied in this context, are likely involved in EAE pathology and symptom development.

Visualizing monocyte behavior in EAE – Association of migration with TG2?

Our *in vivo* data of cr-EAE rats treated with the TG2 inhibitor KCC009 showed a clear reduction in the influx of monocytes into the CNS. Moreover, experiments using an *in vitro* blood-brain barrier revealed that TG2 expressed by monocytes is indeed of relevance for these cells to adhere and migrate over the blood vessel endothelium (**chapter 2**). This suggests that TG2 expressed by monocytes plays a role in their *in vivo* crawling behavior along the blood vessels in the CNS as an initial step to migration. As a first proof of principle we created an experimental setup of intravital microscopy to visualize *in vivo* crawling behavior of monocytes and their interaction with the spinal cord endothelium in EAE mice (**chapter 4**). Mounting a permanent spinal cord window [266, 267] allows studying monocyte adhesion and their migration during EAE using intravital two-photon microscopy (IVM). We visualized monocyte behavior in the spinal cord vasculature during EAE in a time-dependent manner by using CX3CR1 transgenic mice, which contain monocytes, macrophages and microglial cells that express green fluorescent protein (GFP). Very few crawling cells were observed in a naive animal and the number and intraluminal crawling duration of the green fluorescent monocytes was highly increased after immunization. The number of these cells remained elevated and showed extended migratory track length during ongoing clinical EAE disease when compared to adjuvant only injected mice or asymptomatic animals. Therefore it seems that during EAE an extended and potentially firmer interaction of these cells with the endothelium occurs, which might be mediated by soluble or cell surface mediators such as chemokines and cytokines [280, 282, 283], but also TG2 could be involved in this process as suggested by our *in vitro* data (**chapter 2**). Post-mortem analysis confirmed TG2 expression in green labeled microglial cells, monocytes and macrophages in spinal cord EAE lesions and even in cells attached to the luminal side of the vasculature. This indicates that TG2 expression already occurs before extravasation into the parenchyma. TG2 might thereby contribute to adhesion and crawling of monocytes, facilitating extravasation into the CNS in this model. Moreover, this data, together with the early observation of extended monocyte crawling on the spinal cord endothelium (**chapter 4**) and early CNS infiltration [274], leads to the conclusion that interference with monocyte adhesion, by e.g. inhibition of TG2, should be applied at a very early stage of EAE and possibly MS, to effectively combat subsequent pathology. However, therapeutic treatment of EAE animals with TG2 inhibitors after the onset of motor symptoms (**chapters 2 and 5**), still reduced symptom development and suggests that even administration of such treatment during ongoing inflammation, might have beneficial effects. A final proof of interest would be to induce EAE in the transgenic mice, treat them with a TG2 inhibitor and visualize the crawling behavior of monocytes during disease to see if indeed at early stages of EAE, TG2 is involved in the interaction of monocytes with the brain endothelium. If so, this might support our hypothesis of TG2 being a potential target to reduce CNS infiltration in MS. Another very interesting approach of visualization could be the use of fluorescently labeled inhibitors that can give direct information on the time and location of active TG2 in this model, which will provide unique and valuable insight into the mode of action of TG2 in EAE.

With the here used intravital microscopy setup in EAE animals, we laid a ground stone to image monocyte adhesion and migration in the spinal cord *in vivo*. This can be used to combine studies on the effect of TG2 inhibitory compounds (and others) in EAE and the cell types involved.

TG2 in cells in MS and EAE lesions: macrophages only?

In a healthy brain, an intact blood-brain barrier excludes the majority of blood immune cells from the CNS. During MS, however, the integrity of this barrier fails and CNS infiltration of leukocytes from the bloodstream occurs, which can have detrimental effects in the CNS [326]. Therefore, inhibiting the cellular influx into the CNS is of interest for MS treatment (and possibly other neuroinflammatory diseases) to reduce the concomitant tissue damage associated with the inflammation and thereby reduce disease pathology and symptoms. Especially the inhibition of macrophage infiltration is one aspect of treatment that could supplement the currently available MS treatment, which mainly focusses on the blockade of lymphocyte infiltration into the CNS.

Inflammatory processes in the CNS during MS do not only attract cells from the bloodstream but also recruit residential cells such as glial cells [160, 327]. It is assumed that these cells exert various roles in MS pathology, including reduction and containment of inflammation, cleaning up debris and the repair of CNS damage. Therefore, when targeting TG2 as a potential factor to limit monocytes and macrophage infiltration in MS, the effects on pathology involving resident CNS cells need to be taken into account. TG2 is known to be expressed in various glial cell types either constitutively or upon stimulation, e.g. microglia [318], astrocytes [180, 328, 329], oligodendrocyte precursor cells [330] and neurons [76]. All these cell types are involved in MS pathology and found in MS lesions [224]. Thus, whereas the data presented in this thesis indicate that TG2 inhibition might improve EAE symptoms and reduce monocytes and macrophage infiltration of the CNS, the effect on other cell types could have other outcomes. Resident microglia cells act similar to monocyte-derived macrophages in EAE and MS and therefore TG2 inhibition should reduce their migration towards the lesion site, which would help dampen the inflammation in early disease but reduce the phagocytic clean-up capacities of microglia. Also, remyelination can be indirectly affected by microglia-derived TG2 as it stimulates oligodendrocyte precursor cell maturation. This results in functional remyelinating oligodendrocytes, which help to revert the damage of demyelination and this process was hampered by TG2 inhibition [330, 331]. However, despite TG2's role in oligodendrocyte maturation, recent data from our group showed that this is a process limited to the developing human brain and is absent in remyelinating MS lesions [332]. Nevertheless, in a demyelinating mouse model, Tgm2 knockout resulted in impaired remyelination compared to TG2-expressing animals [330] and serves to demonstrate that more research is needed in this area.

Another highly important process in MS pathology is gliosis, the formation of the so-called glial scar, a fibrosis like process. Astrocytes are the main contributors to the glial scar which function is to reduce cellular accessibility of demyelinated areas for the purpose of reparation and therefore hampers remyelination and axonal re-growth [329,

333]. TG2's wide variety of substrates include numerous extracellular proteins, including fibronectin [334, 335], laminin [106], vitronectin and fibrinogen [336] that are involved in gliosis and fibrosis and especially TG2's role in fibrosis has been studied extensively [106, 137, 337]. Crosslinking of the above-mentioned proteins in gliosis and fibrosis increases their proteolytic, chemical and mechanical resistance and also their stiffness. The latter one is thought to assist cell adhesion and migration but also helps closing off lesion areas in gliosis [119, 127]. Therefore, inhibiting TG2 might lower the rigidity of the extracellular matrix and thereby reduce glial scar formation which in turn may increase tissue reparation due to better accessibility of lesions by cells involved in remyelination.

Concluding remarks and future outlook

The data presented in this thesis show that TG2 is expressed in monocytes and in macrophages in MS and EAE lesions and can contribute to the development of symptoms and cellular CNS infiltrates in EAE affected rodents. Pharmacological TG2 inhibition revealed the contribution of TG2 activity to EAE. Its inhibition cannot only reduce macrophage infiltration into the CNS but also reduce lesion formation and paralysis development in EAE affected rodents. We propose that TG2 inhibitory treatment as early as possible will result in the best treatment outcomes in EAE and potentially MS by preventing cellular CNS influx and associated CNS damage. Although our data are promising and EAE is a broadly used animal model for MS research and resulted in currently available valuable MS treatments, it is possible that the situation of TG2 contribution to pathogenesis in MS is different. For that reason, prior to drawing firm conclusions on TG2 as a druggable target in MS, further research is needed. Using primary cells derived from MS patients as well as analyzing CNS biopsies of new and active lesions instead of post-mortem tissue can confirm if our animal-derived data can be transferred to MS patients.

We provide exciting initial data on the contribution of TG2 to EAE development but further research is needed to unravel the contribution or various TG2 expressing cell types and how their functions are affected by TG2 inhibition. Especially the time-dependent factor of inhibiting TG2 during disease progress might result in diverse outcomes of TG2 inhibition. Our data indicated that inhibition of TG2 in early disease phases before massive cellular CNS infiltration has occurred, might be beneficial to reduce this infiltration. However, at later disease stages when cellular infiltrates are already present in the CNS, it might hamper necessary repair mechanisms and cleanup of debris in the lesions. Special attention should also be paid to the cellular locus of action of TG2 inhibition. Our encouraging data with cell-impermeable TG2 inhibitory agents suggests that extracellular TG2 facilitates the migration of macrophages and therefore their CNS infiltration. Furthermore, the development of new and highly specific inhibitors that only target single mechanisms of action of TG2 will greatly contribute to our knowledge of the specific functions of TG2 in EAE and, more importantly, enable proper evaluation of the enzyme's potential as a future therapeutic target in MS. TG2 enzymatic transamidation activity is up to now the focus of these efforts, but specific inhibitors focusing on the interaction of TG2 with extracellular matrix proteins such as fibronectin to study the effect

of TG2 on monocytic transendothelial migration have a large potential and would aid the evaluation of TG2 and its contribution to EAE and MS. Moreover, this is not only of interest for MS patients but also for other diseases that are associated with TG2-ECM interactions and cellular migration like, for example, atherosclerosis and cancer metastasis [338, 339].



APPENDICES

REFERENCES
SUMMARY
ACKNOWLEDGEMENTS
CURRICULUM VITAE
LIST OF PUBLICATIONS

REFERENCES

1. Charcot, J., Histologie de la sclerose en plaques. Gazette des hopitaux, Paris. 41: 554–5, 1868.
2. Kingwell, E., et al., Incidence and prevalence of multiple sclerosis in Europe: a systematic review. BMC Neurol, 2013. 13: p. 128.
3. Milo, R. and E. Kahana, Multiple sclerosis: geoepidemiology, genetics and the environment. Autoimmun Rev, 2010. 9(5): p. A387-94.
4. Compston, A. and A. Coles, Multiple sclerosis. Lancet 2008. 372(9648): p. 1502-17.
5. Rosati, G., The prevalence of multiple sclerosis in the world: an update. Neurol Sci, 2001. 22(2): p. 117-39.
6. Dyment, D.A., A.D. Sadovnick, and G.C. Ebers, Genetics of multiple sclerosis. Hum Mol Genet, 1997. 6(10): p. 1693-8.
7. Hawkes, C.H. and A.J. Macgregor, Twin studies and the heritability of MS: a conclusion. Mult Scler, 2009. 15(6): p. 661-7.
8. Ascherio, A. and K.L. Munger, Environmental risk factors for multiple sclerosis. Part II: Noninfectious factors. Ann Neurol, 2007. 61(6): p. 504-13.
9. Almohmeed, Y.H., et al., Systematic review and meta-analysis of the sero-epidemiological association between Epstein Barr virus and multiple sclerosis. PLoS One, 2013. 8(4): p. e61110.
10. Fierz, W., Multiple sclerosis: an example of pathogenic viral interaction? Virol J, 2017. 14(1): p. 42.
11. Poser, C.M., et al., New diagnostic criteria for multiple sclerosis: guidelines for research protocols. Ann Neurol, 1983. 13(3): p. 227-31.
12. Polman, C.H., et al., Diagnostic criteria for multiple sclerosis: 2010 revisions to the McDonald criteria. Ann Neurol, 2011. 69(2): p. 292-302.
13. Thompson, A.J., et al., Diagnosis of multiple sclerosis: 2017 revisions of the McDonald criteria. Lancet Neurol, 2018. 17(2): p. 162-173.
14. Compston, A. and A. Coles, Multiple sclerosis. The Lancet, 2002. 359(9313): p. 1221-1231.
15. Abraira, V., et al., Utility of oligoclonal IgG band detection for MS diagnosis in daily clinical practice. J Immunol Methods, 2011. 371(1-2): p. 170-3.
16. Bo, L., et al., Intracortical multiple sclerosis lesions are not associated with increased lymphocyte infiltration. Mult Scler, 2003. 9(4): p. 323-31.
17. Lassmann, H., W. Bruck, and C.F. Lucchinetti, The immunopathology of multiple sclerosis: an overview. Brain Pathol, 2007. 17(2): p. 210-8.

18. Peterson, J.W., et al., Transected neurites, apoptotic neurons, and reduced inflammation in cortical multiple sclerosis lesions. Ann Neurol, 2001. 50(3): p. 389-400.
19. Kutzelnigg, A., et al., Cortical demyelination and diffuse white matter injury in multiple sclerosis. Brain, 2005. 128(Pt 11): p. 2705-12.
20. Lucchinetti, C., et al., Heterogeneity of multiple sclerosis lesions: implications for the pathogenesis of demyelination. Ann Neurol, 2000. 47(6): p. 707-17.
21. Popescu, B.F. and C.F. Lucchinetti, Pathology of demyelinating diseases. Annu Rev Pathol, 2012. 7: p. 185-217.
22. Bramow, S., et al., Demyelination versus remyelination in progressive multiple sclerosis. Brain, 2010. 133(10): p. 2983-98.
23. Minagar, A. and J.S. Alexander, Blood-brain barrier disruption in multiple sclerosis. Mult Scler, 2003. 9(6): p. 540-9.
24. Kerfoot, S.M. and P. Kubes, Overlapping roles of P-selectin and alpha 4 integrin to recruit leukocytes to the central nervous system in experimental autoimmune encephalomyelitis. J Immunol, 2002. 169(2): p. 1000-6.
25. Johnston, B. and E.C. Butcher, Chemokines in rapid leukocyte adhesion triggering and migration. Semin Immunol, 2002. 14(2): p. 83-92.
26. Greenwood, J., et al., Review: leucocyte-endothelial cell crosstalk at the blood-brain barrier: a prerequisite for successful immune cell entry to the brain. Neuropathol Appl Neurobiol, 2011. 37(1): p. 24-39.
27. O'Brien, K., B. Gran, and A. Rostami, T-cell based immunotherapy in experimental autoimmune encephalomyelitis and multiple sclerosis. Immunotherapy, 2010. 2(1): p. 99-115.
28. Lalive, P.H., Autoantibodies in inflammatory demyelinating diseases of the central nervous system. Swiss Med Wkly, 2008. 138(47-48): p. 692-707.
29. Bar-Or, A., et al., Abnormal B-cell cytokine responses a trigger of T-cell-mediated disease in MS? Ann Neurol, 2010. 67(4): p. 452-61.
30. Barr, T.A., et al., B cell depletion therapy ameliorates autoimmune disease through ablation of IL-6-producing B cells. J Exp Med, 2012. 209(5): p. 1001-10.
31. Mauri, C. and A. Bosma, Immune regulatory function of B cells. Annu Rev Immunol, 2012. 30: p. 221-41.
32. Abdul-Majid, K.B., et al., Fc receptors are critical for autoimmune inflammatory damage to the central nervous system in experimental autoimmune encephalomyelitis. Scand J Immunol, 2002. 55(1): p. 70-81.

33. Waschbisch, A., et al., Pivotal Role for CD16+ Monocytes in Immune Surveillance of the Central Nervous System. J Immunol, 2016. 196(4): p. 1558-67.
34. Mosser, D.M. and J.P. Edwards, Exploring the full spectrum of macrophage activation. Nat Rev Immunol, 2008. 8(12): p. 958-69.
35. Gordon, S., Alternative activation of macrophages. Nat Rev Immunol, 2003. 3(1): p. 23-35.
36. Martinez, F.O., L. Helming, and S. Gordon, Alternative activation of macrophages: an immunologic functional perspective. Annu Rev Immunol, 2009. 27: p. 451-83.
37. Porcheray, F., et al., Macrophage activation switching: an asset for the resolution of inflammation. Clin Exp Immunol, 2005. 142(3): p. 481-9.
38. Vogel, D.Y., et al., Macrophages in inflammatory multiple sclerosis lesions have an intermediate activation status. J Neuroinflammation, 2013. 10: p. 35.
39. Damal, K., E. Stoker, and J.F. Foley, Optimizing therapeutics in the management of patients with multiple sclerosis: a review of drug efficacy, dosing, and mechanisms of action. Biologics, 2013. 7: p. 247-58.
40. Burton, J.M., et al., Oral versus intravenous steroids for treatment of relapses in multiple sclerosis. Cochrane Database Syst Rev, 2012. 12: p. CD006921.
41. Limmroth, V., N. Putzki, and N.J. Kachuck, The interferon beta therapies for treatment of relapsing-remitting multiple sclerosis: are they equally efficacious? A comparative review of open-label studies evaluating the efficacy, safety, or dosing of different interferon beta formulations alone or in combination. Ther Adv Neurol Disord, 2011. 4(5): p. 281-96.
42. Kieseier, B.C., The mechanism of action of interferon-beta in relapsing multiple sclerosis. CNS Drugs, 2011. 25(6): p. 491-502.
43. Moreno Torres, I. and A. Garcia-Merino, Anti-CD20 monoclonal antibodies in multiple sclerosis. Expert Rev Neurother, 2017. 17(4): p. 359-371.
44. Willis, M.D. and N.P. Robertson, Alemtuzumab for Multiple Sclerosis. Curr Neurol Neurosci Rep, 2016. 16(9): p. 84.
45. Cherwinski, H.M., et al., The immunosuppressant leflunomide inhibits lymphocyte proliferation by inhibiting pyrimidine biosynthesis. J Pharmacol Exp Ther, 1995. 275(2): p. 1043-9.
46. Edan, G., et al., Therapeutic effect of mitoxantrone combined with methylprednisolone in multiple sclerosis: a randomised multicentre study of active disease using MRI and clinical criteria. J Neurol Neurosurg Psychiatry, 1997. 62(2): p. 112-8.

47. Fox, E.J., Management of worsening multiple sclerosis with mitoxantrone: a review. Clin Ther, 2006. 28(4): p. 461-74.
48. Phillips, J.T. and R.J. Fox, BG-12 in multiple sclerosis. Semin Neurol, 2013. 33(1): p. 56-65.
49. Sheridan, J.P., et al., Intermediate-affinity interleukin-2 receptor expression predicts CD56(bright) natural killer cell expansion after daclizumab treatment in the CHOICE study of patients with multiple sclerosis. Mult Scler, 2011. 17(12): p. 1441-8.
50. Gold, R., et al., Daclizumab high-yield process in relapsing-remitting multiple sclerosis (SELECT): a randomised, double-blind, placebo-controlled trial. Lancet, 2013. 381(9884): p. 2167-75.
51. Brinkmann, V., J.G. Cyster, and T. Hla, FTY720: sphingosine 1-phosphate receptor-1 in the control of lymphocyte egress and endothelial barrier function. Am J Transplant, 2004. 4(7): p. 1019-25.
52. Mandala, S., et al., Alteration of lymphocyte trafficking by sphingosine-1-phosphate receptor agonists. Science, 2002. 296(5566): p. 346-9.
53. Kappos, L., et al., A placebo-controlled trial of oral fingolimod in relapsing multiple sclerosis. N Engl J Med, 2010. 362(5): p. 387-401.
54. Vandermeeren, M., et al., Dimethylfumarate is an inhibitor of cytokine-induced E-selectin, VCAM-1, and ICAM-1 expression in human endothelial cells. Biochem Biophys Res Commun, 1997. 234(1): p. 19-23.
55. Loewe, R., et al., Dimethylfumarate inhibits tumor-necrosis-factor-induced CD62E expression in an NF-kappa B-dependent manner. J Invest Dermatol, 2001. 117(6): p. 1363-8.
56. Gold, R. and J.S. Wolinsky, Pathophysiology of multiple sclerosis and the place of teriflunomide. Acta Neurol Scand, 2011. 124(2): p. 75-84.
57. Rice, G.P., H.P. Hartung, and P.A. Calabresi, Anti-alpha4 integrin therapy for multiple sclerosis: mechanisms and rationale. Neurology, 2005. 64(8): p. 1336-42.
58. Kent, S.J., et al., A monoclonal antibody to alpha 4 integrin suppresses and reverses active experimental allergic encephalomyelitis. J Neuroimmunol, 1995. 58(1): p. 1-10.
59. Schwab, N., et al., Natalizumab-associated PML: Challenges with incidence, resulting risk, and risk stratification. Neurology, 2017. 88(12): p. 1197-1205.
60. t Hart, B.A. and S. Amor, The use of animal models to investigate the pathogenesis of neuroinflammatory disorders of the central nervous system. Curr Opin Neurol, 2003. 16(3): p. 375-83.

61. Rangachari, M. and V.K. Kuchroo, Using EAE to better understand principles of immune function and autoimmune pathology. J Autoimmun, 2013. 45: p. 31-9.
62. Kipp, M., et al., Experimental in vivo and in vitro models of multiple sclerosis: EAE and beyond. Mult Scler Relat Disord, 2012. 1(1): p. 15-28.
63. Haanstra, K.G., et al., Induction of experimental autoimmune encephalomyelitis with recombinant human myelin oligodendrocyte glycoprotein in incomplete Freund's adjuvant in three non-human primate species. J Neuroimmune Pharmacol, 2013. 8(5): p. 1251-64.
64. Naidu, K.A., E.S. Fu, and L.D. Prockop, Acute experimental allergic encephalomyelitis increases lumbar spinal cord incorporation of epidurally administered [(3)H]-D-mannitol and [(14)C]-carboxyl-inulin in rabbits. Anesth Analg, 2002. 94(1): p. 208-12, table of contents.
65. Cipriani, B., et al., Upregulation of group 1 CD1 antigen presenting molecules in guinea pigs with experimental autoimmune encephalomyelitis: an immunohistochemical study. Brain Pathol, 2003. 13(1): p. 1-9.
66. Mix, E., et al., Animal models of multiple sclerosis--potentials and limitations. Prog Neurobiol, 2010. 92(3): p. 386-404.
67. Storch, M.K., et al., Autoimmunity to myelin oligodendrocyte glycoprotein in rats mimics the spectrum of multiple sclerosis pathology. Brain Pathol, 1998. 8(4): p. 681-94.
68. Lassmann, H. and M. Bradl, Multiple sclerosis: experimental models and reality. Acta Neuropathol, 2016.
69. Kipp, M., et al., The cuprizone animal model: new insights into an old story. Acta Neuropathol, 2009. 118(6): p. 723-36.
70. Praet, J., et al., Cellular and molecular neuropathology of the cuprizone mouse model: clinical relevance for multiple sclerosis. Neurosci Biobehav Rev, 2014. 47: p. 485-505.
71. Matsushima, G.K. and P. Morell, The neurotoxicant, cuprizone, as a model to study demyelination and remyelination in the central nervous system. Brain Pathol, 2001. 11(1): p. 107-16.
72. Rivera-Quinones, C., et al., Absence of neurological deficits following extensive demyelination in a class I-deficient murine model of multiple sclerosis. Nat Med, 1998. 4(2): p. 187-93.
73. Gilli, F., D.B. Royce, and A.R. Pachner, Measuring Progressive Neurological Disability in a Mouse Model of Multiple Sclerosis. J Vis Exp, 2016(117).
74. Sarkar, N.K., D.D. Clarke, and H. Waelsch, An enzymically catalyzed incorporation of amines into proteins. Biochim Biophys Acta, 1957. 25(2): p. 451-2.

75. Mycek, M.J., et al., Amine incorporation into insulin as catalyzed by transglutaminase. Arch Biochem Biophys, 1959. 84: p. 528-40.
76. Lorand, L. and R.M. Graham, Transglutaminases: crosslinking enzymes with pleiotropic functions. Nat Rev Mol Cell Biol, 2003. 4(2): p. 140-56.
77. Eckert, R.L., et al., Transglutaminase function in epidermis. J Invest Dermatol, 2005. 124(3): p. 481-92.
78. Pietroni, V., et al., Inactive and highly active, proteolytically processed transglutaminase-5 in epithelial cells. J Invest Dermatol, 2008. 128(12): p. 2760-6.
79. Grenard, P., M.K. Bates, and D. Aeschlimann, Evolution of transglutaminase genes: identification of a transglutaminase gene cluster on human chromosome 15q15. Structure of the gene encoding transglutaminase X and a novel gene family member, transglutaminase Z. J Biol Chem, 2001. 276(35): p. 33066-78.
80. Griffin, M., R. Casadio, and C.M. Bergamini, Transglutaminases: nature's biological glues. Biochem J, 2002. 368(Pt 2): p. 377-96.
81. Satchwell, T.J., et al., Protein 4.2: a complex linker. Blood Cells Mol Dis, 2009. 42(3): p. 201-10.
82. Lorand, L., et al., Human plasma factor XIII: subunit interactions and activation of zymogen. Methods Enzymol, 1993. 222: p. 22-35.
83. Torocsik, D., et al., Factor XIII-A is involved in the regulation of gene expression in alternatively activated human macrophages. Thromb Haemost, 2010. 104(4): p. 709-17.
84. Muszbek, L., R. Adany, and H. Mikkola, Novel aspects of blood coagulation factor XIII. I. Structure, distribution, activation, and function. Crit Rev Clin Lab Sci, 1996. 33(5): p. 357-421.
85. Fesus, L. and M. Piacentini, Transglutaminase 2: an enigmatic enzyme with diverse functions. Trends Biochem Sci, 2002. 27(10): p. 534-9.
86. Johnson, G.V., et al., Transglutaminase activity is increased in Alzheimer's disease brain. Brain Res, 1997. 751(2): p. 323-9.
87. Segers-Nolten, I.M., et al., Tissue transglutaminase modulates alpha-synuclein oligomerization. Protein Sci, 2008. 17(8): p. 1395-402.
88. Karpuj, M.V., et al., Transglutaminase aggregates huntingtin into nonamyloidogenic polymers, and its enzymatic activity increases in Huntington's disease brain nuclei. Proc Natl Acad Sci U S A, 1999. 96(13): p. 7388-93.
89. Iannaccone, M., et al., Transglutaminase activity as a possible therapeutical target in neurodegenerative diseases. Recent Pat CNS Drug Discov, 2013. 8(3): p. 235-42.

90. Schuppan, D. and E.G. Hahn, Biomedicine. Gluten and the gut-lessons for immune regulation. Science, 2002. 297(5590): p. 2218-20.
91. Begg, G.E., et al., Mechanism of allosteric regulation of transglutaminase 2 by GTP. Proc Natl Acad Sci U S A, 2006. 103(52): p. 19683-8.
92. Pinkas, D.M., et al., Transglutaminase 2 undergoes a large conformational change upon activation. PLoS Biol, 2007. 5(12): p. e327.
93. Wang, Z. and M. Griffin, TG2, a novel extracellular protein with multiple functions. Amino Acids, 2012. 42(2-3): p. 939-49.
94. Siegel, M., et al., Extracellular transglutaminase 2 is catalytically inactive, but is transiently activated upon tissue injury. PLoS One, 2008. 3(3): p. e1861.
95. Scarpellini, A., et al., Heparan sulfate proteoglycans are receptors for the cell-surface trafficking and biological activity of transglutaminase-2. J Biol Chem, 2009. 284(27): p. 18411-23.
96. Jin, X., et al., Activation of extracellular transglutaminase 2 by thioredoxin. J Biol Chem, 2011. 286(43): p. 37866-73.
97. Hasegawa, G., et al., A novel function of tissue-type transglutaminase: protein disulphide isomerase. Biochem J, 2003. 373(Pt 3): p. 793-803.
98. Achyuthan, K.E. and C.S. Greenberg, Identification of a guanosine triphosphate-binding site on guinea pig liver transglutaminase. Role of GTP and calcium ions in modulating activity. J Biol Chem, 1987. 262(4): p. 1901-6.
99. Nakaoka, H., et al., Gh: a GTP-binding protein with transglutaminase activity and receptor signaling function. Science, 1994. 264(5165): p. 1593-6.
100. Mishra, S. and L.J. Murphy, Tissue transglutaminase has intrinsic kinase activity: identification of transglutaminase 2 as an insulin-like growth factor-binding protein-3 kinase. J Biol Chem, 2004. 279(23): p. 23863-8.
101. Lesort, M., et al., Distinct nuclear localization and activity of tissue transglutaminase. J Biol Chem, 1998. 273(20): p. 11991-4.
102. Balajthy, Z., et al., Tissue-transglutaminase contributes to neutrophil granulocyte differentiation and functions. Blood, 2006. 108(6): p. 2045-54.
103. Hodrea, J., et al., Transglutaminase 2 is expressed and active on the surface of human monocyte-derived dendritic cells and macrophages. Immunol Lett, 2010. 130(1-2): p. 74-81.
104. Wilhelmus, M.M., et al., Presence of tissue transglutaminase in granular endoplasmic reticulum is characteristic of melanized neurons in Parkinson's disease brain. Brain Pathol, 2011. 21(2): p. 130-9.

105. Nurminskaya, M.V. and A.M. Belkin, Cellular functions of tissue transglutaminase. Int Rev Cell Mol Biol, 2012. 294: p. 1-97.
106. Aeschlimann, D. and V. Thomazy, Protein crosslinking in assembly and remodelling of extracellular matrices: the role of transglutaminases. Connect Tissue Res, 2000. 41(1): p. 1-27.
107. Park, D., S.S. Choi, and K.S. Ha, Transglutaminase 2: a multi-functional protein in multiple subcellular compartments. Amino Acids, 2010. 39(3): p. 619-31.
108. Iismaa, S.E., et al., Transglutaminases and disease: lessons from genetically engineered mouse models and inherited disorders. Physiol Rev, 2009. 89(3): p. 991-1023.
109. Mirza, A., et al., A role for tissue transglutaminase in hepatic injury and fibrogenesis, and its regulation by NF-kappaB. Am J Physiol, 1997. 272(2 Pt 1): p. G281-8.
110. Lu, S., et al., Isolation and characterization of the human tissue transglutaminase gene promoter. J Biol Chem, 1995. 270(17): p. 9748-56.
111. Ritter, S.J. and P.J. Davies, Identification of a transforming growth factor-beta1/bone morphogenetic protein 4 (TGF-beta1/BMP4) response element within the mouse tissue transglutaminase gene promoter. J Biol Chem, 1998. 273(21): p. 12798-806.
112. Tovar-Vidales, T., A.F. Clark, and R.J. Wordinger, Transforming growth factor-beta2 utilizes the canonical Smad-signaling pathway to regulate tissue transglutaminase expression in human trabecular meshwork cells. Exp Eye Res, 2011. 93(4): p. 442-51.
113. Kuncio, G.S., et al., TNF-alpha modulates expression of the tissue transglutaminase gene in liver cells. Am J Physiol, 1998. 274(2 Pt 1): p. G240-5.
114. Frisdal, E., et al., Interleukin-6 protects human macrophages from cellular cholesterol accumulation and attenuates the proinflammatory response. J Biol Chem, 2011. 286(35): p. 30926-36.
115. Johnson, K., et al., Interleukin-1 Induces Pro-Mineralizing Activity of Cartilage Tissue Transglutaminase and Factor XIIIa. The American Journal of Pathology, 2001. 159(1): p. 149-163.
116. Jung, S.A., et al., Upregulation of TGF-beta-induced tissue transglutaminase expression by PI3K-Akt pathway activation in human subconjunctival fibroblasts. Invest Ophthalmol Vis Sci, 2007. 48(5): p. 1952-8.
117. Gratchev, A., et al., Interleukin-4 and dexamethasone counterregulate extracellular matrix remodelling and phagocytosis in type-2 macrophages. Scand J Immunol, 2005. 61(1): p. 10-7.

118. Gentile, V., et al., Expression of tissue transglutaminase in Balb-C 3T3 fibroblasts: effects on cellular morphology and adhesion. J Cell Biol, 1992. 119(2): p. 463-74.
119. Akimov, S.S. and A.M. Belkin, Cell surface tissue transglutaminase is involved in adhesion and migration of monocytic cells on fibronectin. Blood, 2001. 98(5): p. 1567-76.
120. Turner, P.M. and L. Lorand, Complexation of fibronectin with tissue transglutaminase. Biochemistry, 1989. 28(2): p. 628-35.
121. Pankov, R. and K.M. Yamada, Fibronectin at a glance. J Cell Sci, 2002. 115(Pt 20): p. 3861-3.
122. Akimov, S.S., et al., Tissue transglutaminase is an integrin-binding adhesion coreceptor for fibronectin. J Cell Biol, 2000. 148(4): p. 825-38.
123. Marchisio, P.C., et al., Rous sarcoma virus-transformed fibroblasts and cells of monocytic origin display a peculiar dot-like organization of cytoskeletal proteins involved in microfilament-membrane interactions. Exp Cell Res, 1987. 169(1): p. 202-14.
124. DeFife, K.M., et al., Cytoskeletal and adhesive structural polarizations accompany IL-13-induced human macrophage fusion. J Histochem Cytochem, 1999. 47(1): p. 65-74.
125. Gaudry, C.A., et al., Tissue transglutaminase is an important player at the surface of human endothelial cells: evidence for its externalization and its colocalization with the beta(1) integrin. Exp Cell Res, 1999. 252(1): p. 104-13.
126. Akimov, S.S. and A.M. Belkin, Cell-surface transglutaminase promotes fibronectin assembly via interaction with the gelatin-binding domain of fibronectin: a role in TGFbeta-dependent matrix deposition. J Cell Sci, 2001. 114(Pt 16): p. 2989-3000.
127. Balklava, Z., et al., Analysis of tissue transglutaminase function in the migration of Swiss 3T3 fibroblasts: the active-state conformation of the enzyme does not affect cell motility but is important for its secretion. J Biol Chem, 2002. 277(19): p. 16567-75.
128. Huelsz-Prince, G., et al., Activation of extracellular transglutaminase 2 by mechanical force in the arterial wall. J Vasc Res, 2013. 50(5): p. 383-95.
129. Sheetz, M.P., D.P. Felsenfeld, and C.G. Galbraith, Cell migration: regulation of force on extracellular-matrix-integrin complexes. Trends Cell Biol, 1998. 8(2): p. 51-4.
130. Giannone, G. and M.P. Sheetz, Substrate rigidity and force define form through tyrosine phosphatase and kinase pathways. Trends Cell Biol, 2006. 16(4): p. 213-23.

131. Antonyak, M.A., et al., Tissue transglutaminase is an essential participant in the epidermal growth factor-stimulated signaling pathway leading to cancer cell migration and invasion. J Biol Chem, 2009. 284(27): p. 17914-25.
132. Wakshlag, J.J., et al., Effects of tissue transglutaminase on beta -amyloid1-42-induced apoptosis. Protein J, 2006. 25(1): p. 83-94.
133. Mains, P.E., I.A. Sulston, and W.B. Wood, Dominant maternal-effect mutations causing embryonic lethality in Caenorhabditis elegans. Genetics, 1990. 125(2): p. 351-69.
134. Honing, H., et al., RhoA activation promotes transendothelial migration of monocytes via ROCK. J Leukoc Biol, 2004. 75(3): p. 523-8.
135. Janiak, A., E.A. Zemskov, and A.M. Belkin, Cell surface transglutaminase promotes RhoA activation via integrin clustering and suppression of the Src-p190RhoGAP signaling pathway. Mol Biol Cell, 2006. 17(4): p. 1606-19.
136. Schnoor, M., Endothelial actin-binding proteins and actin dynamics in leukocyte transendothelial migration. J Immunol, 2015. 194(8): p. 3535-41.
137. Collighan, R.J. and M. Griffin, Transglutaminase 2 cross-linking of matrix proteins: biological significance and medical applications. Amino Acids, 2009. 36(4): p. 659-70.
138. Ahn, J.S., et al., Tissue transglutaminase-induced down-regulation of matrix metalloproteinase-9. Biochem Biophys Res Commun, 2008. 376(4): p. 743-7.
139. Kessenbrock, K., V. Plaks, and Z. Werb, Matrix metalloproteinases: regulators of the tumor microenvironment. Cell, 2010. 141(1): p. 52-67.
140. Kim, S.Y., Transglutaminase 2 in inflammation. Front Biosci, 2006. 11: p. 3026-35.
141. Rauhavirta, T., et al., Transglutaminase 2 and Transglutaminase 2 Autoantibodies in Celiac Disease: a Review. Clin Rev Allergy Immunol, 2016.
142. Grosso, H. and M.M. Mouradian, Transglutaminase 2: biology, relevance to neurodegenerative diseases and therapeutic implications. Pharmacol Ther, 2012. 133(3): p. 392-410.
143. Ientile, R., M. Curro, and D. Caccamo, Transglutaminase 2 and neuroinflammation. Amino Acids, 2015. 47(1): p. 19-26.
144. Mangala, L.S. and K. Mehta, Tissue transglutaminase (TG2) in cancer biology. Prog Exp Tumor Res, 2005. 38: p. 125-38.
145. Mehta, K., A. Kumar, and H.I. Kim, Transglutaminase 2: a multi-tasking protein in the complex circuitry of inflammation and cancer. Biochem Pharmacol, 2010. 80(12): p. 1921-9.

146. Szondy, Z., et al., Transglutaminase 2-/- mice reveal a phagocytosis-associated crosstalk between macrophages and apoptotic cells. Proc Natl Acad Sci U S A, 2003. 100(13): p. 7812-7.
147. Leblanc, A., et al., Kinetic studies of guinea pig liver transglutaminase reveal a general-base-catalyzed deacylation mechanism. Biochemistry, 2001. 40(28): p. 8335-42.
148. Dedeoglu, A., et al., Therapeutic effects of cystamine in a murine model of Huntington's disease. J Neurosci, 2002. 22(20): p. 8942-50.
149. Stack, E.C., et al., Therapeutic attenuation of mitochondrial dysfunction and oxidative stress in neurotoxin models of Parkinson's disease. Biochim Biophys Acta, 2008. 1782(3): p. 151-62.
150. Karpuj, M.V., et al., Prolonged survival and decreased abnormal movements in transgenic model of Huntington disease, with administration of the transglutaminase inhibitor cystamine. Nat Med, 2002. 8(2): p. 143-9.
151. Bailey, C.D. and G.V. Johnson, Tissue transglutaminase contributes to disease progression in the R6/2 Huntington's disease mouse model via aggregate-independent mechanisms. J Neurochem, 2005. 92(1): p. 83-92.
152. DiRaimondo, T.R., et al., Elevated transglutaminase 2 activity is associated with hypoxia-induced experimental pulmonary hypertension in mice. ACS Chem Biol, 2014. 9(1): p. 266-75.
153. Dafik, L., et al., Activation and inhibition of transglutaminase 2 in mice. PLoS One, 2012. 7(2): p. e30642.
154. Yuan, L., et al., Tissue transglutaminase 2 inhibition promotes cell death and chemosensitivity in glioblastomas. Mol Cancer Ther, 2005. 4(9): p. 1293-302.
155. Johnson, T.S., et al., Transglutaminase inhibition reduces fibrosis and preserves function in experimental chronic kidney disease. J Am Soc Nephrol, 2007. 18(12): p. 3078-88.
156. Huang, L., et al., Transglutaminase inhibition ameliorates experimental diabetic nephropathy. Kidney Int, 2009. 76(4): p. 383-94.
157. Yakubov, B., et al., Small molecule inhibitors target the tissue transglutaminase and fibronectin interaction. PLoS One, 2014. 9(2): p. e89285.
158. Esposito, C., et al., Anti-tissue transglutaminase antibodies from coeliac patients inhibit transglutaminase activity both in vitro and in situ. Gut, 2002. 51(2): p. 177-81.
159. Noseworthy, J.H., et al., Multiple sclerosis. N Engl J Med, 2000. 343(13): p. 938-52.

160. Al-Omaishi, J., R. Bashir, and H.E. Gendelman, The cellular immunology of multiple sclerosis. J Leukoc Biol, 1999. 65(4): p. 444-52.
161. Lassmann, H., Basic mechanisms of brain inflammation. J Neural Transm Suppl, 1997. 50: p. 183-90.
162. Ubogu, E.E., M.B. Cossoy, and R.M. Ransohoff, The expression and function of chemokines involved in CNS inflammation. Trends Pharmacol Sci, 2006. 27(1): p. 48-55.
163. Steffen, B.J., E.C. Butcher, and B. Engelhardt, Evidence for involvement of ICAM-1 and VCAM-1 in lymphocyte interaction with endothelium in experimental autoimmune encephalomyelitis in the central nervous system in the SJL/J mouse. Am J Pathol, 1994. 145(1): p. 189-201.
164. Yednock, T.A., et al., Prevention of experimental autoimmune encephalomyelitis by antibodies against alpha 4 beta 1 integrin. Nature, 1992. 356(6364): p. 63-6.
165. Webster, N.L. and S.M. Crowe, Matrix metalloproteinases, their production by monocytes and macrophages and their potential role in HIV-related diseases. J Leukoc Biol, 2006. 80(5): p. 1052-66.
166. Farias, A.S., et al., Nitric oxide and TNFalpha effects in experimental autoimmune encephalomyelitis demyelination. Neuroimmunomodulation, 2007. 14(1): p. 32-8.
167. van der Laan, L.J., et al., Macrophage phagocytosis of myelin in vitro determined by flow cytometry: phagocytosis is mediated by CR3 and induces production of tumor necrosis factor-alpha and nitric oxide. J Neuroimmunol, 1996. 70(2): p. 145-52.
168. Engelhardt, B. and L. Kappos, Natalizumab: targeting alpha4-integrins in multiple sclerosis. Neurodegener Dis, 2008. 5(1): p. 16-22.
169. Rudick, R.A., et al., In vivo effects of interferon beta-1a on immunosuppressive cytokines in multiple sclerosis. Neurology, 1998. 50(5): p. 1294-300.
170. Scott, L.J. and D.P. Figgitt, Mitoxantrone: a review of its use in multiple sclerosis. CNS Drugs, 2004. 18(6): p. 379-96.
171. Kim, S.Y., et al., Differential expression of multiple transglutaminases in human brain. Increased expression and cross-linking by transglutaminases 1 and 2 in Alzheimer's disease. J Biol Chem, 1999. 274(43): p. 30715-21.
172. Ruan, Q. and G.V. Johnson, Transglutaminase 2 in neurodegenerative disorders. Front Biosci, 2007. 12: p. 891-904.
173. Monsonego, A., et al., Expression of GTP-dependent and GTP-independent tissue-type transglutaminase in cytokine-treated rat brain astrocytes. J Biol Chem, 1997. 272(6): p. 3724-32.

174. Han, M.H., et al., Proteomic analysis of active multiple sclerosis lesions reveals therapeutic targets. Nature, 2008. 451(7182): p. 1076-81.
175. Singh, U.S., et al., Tissue transglutaminase mediates activation of RhoA and MAP kinase pathways during retinoic acid-induced neuronal differentiation of SH-SY5Y cells. J Biol Chem, 2003. 278(1): p. 391-9.
176. Bo, L., et al., Detection of MHC class II-antigens on macrophages and microglia, but not on astrocytes and endothelia in active multiple sclerosis lesions. J Neuroimmunol, 1994. 51(2): p. 135-46.
177. De Groot, C.J., et al., Post-mortem MRI-guided sampling of multiple sclerosis brain lesions: increased yield of active demyelinating and (p)reactive lesions. Brain, 2001. 124(Pt 8): p. 1635-45.
178. Trapp, B.D., et al., Axonal transection in the lesions of multiple sclerosis. N Engl J Med, 1998. 338(5): p. 278-85.
179. van der Valk, P. and C.J. De Groot, Staging of multiple sclerosis (MS) lesions: pathology of the time frame of MS. Neuropathol Appl Neurobiol, 2000. 26(1): p. 2-10.
180. van Strien, M.E., et al., Appearance of tissue transglutaminase in astrocytes in multiple sclerosis lesions: a role in cell adhesion and migration? Brain Pathol, 2011. 21(1): p. 44-54.
181. Choi, K., et al., Chemistry and biology of dihydroisoxazole derivatives: selective inhibitors of human transglutaminase 2. Chem Biol, 2005. 12(4): p. 469-75.
182. Yuan, L., et al., Transglutaminase 2 inhibitor, KCC009, disrupts fibronectin assembly in the extracellular matrix and sensitizes orthotopic glioblastomas to chemotherapy. Oncogene, 2007. 26(18): p. 2563-73.
183. Ientile, R., et al., Cystamine inhibits transglutaminase and caspase-3 cleavage in glutamate-exposed astroglial cells. J Neurosci Res, 2003. 74(1): p. 52-9.
184. Lesort, M., et al., Cystamine inhibits caspase activity. Implications for the treatment of polyglutamine disorders. J Biol Chem, 2003. 278(6): p. 3825-30.
185. De Laurenzi, V. and G. Melino, Gene disruption of tissue transglutaminase. Mol Cell Biol, 2001. 21(1): p. 148-55.
186. Kuijk, L.M., et al., Soluble helminth products suppress clinical signs in murine experimental autoimmune encephalomyelitis and differentially modulate human dendritic cell activation. Mol Immunol, 2012. 51(2): p. 210-8.
187. Lee, K.N., et al., Development of selective inhibitors of transglutaminase. Phenylthiourea derivatives. J Biol Chem, 1985. 260(27): p. 14689-94.

188. Imai, Y., et al., A novel gene iba1 in the major histocompatibility complex class III region encoding an EF hand protein expressed in a monocytic lineage. Biochem Biophys Res Commun, 1996. 224(3): p. 855-62.
189. Breve, J.J., et al., Validated sandwich ELISA for the quantification of tissue transglutaminase in tissue homogenates and cell lysates of multiple species. J Immunol Methods, 2008. 332(1-2): p. 142-50.
190. de Vries, H.E., et al., Signal-Regulatory Protein -CD47 Interactions Are Required for the Transmigration of Monocytes Across Cerebral Endothelium. The Journal of Immunology, 2002. 168(11): p. 5832-5839.
191. Sakly, W., et al., A role for tissue transglutaminase in alpha-gliadin peptide cytotoxicity. Clin Exp Immunol, 2006. 146(3): p. 550-8.
192. Reijerkerk, A., et al., Diapedesis of monocytes is associated with MMP-mediated occludin disappearance in brain endothelial cells. FASEB J, 2006. 20(14): p. 2550-2.
193. Ren, X.D. and M.A. Schwartz, Determination of GTP loading on Rho. Methods Enzymol, 2000. 325: p. 264-72.
194. Greenberg, C.S., et al., The transglutaminase in vascular cells and tissues could provide an alternate pathway for fibrin stabilization. Blood, 1987. 70(3): p. 702-9.
195. Thomazy, V. and L. Fesus, Differential expression of tissue transglutaminase in human cells. An immunohistochemical study. Cell Tissue Res, 1989. 255(1): p. 215-24.
196. Wilhelmus, M.M., et al., Transglutaminases and transglutaminase-catalyzed cross-links colocalize with the pathological lesions in Alzheimer's disease brain. Brain Pathol, 2009. 19(4): p. 612-22.
197. Szekanecz, Z., M.J. Humphries, and A. Ager, Lymphocyte adhesion to high endothelium is mediated by two beta 1 integrin receptors for fibronectin, alpha 4 beta 1 and alpha 5 beta 1. J Cell Sci, 1992. 101 (Pt 4): p. 885-94.
198. Oh, K., et al., Transglutaminase 2 exacerbates experimental autoimmune encephalomyelitis through positive regulation of encephalitogenic T cell differentiation and inflammation. Clin Immunol, 2012. 145(2): p. 122-32.
199. van Strien, M.E., et al., Astrocyte-derived tissue transglutaminase interacts with fibronectin: a role in astrocyte adhesion and migration? PLoS One, 2011. 6(9): p. e25037.
200. Gahl, W.A., J.G. Thoene, and J.A. Schneider, Cystinosis. N Engl J Med, 2002. 347(2): p. 111-21.
201. Bungay, P.J., J.M. Potter, and M. Griffin, The inhibition of glucose-stimulated insulin secretion by primary amines. A role for transglutaminase in the secretory mechanism. Biochem J, 1984. 219(3): p. 819-27.

202. de Vos, A.F., et al., Transfer of central nervous system autoantigens and presentation in secondary lymphoid organs. J Immunol, 2002. 169(10): p. 5415-23.
203. Martin, R., H.F. McFarland, and D.E. McFarlin, Immunological aspects of demyelinating diseases. Annu Rev Immunol, 1992. 10: p. 153-87.
204. Steinman, L., Multiple sclerosis: a coordinated immunological attack against myelin in the central nervous system. Cell, 1996. 85(3): p. 299-302.
205. Qiao, S.W., et al., Tissue transglutaminase-mediated formation and cleavage of histamine-gliadin complexes: biological effects and implications for celiac disease. J Immunol, 2005. 174(3): p. 1657-63.
206. Hall, A., Rho GTPases and the actin cytoskeleton. Science, 1998. 279(5350): p. 509-14.
207. Worthylake, R.A., et al., RhoA is required for monocyte tail retraction during transendothelial migration. J Cell Biol, 2001. 154(1): p. 147-60.
208. Martin-Saavedra, F.M., et al., Beta-interferon unbalances the peripheral T cell proinflammatory response in experimental autoimmune encephalomyelitis. Mol Immunol, 2007. 44(14): p. 3597-607.
209. Ruuls, S.R., et al., Aggravation of experimental allergic encephalomyelitis (EAE) by administration of nitric oxide (NO) synthase inhibitors. Clin Exp Immunol, 1996. 103(3): p. 467-74.
210. Van Dam, A.M., et al., Appearance of inducible nitric oxide synthase in the rat central nervous system after rabies virus infection and during experimental allergic encephalomyelitis but not after peripheral administration of endotoxin. J Neurosci Res, 1995. 40(2): p. 251-60.
211. Pugliatti, M., S. Sotgiu, and G. Rosati, The worldwide prevalence of multiple sclerosis. Clin Neurol Neurosurg, 2002. 104(3): p. 182-91.
212. Sospedra, M. and R. Martin, Immunology of multiple sclerosis. Annu Rev Immunol, 2005. 23: p. 683-747.
213. Kutzelnigg, A. and H. Lassmann, Pathology of multiple sclerosis and related inflammatory demyelinating diseases. Handb Clin Neurol, 2014. 122: p. 15-58.
214. Cheng, Y., et al., Diversity of immune cell types in multiple sclerosis and its animal model: Pathological and therapeutic implications. J Neurosci Res, 2017. 95(10): p. 1973-1983.
215. Ley, K., et al., Getting to the site of inflammation: the leukocyte adhesion cascade updated. Nat Rev Immunol, 2007. 7(9): p. 678-89.
216. Wekerle, H., B cells in multiple sclerosis. Autoimmunity, 2017. 50(1): p. 57-60.

217. Minogue, A.M., Role of infiltrating monocytes/macrophages in acute and chronic neuroinflammation: Effects on cognition, learning and affective behaviour. Prog Neuropsychopharmacol Biol Psychiatry, 2017. 79(Pt A): p. 15-18.
218. Wlodarczyk, A., et al., Pathologic and Protective Roles for Microglial Subsets and Bone Marrow- and Blood-Derived Myeloid Cells in Central Nervous System Inflammation. Front Immunol, 2015. 6: p. 463.
219. Berkovich, R., Treatment of acute relapses in multiple sclerosis. Neurotherapeutics, 2013. 10(1): p. 97-105.
220. Oh, J. and P.W. O'Connor, Established disease-modifying treatments in relapsing-remitting multiple sclerosis. Curr Opin Neurol, 2015. 28(3): p. 220-9.
221. Blumenfeld, S., E. Staun-Ram, and A. Miller, Fingolimod therapy modulates circulating B cell composition, increases B regulatory subsets and production of IL-10 and TGFbeta in patients with Multiple Sclerosis. J Autoimmun, 2016. 70: p. 40-51.
222. Diebold, M., et al., Dimethyl fumarate influences innate and adaptive immunity in multiple sclerosis. J Autoimmun, 2018. 86: p. 39-50.
223. Delbue, S., M. Comar, and P. Ferrante, Natalizumab treatment of multiple sclerosis: new insights. Immunotherapy, 2017. 9(2): p. 157-171.
224. Rahmanzadeh, R., et al., Multiple sclerosis pathogenesis: missing pieces of an old puzzle. Rev Neurosci, 2018. 30(1): p. 67-83.
225. Huitinga, I., et al., Suppression of experimental allergic encephalomyelitis in Lewis rats after elimination of macrophages. J Exp Med, 1990. 172(4): p. 1025-33.
226. Duffy, S.S., J.G. Lees, and G. Moalem-Taylor, The contribution of immune and glial cell types in experimental autoimmune encephalomyelitis and multiple sclerosis. Mult Scler Int, 2014. 2014: p. 285245.
227. Leu, R.W., et al., Enhanced transglutaminase activity associated with macrophage activation. Possible role in Fc-mediated phagocytosis. Exp Cell Res, 1982. 141(1): p. 191-9.
228. Bogie, J.F., P. Stinissen, and J.J. Hendriks, Macrophage subsets and microglia in multiple sclerosis. Acta Neuropathol, 2014. 128(2): p. 191-213.
229. van Strien, M.E., et al., Tissue Transglutaminase contributes to experimental multiple sclerosis pathogenesis and clinical outcome by promoting macrophage migration. Brain Behav Immun, 2015. 50: p. 141-154.

230. Chrobok, N.L., et al., Is monocyte- and macrophage-derived tissue transglutaminase involved in inflammatory processes? Amino Acids, 2017. 49(3): p. 441-452.
231. Espitia Pinzon, N., et al., Tissue transglutaminase in marmoset experimental multiple sclerosis: discrepancy between white and grey matter. PLoS One, 2014. 9(6): p. e100574.
232. Hendrickx, D.A.E., et al., Staining of HLA-DR, Iba1 and CD68 in human microglia reveals partially overlapping expression depending on cellular morphology and pathology. J Neuroimmunol, 2017. 309: p. 12-22.
233. Walker, D.G. and L.F. Lue, Immune phenotypes of microglia in human neurodegenerative disease: challenges to detecting microglial polarization in human brains. Alzheimers Res Ther, 2015. 7(1): p. 56.
234. Hulshof, S., et al., CX3CL1 and CX3CR1 expression in human brain tissue: noninflammatory control versus multiple sclerosis. J Neuropathol Exp Neurol, 2003. 62(9): p. 899-907.
235. Holness, C.L. and D.L. Simmons, Molecular cloning of CD68, a human macrophage marker related to lysosomal glycoproteins. Blood, 1993. 81(6): p. 1607-13.
236. Panek, C.A., et al., Differential expression of the fractalkine chemokine receptor (CX3CR1) in human monocytes during differentiation. Cell Mol Immunol, 2015. 12(6): p. 669-80.
237. Eligini, S., et al., Human monocyte-derived macrophages are heterogenous: Proteomic profile of different phenotypes. J Proteomics, 2015. 124: p. 112-23.
238. Dutta, R. and B.D. Trapp, Relapsing and progressive forms of multiple sclerosis: insights from pathology. Curr Opin Neurol, 2014. 27(3): p. 271-8.
239. Constantinescu, C.S. and B. Gran, The essential role of T cells in multiple sclerosis: a reappraisal. Biomed J, 2014. 37(2): p. 34-40.
240. Sestito, C., et al., Monocyte-derived tissue transglutaminase in multiple sclerosis patients: reflecting an anti-inflammatory status and function of the cells? J Neuroinflammation, 2017. 14(1): p. 257.
241. Illes, Z., et al., Differential expression of NK T cell V alpha 24J alpha Q invariant TCR chain in the lesions of multiple sclerosis and chronic inflammatory demyelinating polyneuropathy. J Immunol, 2000. 164(8): p. 4375-81.
242. Durrenberger, P.F., et al., Innate immunity in multiple sclerosis white matter lesions: expression of natural cytotoxicity triggering receptor 1 (NCR1). J Neuroinflammation, 2012. 9: p. 1.
243. Rumble, J.M., et al., Neutrophil-related factors as biomarkers in EAE and MS. J Exp Med, 2015. 212(1): p. 23-35.

244. Seiving, B., et al., Transglutaminase differentiation during maturation of human blood monocytes to macrophages. Eur J Haematol, 1991. 46(5): p. 263-71.
245. Murray, P.J., et al., Macrophage activation and polarization: nomenclature and experimental guidelines. Immunity, 2014. 41(1): p. 14-20.
246. Nadella, V., et al., Transglutaminase 2 interacts with syndecan-4 and CD44 at the surface of human macrophages to promote removal of apoptotic cells. Biochim Biophys Acta, 2015. 1853(1): p. 201-12.
247. Fesus, L., et al., Immune-complex-induced transglutaminase activation: its role in the Fc-receptor-mediated transmembrane effect on peritoneal macrophages. Mol Immunol, 1981. 18(7): p. 633-8.
248. Murtaugh, M.P., W.P. Arend, and P.J. Davies, Induction of tissue transglutaminase in human peripheral blood monocytes. J Exp Med, 1984. 159(1): p. 114-25.
249. Lampron, A., et al., Inefficient clearance of myelin debris by microglia impairs remyelinating processes. J Exp Med, 2015. 212(4): p. 481-95.
250. Boven, L.A., et al., Myelin-laden macrophages are anti-inflammatory, consistent with foam cells in multiple sclerosis. Brain, 2006. 129(Pt 2): p. 517-26.
251. Martinez, F.O., et al., Genetic programs expressed in resting and IL-4 alternatively activated mouse and human macrophages: similarities and differences. Blood, 2013. 121(9): p. e57-69.
252. Jeong, H.K., et al., Brain inflammation and microglia: facts and misconceptions. Exp Neurobiol, 2013. 22(2): p. 59-67.
253. Bobholz, J.A. and S.M. Rao, Cognitive dysfunction in multiple sclerosis: a review of recent developments. Curr Opin Neurol, 2003. 16(3): p. 283-8.
254. Kornek, B. and H. Lassmann, Neuropathology of multiple sclerosis-new concepts. Brain Res Bull, 2003. 61(3): p. 321-6.
255. Pucci, E., et al., Natalizumab for relapsing remitting multiple sclerosis. Cochrane Database Syst Rev, 2011(10): p. CD007621.
256. Ajami, B., et al., Infiltrating monocytes trigger EAE progression, but do not contribute to the resident microglia pool. Nat Neurosci, 2011. 14(9): p. 1142-9.
257. Man, S., E.E. Ubogu, and R.M. Ransohoff, Inflammatory cell migration into the central nervous system: a few new twists on an old tale. Brain Pathol, 2007. 17(2): p. 243-50.
258. Gerhardt, T. and K. Ley, Monocyte trafficking across the vessel wall. Cardiovasc Res, 2015. 107(3): p. 321-30.

259. Metha, K., J. Turpin, and G. Lopez-Berestein, Induction of tissue transglutaminase in human peripheral blood monocytes by intracellular delivery of retinoids. J Leukoc Biol, 1987. 41(4): p. 341-8.
260. Eckert, R.L., et al., Transglutaminase regulation of cell function. Physiol Rev, 2014. 94(2): p. 383-417.
261. Laudanna, C., et al., Rapid leukocyte integrin activation by chemokines. Immunol Rev, 2002. 186: p. 37-46.
262. Rausch, M., et al., MRI-based monitoring of inflammation and tissue damage in acute and chronic relapsing EAE. Magn Reson Med, 2003. 50(2): p. 309-14.
263. Pirko, I., et al., Magnetic resonance imaging of immune cells in inflammation of central nervous system. Croat Med J, 2003. 44(4): p. 463-8.
264. Floris, S., et al., Blood-brain barrier permeability and monocyte infiltration in experimental allergic encephalomyelitis: a quantitative MRI study. Brain, 2004. 127(Pt 3): p. 616-27.
265. Jung, S., et al., Analysis of fractalkine receptor CX(3)CR1 function by targeted deletion and green fluorescent protein reporter gene insertion. Mol Cell Biol, 2000. 20(11): p. 4106-14.
266. Fenrich, K.K., et al., Long-term in vivo imaging of normal and pathological mouse spinal cord with subcellular resolution using implanted glass windows. J Physiol, 2012. 590(16): p. 3665-75.
267. Fenrich, K.K., et al., Implanting glass spinal cord windows in adult mice with experimental autoimmune encephalomyelitis. J Vis Exp, 2013(82): p. e50826.
268. Fenrich, K.K., et al., Long- and short-term intravital imaging reveals differential spatiotemporal recruitment and function of myelomonocytic cells after spinal cord injury. J Physiol, 2013. 591(19): p. 4895-902.
269. Nikic, I., et al., A reversible form of axon damage in experimental autoimmune encephalomyelitis and multiple sclerosis. Nat Med, 2011. 17(4): p. 495-9.
270. Meijering, E., O. Dzyubachyk, and I. Smal, Methods for cell and particle tracking. Methods Enzymol, 2012. 504: p. 183-200.
271. Schindelin, J., et al., Fiji: an open-source platform for biological-image analysis. Nat Methods, 2012. 9(7): p. 676-82.
272. Harrison, M., et al., Vertebral landmarks for the identification of spinal cord segments in the mouse. Neuroimage, 2013. 68: p. 22-9.
273. Sandor, K., et al., Transcriptional control of transglutaminase 2 expression in mouse apoptotic thymocytes. Biochim Biophys Acta, 2016. 1859(8): p. 964-74.

274. Barthelmes, J., et al., Induction of Experimental Autoimmune Encephalomyelitis in Mice and Evaluation of the Disease-dependent Distribution of Immune Cells in Various Tissues. J Vis Exp, 2016(111).
275. Huang, D., et al., The neuronal chemokine CX3CL1/fractalkine selectively recruits NK cells that modify experimental autoimmune encephalomyelitis within the central nervous system. FASEB J, 2006. 20(7): p. 896-905.
276. Auffray, C., et al., Monitoring of blood vessels and tissues by a population of monocytes with patrolling behavior. Science, 2007. 317(5838): p. 666-70.
277. Carlin, L.M., C. Auffray, and F. Geissmann, Measuring intravascular migration of mouse Ly6C(low) monocytes in vivo using intravital microscopy. Curr Protoc Immunol, 2013. Chapter 14: p. Unit 14 33 1-16.
278. Kuerten, S., et al., MP4- and MOG:35-55-induced EAE in C57BL/6 mice differentially targets brain, spinal cord and cerebellum. J Neuroimmunol, 2007. 189(1-2): p. 31-40.
279. Recks, M.S., K. Addicks, and S. Kuerten, Spinal cord histopathology of MOG peptide 35-55-induced experimental autoimmune encephalomyelitis is time- and score-dependent. Neurosci Lett, 2011. 494(3): p. 227-31.
280. Redford, E.J., et al., A combined inhibitor of matrix metalloproteinase activity and tumour necrosis factor-alpha processing attenuates experimental autoimmune neuritis. Brain, 1997. 120 (Pt 10): p. 1895-905.
281. Leppert, D., et al., Matrix metalloproteinases: multifunctional effectors of inflammation in multiple sclerosis and bacterial meningitis. Brain Res Brain Res Rev, 2001. 36(2-3): p. 249-57.
282. Goldmann, T. and M. Prinz, Role of microglia in CNS autoimmunity. Clin Dev Immunol, 2013. 2013: p. 208093.
283. Rossi, B., et al., Vascular inflammation in central nervous system diseases: adhesion receptors controlling leukocyte-endothelial interactions. J Leukoc Biol, 2011. 89(4): p. 539-56.
284. Yin, J.X., et al., Centrally administered pertussis toxin inhibits microglia migration to the spinal cord and prevents dissemination of disease in an EAE mouse model. PLoS One, 2010. 5(8): p. e12400.
285. Chastain, E.M., et al., The role of antigen presenting cells in multiple sclerosis. Biochim Biophys Acta, 2011. 1812(2): p. 265-74.
286. Tatsukawa, H., et al., Transglutaminase 2 has opposing roles in the regulation of cellular functions as well as cell growth and death. Cell Death Dis, 2016. 7(6): p. e2244.

287. Irony-Tur-Sinai, M., et al., Immunomodulation of EAE by alpha-fetoprotein involves elevation of immune cell apoptosis markers and the transcription factor FoxP3. J Neurol Sci, 2009. 279(1-2): p. 80-7.
288. Kipp, M., et al., Multiple sclerosis animal models: a clinical and histopathological perspective. Brain Pathol, 2016.
289. Sheremata, W.A., et al., The role of alpha-4 integrin in the aetiology of multiple sclerosis: current knowledge and therapeutic implications. CNS Drugs, 2005. 19(11): p. 909-22.
290. Gundemir, S., et al., Transglutaminase 2: a molecular Swiss army knife. Biochim Biophys Acta, 2012. 1823(2): p. 406-19.
291. Espitia Pinzon, N., et al., Astrocyte-derived tissue Transglutaminase affects fibronectin deposition, but not aggregation, during cuprizone-induced demyelination. Sci Rep, 2017. 7: p. 40995.
292. Oertel, K., et al., A highly sensitive fluorometric assay for determination of human coagulation factor XIII in plasma. Anal Biochem, 2007. 367(2): p. 152-8.
293. van der Wildt, B., et al., Development of carbon-11 labeled acryl amides for selective PET imaging of active tissue transglutaminase. Nucl Med Biol, 2016. 43(4): p. 232-42.
294. Dafik, L. and C. Khosla, Dihydroisoxazole analogs for labeling and visualization of catalytically active transglutaminase 2. Chem Biol, 2011. 18(1): p. 58-66.
295. Watts, R.E., M. Siegel, and C. Khosla, Structure-activity relationship analysis of the selective inhibition of transglutaminase 2 by dihydroisoxazoles. J Med Chem, 2006. 49(25): p. 7493-501.
296. Verhaar, R., et al., Blockade of enzyme activity inhibits tissue transglutaminase-mediated transamidation of alpha-synuclein in a cellular model of Parkinson's disease. Neurochem Int, 2011. 58(7): p. 785-93.
297. Miller, S.D. and W.J. Karpus, Experimental autoimmune encephalomyelitis in the mouse. Curr Protoc Immunol, 2007. Chapter 15: p. Unit 15 1.
298. de Jager, M., et al., Tissue transglutaminase colocalizes with extracellular matrix proteins in cerebral amyloid angiopathy. Neurobiol Aging, 2013. 34(4): p. 1159-69.
299. Ye, J., et al., Primer-BLAST: a tool to design target-specific primers for polymerase chain reaction. BMC Bioinformatics, 2012. 13: p. 134.
300. Bustin, S.A., et al., The MIQE guidelines: minimum information for publication of quantitative real-time PCR experiments. Clin Chem, 2009. 55(4): p. 611-22.

301. Ruijter, J.M., et al., Amplification efficiency: linking baseline and bias in the analysis of quantitative PCR data. Nucleic Acids Res, 2009. 37(6): p. e45.
302. Ferrara, G., et al., NG2, a common denominator for neuroinflammation, blood-brain barrier alteration, and oligodendrocyte precursor response in EAE, plays a role in dendritic cell activation. Acta Neuropathol, 2016. 132(1): p. 23-42.
303. Junqueira, S.C., et al., Inosine, an Endogenous Purine Nucleoside, Suppresses Immune Responses and Protects Mice from Experimental Autoimmune Encephalomyelitis: a Role for A2A Adenosine Receptor. Mol Neurobiol, 2016.
304. Chrobok, N.L., et al., Monocyte behaviour and tissue transglutaminase expression during experimental autoimmune encephalomyelitis in transgenic CX3CR1gfp/gfp mice. Amino Acids, 2016.
305. Cristofanilli, M., et al., Transglutaminase-6 is an autoantigen in progressive multiple sclerosis and is upregulated in reactive astrocytes. Mult Scler, 2017. 23(13): p. 1707-1715.
306. van Horssen, J., et al., Extensive extracellular matrix depositions in active multiple sclerosis lesions. Neurobiol Dis, 2006. 24(3): p. 484-91.
307. Clerico, M., et al., Long-term safety evaluation of natalizumab for the treatment of multiple sclerosis. Expert Opin Drug Saf, 2017. 16(8): p. 963-972.
308. Hoepner, R., et al., Efficacy and side effects of natalizumab therapy in patients with multiple sclerosis. J Cent Nerv Syst Dis, 2014. 6: p. 41-9.
309. Brosnan, C.F., M.B. Bornstein, and B.R. Bloom, The effects of macrophage depletion on the clinical and pathologic expression of experimental allergic encephalomyelitis. J Immunol, 1981. 126(2): p. 614-20.
310. Mehta, K., et al., Interferon-gamma requires serum retinoids to promote the expression of tissue transglutaminase in cultured human blood monocytes. J Immunol, 1985. 134(4): p. 2053-6.
311. Yamaguchi, M., et al., PLA2G5 regulates transglutaminase activity of human IL-4-activated M2 macrophages through PGE2 generation. J Leukoc Biol, 2016.
312. Martin, E., et al., Analysis of Microglia and Monocyte-derived Macrophages from the Central Nervous System by Flow Cytometry. J Vis Exp, 2017(124).
313. Baker, D. and S. Amor, Experimental autoimmune encephalomyelitis is a good model of multiple sclerosis if used wisely. Mult Scler Relat Disord, 2014. 3(5): p. 555-64.

314. Fletcher, J.M., et al., T cells in multiple sclerosis and experimental autoimmune encephalomyelitis. Clin Exp Immunol, 2010. 162(1): p. 1-11.
315. Fisniku, L.K., et al., Disability and T2 MRI lesions: a 20-year follow-up of patients with relapse onset of multiple sclerosis. Brain, 2008. 131(Pt 3): p. 808-17.
316. Wuerfel, J., et al., Mouse model mimics multiple sclerosis in the clinico-radiological paradox. Eur J Neurosci, 2007. 26(1): p. 190-8.
317. Belkin, A.M., Extracellular TG2: emerging functions and regulation. FEBS J, 2011. 278(24): p. 4704-16.
318. Park, K.C., et al., Transglutaminase 2 induces nitric oxide synthesis in BV-2 microglia. Biochem Biophys Res Commun, 2004. 323(3): p. 1055-62.
319. Kawabe, K., et al., Lipopolysaccharide-Stimulated Transglutaminase 2 Expression Enhances Endocytosis Activity in the Mouse Microglial Cell Line BV-2. Neuroimmunomodulation, 2015. 22(4): p. 243-9.
320. Kuo, T.F., H. Tatsukawa, and S. Kojima, New insights into the functions and localization of nuclear transglutaminase 2. FEBS J, 2011. 278(24): p. 4756-67.
321. Verhaar, R., et al., Increase in endoplasmic reticulum-associated tissue transglutaminase and enzymatic activation in a cellular model of Parkinson's disease. Neurobiol Dis, 2012. 45(3): p. 839-50.
322. Zemskov, E.A., et al., The role of tissue transglutaminase in cell-matrix interactions. Front Biosci, 2006. 11: p. 1057-76.
323. Verma, A., et al., Tissue transglutaminase regulates focal adhesion kinase/AKT activation by modulating PTEN expression in pancreatic cancer cells. Clin Cancer Res, 2008. 14(7): p. 1997-2005.
324. Herman, J.F., L.S. Mangala, and K. Mehta, Implications of increased tissue transglutaminase (TG2) expression in drug-resistant breast cancer (MCF-7) cells. Oncogene, 2006. 25(21): p. 3049-58.
325. Verma, A., et al., Increased expression of tissue transglutaminase in pancreatic ductal adenocarcinoma and its implications in drug resistance and metastasis. Cancer Res, 2006. 66(21): p. 10525-33.
326. Alvarez, J.I., R. Cayrol, and A. Prat, Disruption of central nervous system barriers in multiple sclerosis. Biochim Biophys Acta, 2011. 1812(2): p. 252-64.
327. Bauer, S., B.J. Kerr, and P.H. Patterson, The neuropoietic cytokine family in development, plasticity, disease and injury. Nat Rev Neurosci, 2007. 8(3): p. 221-32.
328. Hostenbach, S., et al., Astrocyte loss and astrogliosis in neuroinflammatory disorders. Neurosci Lett, 2014. 565: p. 39-41.

329. Espitia Pinzon, N., et al., Tissue transglutaminase in astrocytes is enhanced by inflammatory mediators and is involved in the formation of fibronectin fibril-like structures. J Neuroinflammation, 2017. 14(1): p. 260.
330. Van Strien, M.E., et al., Tissue transglutaminase activity is involved in the differentiation of oligodendrocyte precursor cells into myelin-forming oligodendrocytes during CNS remyelination. Glia, 2011. 59(11): p. 1622-34.
331. Giera, S., et al., Microglial transglutaminase-2 drives myelination and myelin repair via GPR56/ADGRG1 in oligodendrocyte precursor cells. Elife, 2018. 7.
332. Espitia Pinzon, N., et al., Tissue Transglutaminase Promotes Early Differentiation of Oligodendrocyte Progenitor Cells. Front Cell Neurosci, 2019. 13: p. 281.
333. Williams, A., G. Piaton, and C. Lubetzki, Astrocytes--friends or foes in multiple sclerosis? Glia, 2007. 55(13): p. 1300-12.
334. Jones, R.A., et al., Reduced expression of tissue transglutaminase in a human endothelial cell line leads to changes in cell spreading, cell adhesion and reduced polymerisation of fibronectin. J Cell Sci, 1997. 110 (Pt 19): p. 2461-72.
335. Mosher, D.F., Cross-linking of fibronectin to collagenous proteins. Mol Cell Biochem, 1984. 58(1-2): p. 63-8.
336. Sane, D.C., et al., Vitronectin is a substrate for transglutaminases. Biochem Biophys Res Commun, 1988. 157(1): p. 115-20.
337. Griffin, M., L.L. Smith, and J. Wynne, Changes in transglutaminase activity in an experimental model of pulmonary fibrosis induced by paraquat. Br J Exp Pathol, 1979. 60(6): p. 653-61.
338. Moore, K.J., F.J. Sheedy, and E.A. Fisher, Macrophages in atherosclerosis: a dynamic balance. Nat Rev Immunol, 2013. 13(10): p. 709-21.
339. Van Herck, J.L., et al., Transglutaminase 2 deficiency decreases plaque fibrosis and increases plaque inflammation in apolipoprotein-E-deficient mice. J Vasc Res, 2010. 47(3): p. 231-40.

SUMMARY

Multiple Sclerosis (MS) is an inflammatory disease of the central nervous system (CNS) that is characterized by demyelination and axonal damage. It is one of the most common neurological disorders among young adults. MS causes serious physical disabilities together with cognitive impairment, which highly affect the quality of life. The most common form of MS pathologically presents itself with a massive migration of leukocytes from the bloodstream into the CNS facilitated by functional disturbances of the blood-brain barrier. These infiltrated cells, together with activated resident cells of the CNS, damage the insulating myelin sheath of the axons and are responsible for the serious disabling symptoms in MS patients.

Unfortunately, up to now, no preventive or curing treatment is available and MS therapy traditionally applies general anti-inflammatory treatment. In recent years a more specific approach has been applied, that targets the influx of CNS infiltrating lymphocytes. With this goal in mind, detailed understanding of the cell types and mechanisms involved in the pathogenesis of MS is of crucial importance to develop new therapeutic agents, with possibly less side effects. Previous research has shown that monocytes and/or macrophages have detrimental influence in the early stage of MS pathogenesis and in its animal model experimental autoimmune encephalomyelitis (EAE). Besides, they constitute the majority of infiltrated immune cells in the CNS lesions. Thus far, monocytes/macrophages are not specifically targeted by therapeutic drugs available in MS. To obtain more knowledge on the pathogenesis of MS, research is often done with experimental models, mimicking certain aspects of the disease. In this thesis we used EAE models in rodents, which are the most commonly used models for studying neuroinflammatory processes as present in MS pathology.

Tissue Transglutaminase (TG2) is a multifunctional enzyme of the Transglutaminase family. It is best known for its enzymatic protein cross-linking activity but additionally exhibits various other enzymatic functions including GTPase, disulfide isomerase and protein kinase activity as well as enzymatic independent functions. TG2 is associated with important functions in both physiological and pathological conditions and is ubiquitously expressed in many cell types, including monocytes and macrophages. The enzyme is predominantly present in the cytoplasm, but has also been found in the nucleus, mitochondria, endoplasmic reticulum, on the cell surface and extracellularly in the extracellular matrix (ECM). Increased TG2 expression and transamidation activity is often observed under inflammatory conditions and TG2 can contribute to many fundamental processes, including cellular adhesion and migration, cytoskeletal rearrangement and cell differentiation. Previous research found both neuroinflammation and degeneration facilitated by dysregulated expression and activity of TG2 in several neurodegenerative diseases including Alzheimer's, Parkinson's and Huntington's disease.

The studies presented in this thesis aimed at identifying the cellular expression of TG2 in post-mortem CNS material of MS patients and of rodents subjected to EAE. To elucidate the role of TG2 in EAE symptom development and pathology, we investigated TG2's contribution and potential as druggable target in rat and mouse EAE.

Our immunohistochemical studies showed that TG2 is expressed in inflammatory white matter MS lesions in post-mortem CNS tissue from MS patients (chapters 2 and 3) and in EAE lesions of rats (chapter 2) and mice (chapters 4 and 5). In both pathologies, under condition of inflammatory activity in the lesions, cells appeared to express TG2 and are identified as leukocytes and more specifically macrophages. The restriction of TG2 expression to specific cell types that are major players in disease pathology of MS and EAE indicate that TG2 may be involved in both disease pathologies, which makes TG2 a potential exciting therapeutic target. Interestingly, we found evidence that TG2 upregulation in monocytes in EAE might already occur previous to their extravasation into the CNS parenchyma. The upregulation of TG2 in peripheral monocytes might then very well be a prelude to further involvement of TG2 in MS and EAE pathology.

Although post-mortem tissue provides valuable information about CNS lesions of MS and EAE, imaging the interaction with monocytes in the spinal cord adds more detailed information about monocyte behavior during EAE in vivo. In chapter 4, we studied the behavior of crawling, fluorescent monocytes and their interaction with the spinal cord endothelium, in EAE mice, in real time using 2-photon microscopy. The cells were visualized in CX3CR1 transgenic mice, in which monocytes, macrophages and microglial cells express green fluorescent protein (GFP). We showed that the amount of crawling cells are increased and their track lengths extended during EAE, indicating a potentially firmer interaction of the cells with the endothelium. One of the mediators of these processes could be TG2, which expression in brain endothelium attached monocytes was confirmed in post-mortem tissue from these transgenic mice.

To investigate a potential causal contribution of TG2 to EAE motor symptom development and pathology, we pharmacologically manipulated TG2 activity in rodent EAE models (chapters 2 and 5). Rats and mice suffering from EAE were treated with various TG2 inhibitory compounds just after onset of disease symptoms. The pharmacological inhibition of TG2 activity could drastically reduce EAE motor symptoms and pathology, confirming a role of TG2 in the development of EAE symptoms. Especially the administration of one compound (KCC009) highly reduced the leukocyte infiltration in the CNS and lesion formation. Together with in vitro reduction of monocyte adhesion to and migration across blood-brain barrier cells after TG2 inhibition, this points towards monocyte and macrophage derived TG2 playing a role in their in vivo crawling behavior along the blood vessels in the CNS as an initial step to CNS infiltration. Promising for potential treatment of MS with TG2 inhibitors is, that therapeutic treatment approach after onset of disease symptoms, comparable to treating MS patients, is effective. Although the administration of TG2 activity inhibitors demonstrated clear beneficial effects in our animal models, the detailed process and mechanisms are not fully revealed. We observed a better effect when using a TG2 inhibitor that does not penetrate the cells, suggestive for an important role for surface/extracellular TG2 in reducing EAE symptoms and especially CNS infiltration of immune cells. Therefore it is likely that an interplay of TG2's transamidation function and possibly other actions of TG2, that have not been specifically studied in this context, are involved in EAE pathology and symptom development.

In conclusion, our studies demonstrate that TG2 is expressed in monocytes and macrophages in inflammatory MS and EAE lesions. Our encouraging results of pharmacological TG2 inhibition in rodents suffering from EAE revealed that TG2 is involved in monocyte/macrophage migration into the CNS. In addition, TG2 contributes to motor impairment in EAE and hence TG2 could be a potential target of interest in MS patients. The here presented studies support the investigation of monocyte and macrophage derived TG2 as a potential druggable target of interest for the treatment of MS patients.

ACKNOWLEDGEMENTS

I would like to express my sincere gratitude to all the people who have helped and supported me during the long course of my PhD.

In particular, I am very thankful to my supervisor Anne-Marie van Dam who supported me as a PhD student. I cannot thank her enough for her revisions of my manuscripts, encouragement and unlimited optimism! I also want to thank my promotor Benjamin Drukarch and my co-promotor Micha Wilhelmus for their valuable input and support in planning my research, revising my manuscripts and this thesis.

My sincere thanks goes to all the members of the reading commission (Sandra Amor, Paul v. d. Valk, Erik Bakker, Paul Lucassen, Joost Smolders, Gijs Kooij) for spending some of their precious time and examining my thesis.

I wish to cordially thank all the members of the ANW department and especially the PhD students of my group and the other ANW PhD students “down the hallway”, and all the ones I only got to know after moving to the O2 building.

I am especially thankful to John Bol, Kees Jongenelen and John Brevé for all their hard work doing experiments for me, their input in performing laboratory experiments, their motivation and always making time for a chat for work and non-work related topics!

Without collaborators and many other people, this thesis would not have been possible. These include Paul van der Valk and Sandra Amor, Wouter Gerritsen, Regina Peferoen-Baart from the VUmc pathology department; the team from the Netherlands Brain Bank (NBB), especially Michiel Kooreman and Corbert van Eden; the staff from the Universitair Proefdier centrum for taking good care of my animals during experiments; Jos Twisk was a great help with the statistical analysis of the EAE animal experiments and he gave me some new insights into statistics; the members of the MCBI department, especially, Elga de Vries, Tanja Konijn, Henrike Veninga, Susanne van der Pol and Tom O’Toole.

The study on the intravital microscopy of the murine spinal cord would not have been possible without our collaborators in Marseille. I would like to thank Franck Debarbieux to welcome me into his lab. Thanks to Keith Fenrich and Alexandre Jaouen for patiently explaining the surgical techniques as well as assisting with surgery, microscopical acquisition and analysis. Although it was a short time I spend in Marseille, I enjoyed it very much.

I joined Covalab for one month only, but I had a good time in Lyon and want to thank Said El Alaoui, Javier Fidalgo Lopez, Vincent Thomas, Valérie Attuil, Sabrina Lareure, Christine Dufour and the other employees for this.

As a member of the Marie Curie ITN Transpath, I would like to thank all the members for making it a good time being part of this ITN and especially the other PhD students and postdocs.

Last but not least, I am deeply grateful for my family and friends who supported me during my ups and downs of this long process. I very much appreciate their invaluable encouragement and support.

Mama, danke für alles! Du hast mich seit der Schule immer motiviert und mir beigestanden, wenn es gerade nicht so gut lief und dich so wunderbar mit mir gefreut, wenn alles gut klappte. Es hat zwar etwas gedauert, aber jetzt sind beide deine Kinder fertig mit ihrer Doktoarbeit und du kannst unglaublich stolz sein uns dabei unterstützt zu haben!

Michael, mein großer Bruder. Ich habe es ja schon lange gesagt und tatsächlich hat du deinen PhD noch vor mir bekommen. Vielen Dank für die guten wissenschaftlichen Diskussionen und Hilfe mit Durchflusszytometrie, auch wenn daraus am Ende nichts geworden ist. Du hast mich immer unterstützt und motiviert durchzuhalten.

Ralf, even though I did not know you when I started my PhD, you are the one person, besides me, on which this work had the highest impact. With so many downs and moments when I wanted to give up, you were always optimistic, supportive and encouraging beyond belief. Thanks for sticking with me through all these years finishing this up!

Antonie, wir hätten zwar beide nie gedacht, dass es so lange dauert bis das Ding fertig ist, aber unsere Freundschaft ist definitiv gleichzeitig mit meiner Doktorarbeit gewachsen (wenn auch etwas schneller). Danke, für den ganzen Spaß und das gute Zureden.

CURRICULUM VITAE

Navina Chrobok was born on July 17th, 1986 in Hannover, Germany. She attended the Kaiser-Wilhelm- und Ratsgymnasium in Hannover and received her diploma (Abitur) in 2005. After obtaining a Bachelor's degree in Biochemistry (Universität Bayreuth, Germany), she graduated from Universität zu Lübeck (Germany) with a Master's degree in Molecular Life Sciences. During her Master's she completed a three month internship at the University of Toronto, Canada, and a three and a half month internship at the University of Oxford, United Kingdom. For her Master's thesis she worked for 7 month at the University of Calgary in the group of Paul Kubes under the supervision of Connie Wong. There she applied intra-vital confocal microscopy to study platelet aggregation in the mouse liver caused by *Bacillus cereus*. After a short research intermezzo at the Universität zu Lübeck, she started her PhD research in 2012 as a Marie Curie Early Stage researcher at the VUmc in Amsterdam, Netherlands. Under the supervision of Anne-Marie van Dam she focused on the presence and role of tissue transglutaminase in multiple sclerosis lesions and the experimental autoimmune encephalomyelitis rodent models. The results of this work is described in the present thesis. After her PhD she started as junior project manager at Virology Education, Utrecht, Netherlands, and assisted with the organization of international scientific conferences. In 2019 Navina joined the Vaccine Analysis group of the Development & Technology department of MSD Animal Health, Boxmeer, Netherlands, to develop an *in vitro* potency test for vaccines against the Foot-and-mouth disease virus.

LIST OF PUBLICATIONS

Chrobok NL, Bol JGJM, Wilhelmus MMM, Drukarch B, van Dam AM (2019); Tissue Transglutaminase Appears in Monocytes and Macrophages but Not in Lymphocytes in White Matter Multiple Sclerosis Lesions. J Neuropathol Exp Neurol. 2019. Vol. 78, No. 6, June 2019, pp. 492–500.

Chrobok NL, Bol JGJM, Jongenelen CA, Brevé JJP, El Alaoui S, Fidalgo-Lopez J, Fournet G, Joseph B, Wilhelmus MMM, Drukarch B, van Dam AM (2018); Characterization of Transglutaminase 2 activity inhibitors in monocytes *in vitro* and their effect in a mouse model for multiple sclerosis. PLoS One. 2018. 13(4): p. e0196433. Correction in: PLoS One, 2018. **13**(12): p. e0209522.

Chrobok NL, Jaouen A, Fenrich KK, Bol JG, Wilhelmus MM, Drukarch B, Debarbieux F, van Dam AM (2017); Monocyte behaviour and tissue transglutaminase expression during experimental autoimmune encephalomyelitis in transgenic CX3CR1$^{gfp/gfp}$ mice. Amino Acids. 2017 Mar;49(3):643-658.

Chrobok NL, Sestito C, Wilhelmus MM, Drukarch B, van Dam AM (2017); Is monocyte- and macrophage-derived tissue transglutaminase involved in inflammatory processes? Amino Acids. 2017 Mar;49(3):441-452.

van Strien ME, **Chrobok NL**, de Vries HE, Bol JG, Breve JJ, van der Pol SM, Kooij G, van Buul JD, Karpuj M, Steinman L, Wilhelmus MM, Sestito C, Drukarch B, Van Dam AM (2015); Tissue Transglutaminase contributes to experimental multiple sclerosis pathogenesis and clinical outcome by promoting macrophage migration. Brain Behav Immun 50:141-154.

Iwata H, Bieber K, Tiburzy B, **Chrobok N**, Kalies K, Shimizu A, Leineweber S, Ishiko A, Vorobyev A, Zillikens D, Kohl J, Westermann J, Seeger K, Manz R, Ludwig RJ (2013); B cells, dendritic cells, and macrophages are required to induce an autoreactive CD4 helper T cell response in experimental epidermolysis bullosa acquisita. J Immunol 191 (6):2978-2988.

Tiburzy B, Szyska M, Iwata H, **Chrobok N,** Kulkarni U, Hirose M, Ludwig RJ, Kalies K, Westermann J, Wong D, Manz RA (2013); Persistent autoantibody-production by intermediates between short-and long-lived plasma cells in inflamed lymph nodes of experimental epidermolysis bullosa acquisita. PLoS One 8 (12):e83631.

Wong CH, Jenne CN, Petri B, **Chrobok NL**, Kubes P (2013); Nucleation of platelets with blood-borne pathogens on Kupffer cells precedes other innate immunity and contributes to bacterial clearance. Nat Immunol 14 (8):785-792.

